IMIDAZOLIUM IONOMER DERIVATIVES OF ISOBUTYLENE-RICH ELASTOMERS:

THERMOSETS, EMULSIONS, FILLER COMPOSITES and CLAY NANOCOMPOSITES

By

Monika Robyn Kleczek

A thesis submitted to the Department of Chemical Engineering
in conformity with the requirements for the degree of
Doctor of Philosophy

Queen's University
Kingston, Ontario, Canada
December 2013

ABSTRACT

Ionomers are valued for their exceptional physical properties, antimicrobial activity and superior adhesion to high surface energy solids and polymer blend components. Carboxylate, or sulfonate derivatives, of ethylene-rich thermoplastics are the most commercially available ionomers. Elastomeric ionomers bearing quaternary ammonium and phosphonium halide functionality have a literary standing in both scientific and patent-based publications. Currently cationic ionomers have shown great prominence in their inactivity to a wide range of bacteria and fungi.

The specific focus of this research is in the derivatives of isobutylene-rich elastomers due to their exceptional impermeability, oxidative stability and vibration dampening characteristics. Imidazole-derived ionomers support a wider range of ionomer chemistry compared to ammonium and phosphonium analogues. N-alkylation of nucleophiles including butyl imidazole, vinyl imidazole and 1,1'(1,4-butanediyl)bis(imidazole) by brominated poly(isobutylene-*co*-isoprene) yield thermally stable imidazolium bromide salts capable of supporting free radical cures and/or siliceous filler dispersions through further chemical modifications.

The versatility of imidazole chemistry extends to the synthesis of isobutylene-rich thermoset ionomers. This derives material properties from both a network of covalent crosslinks and a network of ion pair aggregates. Un-crosslinked elastomers are prone to creep and stress relaxation, hence a need for thermoset ionomer chemistry. Ion pairs are poorly solvated by the low dielectric constant of the polymer backbone and favoured thermodynamically by way of self-assembly of the ionic functionality. The aggregation of ion pairs establishes a non-covalent network of polymer chains whose dynamic mechanical properties approach those of conventional covalent thermosets comprised of carbon-carbon and/or sulfide crosslinks. However, the lability of this ionic network leads to a poor response to static loads leaving the thermoformable ionomers unqualified for engineering applications. A direct route is a more desirable method in preparing thermoset ionomers comprised of covalent crosslink networks and ionic functionality.

In all, these reactive imidazolium ionomers look promising in supporting new value-added applications for isobutylene-rich derivatives, which include yet are not limited to elastomer thermosets, emulsions, filler composites and clay nanocomposites.

ACKNOWLEDGEMENTS

This day on the completion of my thesis for the degree of Doctor of Philosophy, I extend my gratitude, debt and sincere thanks to Queen's University and their Departments of Chemical Engineering and Chemistry, my colleagues, peers, and friends.

Many thanks to Professor Dr. J. Scott Parent and Dr. Ralph A. Whitney for their mentoring, encouragement, optimism and generous offering of expertise and time. Their untiring energy was inspiring providing me the opportunity to experience their wisdom and friendship.

To my parents, I express my sincere gratitude for their sacrifice, friendship, forbearance, encouragement and help through the years.

TABLE OF CONTENTS

CHAPTER 4

Properties of a Vinylimidazolium Bromide Derivative of Poly(Isobutylene-Co-Isoprene) O/W Emulsion

CHAPTER 5

Filler Compounding and Clay Nanocomposites of a Mixed N-Vinylimidazolium and N-Butylimidazolium Derivative of BIMS

CHAPTER 6

Conclusions and Recommendations

APPENDIX A

LIST OF TABLES

LIST OF FIGURES

LIST OF SCHEMES

ABBREVIATIONS

AA	Acrylate
Ac	Acetate
APA	Advanced Polymer Analyzer
BIIR	Brominated Poly(isobutylene-*co*-isoprene)
BIMS	Brominated Poly(Isobutylene-*co*-*para*-methylstyrene)
BPMN	Brominated 2,2,4,8,8-Tetramethyl-4-Nonene
BuIm	Butylimidazole
Cin	Cinnamate
CMC	Critical Micelle Concentration
Crot	Crotonate
DCP	Dicumyl Peroxide
DLS	Dynamic Light Scattering
DMBA	3,3-Dimethylbutyrate
G*	Complex Modulus
G'	Storage Modulus
G"	Loss Modulus
GC	Gas Chromatography
IIR	Poly(Isobutylene-*co*-isoprene) / Butyl Rubber
Im	Imidazole
IMS	Poly(Isobutylene-*co*-para-methylstyrene)
IP	Isoprene
MA	Mixed Alkylation
MAA	Methacrylate
MMT	Montmorillonite
MS	Mass Spectrometry
NMR	Nuclear Magnetic Resonance
NR_3	Tertiary Amine
O/W	Oil In Water
PIB	Polyisobutylene
PLSNs	Polymer-Layered Silicate Nanocomposites
PPH_3	Triphenylphosphine
PTC	Phase Transfer Catalysis
ROOR	Organic Peroxide
TBA	Tetrabutylmmonium
TBAB	Tetrabutylammonium Bromide
TEM	Transmission Electron Microscopy
TGA	Thermogravimetric Analysis
TSB	Tryptic Soy Broth
UD	Undecenoate
VIm	Vinylimidazole
VOC	Volatile Organic Compounds
W/O	Water in Oil
XL	Crosslinked
δ	Loss Tangent

CHAPTER 1

INTRODUCTION

1.1 Isobutylene-Rich Elastomers

Poly(isobutylene), PIB, (Figure 1.1 below) can be found in typical day-to-day products like adhesives, sealants, and chewing gum. It provides superior thermal and oxidative stability, vibration dampening and gas impermeability qualities.[1] The elastomer is commercially available at a molecular weight on the order of 100 kg/mole. It is an amorphous homopolymer with a glass-transition temperature of approximately -60°C, providing uncured elastomer properties of high elongation at break and low stiffness (Young's modulus).

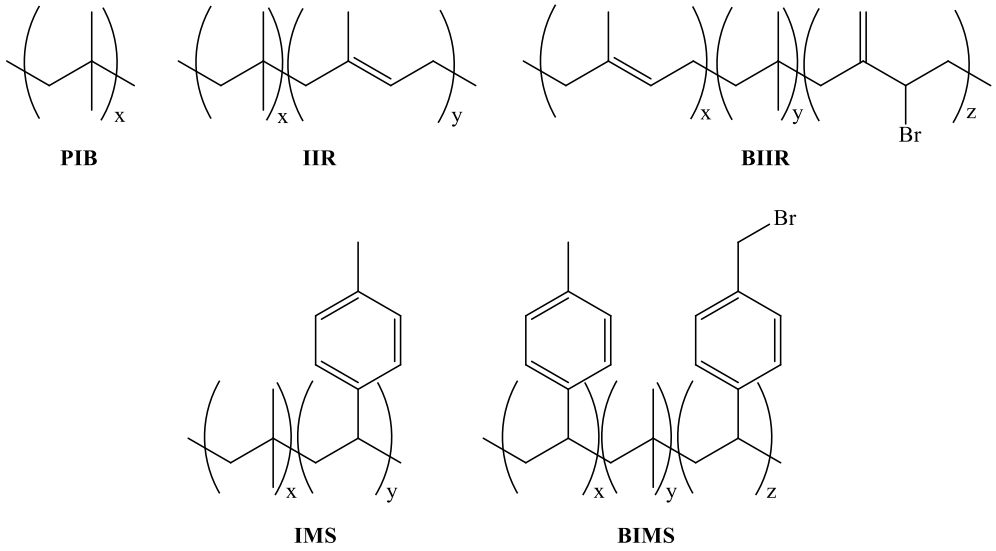

FIGURE 1.1 – Structures of isobutylene-rich elastomers

Unfortunately, PIB reacts poorly towards crosslinking. Un-crosslinked rubber is a viscoelastic material that deforms irreversibly under applied stress rendering the elastomer useless for engineering applications. Vulcanization, alternatively referred to as curing or crosslinking, generates a covalent network among polymer chains (Figure 1.2 on page 2) preventing chain segment relaxation when subjected to sustained loads. Property characteristics like improved modulus, tensile failure and long-term creep resistance allow for the use of this polymer in a wide array of consumer goods.

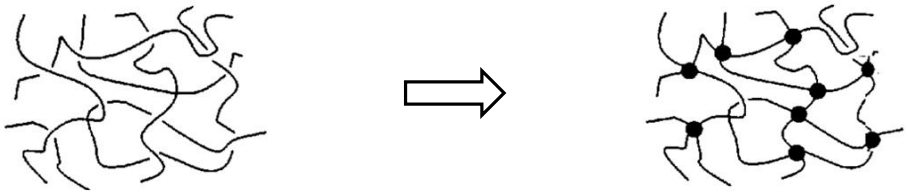

FIGURE 1.2 – A polymer crosslink network[1]

Modulus, or stiffness, is a measure of the stress response of a material to an applied sinusoidal strain and is resolved into two components: the elastic component, an in-phase stress response called the storage modulus (G'), and the viscous component, an out-of-phase stress response called the loss modulus (G'').

The physical properties of viscoelastic materials contain contributions from both the storage and loss moduli quantified by the complex modulus (G*):

$$G' = \sqrt{\left(G'\right)^2 + \left(G''\right)^2} \qquad (1)$$

The loss tangent is the ratio of the loss modulus to the storage modulus:

$$\tan\delta = \frac{G''}{G'} \qquad (2)$$

An ideal elastic solid has a tan δ value of zero, whereas an ideal viscous liquid has a tan δ value approaching infinity.[2]

A rheometer monitors crosslinking reactions. By placing a polymer/curative mixture between two oscillating biconical discs, the rheometer measures the torque required to oscillate the bottom disc relative to the top disc as a function of time at a controlled temperature. To measure the modulus requires a measured torque calibrated to a standard rubber sample.[2] Figure 1.3 on page 3 depicts the three phases of a typical crosslinking curve obtained from a rheometer. The delay phase provides the time for a polymer to flow into a mold before crosslinking occurs, an important industrial consideration. A curing phase follows the delay phase, where formation of a crosslink network occurs. Fast crosslinking reactions are desirable in preventing material degradation at high temperatures. The final phase of crosslink network

formation is dependent on the stability of the crosslinks. The modulus may do the following: reach a stable plateau, increase (marching modulus) because of continued crosslinking, or decrease (reversion) because of crosslink degradation.

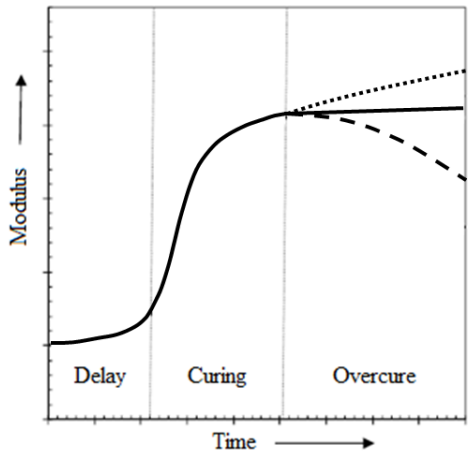

FIGURE 1.3 – A typical crosslinking curve for a rubber mixture[2]

In 1940 Standard Oil Development Company invented poly(isobutylene-*co*-isoprene) (IIR, Figure 1.1 on page 1) thus resolving the complications of cure deficiencies with PIB.[8] IIR, commonly known as butyl rubber, is a random copolymer comprised of 1-2 mole% 2-methylbut-1,3-diene (isoprene) and 98-99 mole% 2-methylprop-1-ene (isobutylene). The isoprene mers are incorporated randomly and predominately by 1,4-addition.[3] It also provides residual unsaturation amenable for chemical modification. For example, vulcanization by sulfur curing formulations adapts butyl rubber for tire inner-tube applications, a principal market for IIR in developing countries. Diene-rich materials, which include poly(butadiene) and poly(isoprene), allow for faster cures as compared to IIR, owing to the larger amount of unsaturation. Hence, these materials are included in tire sidewalls and tread compounds.

It is essential for the inner-liner of tubeless tires to cure at rates equal to other tire component materials, but IIR is not reactive enough for this application.[4] To increase vulcanization rates, IIR was halogenated to yield brominated poly(isobutylene-*co*-isoprene) (BIIR, Scheme 1.1 on page 4) and to provide allylic bromide functionality with a heightened reactivity towards nucleophilic displacement by sulfur. At 85%, the majority of the commercial market for BIIR is

comprised of tire inner-liners, with the balance as pharmaceutical stoppers and other consumer goods.

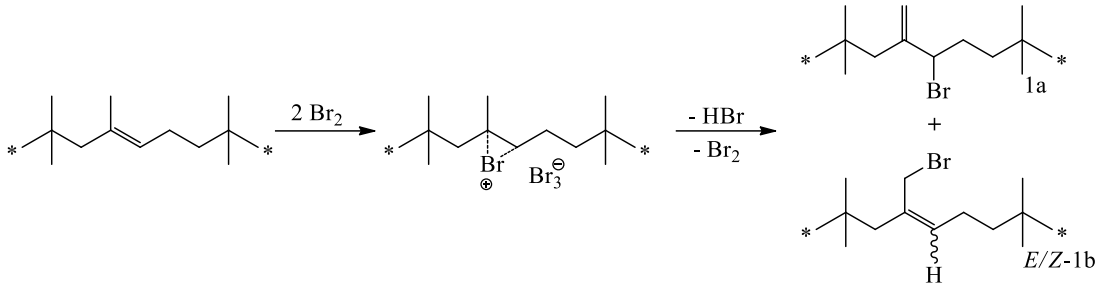

SCHEME 1.1 – Bromination of IIR

In 1989 there was a patent issued for a random copolymer comprising 1-5 mole% 1-methyl-*para*-vinylbenzene (*para*-methylstyrene) and 95-99 mole% isobutylene, also known as poly(isobutylene-*co*-*para*-methylstyrene) (IMS, Figure 1.1 on page 1).[5] The air and moisture permeability of IMS is comparable to IIR, a result of the isobutylene-rich backbone.[6] However, because of the lack of backbone unsaturation it provides improved oxidative and thermal stability. Unfortunately, the incorporation of *para*-methylstyrene has little practical use for any application owing to its inactivity towards conventional cure formulations. To aid in crosslinking reactions, the bromination of the *para*-methylstyrene functionality provides a brominated derivative of poly(isobutylene-*co*-*para*-methylstyrene) (BIMS, Figure 1.1 on page 1) containing a reactive benzylic bromide species. This functionality is reactive towards a number of conventional rubber crosslinking reactions, similar to the allylic bromide species in BIIR, thus offering a usage in various applications similar to BIIR.

1.2 Chemical Modification of BIIR and BIMS

BIIR and BIMS are attractive starting materials for the synthesis of functional isobutylene-rich elastomers owing to the allylic and benzylic halide functionality, respectively, being reactive towards a wide range of nucleophiles. However, the allylic bromide within BIIR is susceptible to undesirable side-reactions including isomerization and hydrogen bromide elimination.[7] Scheme 1.2 on page 5 illustrates well established reactions for

brominated 2,2,4,8,8-tetramethyl-4-nonene (BPMN), a model compound[8] for the allylic bromide groups within BIIR.

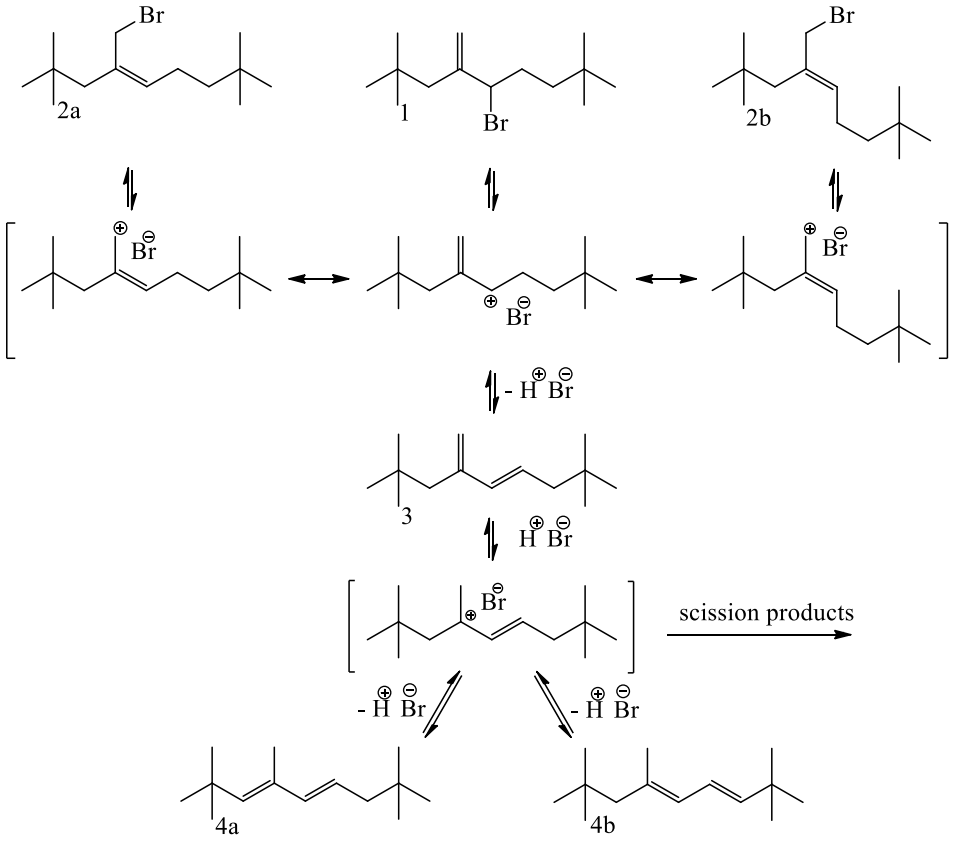

SCHEME 1.2 – Isomerization and elimination reactions of BPMN

At elevated temperatures the kinetically favoured halogenation product, the exomethylene isomer (**1**, Exo-Br), isomerizes to the thermodynamically more stable *E/Z*-endo-bromomethyl isomers (**2a**, **2b**). This rearrangement proceeds through the ionization/ion pair collapse mechanism and, if accompanied by allyl cation deprotonation, provides an exo-conjugated diene (**3**). Acid-catalyzed isomerization of this functionality leads to other conjugated dienes (**4a**, **4b**) and may lead to molecular weight degradation through β-scission of cationic intermediates.

HBr elimination is an undesired side-reaction likely consuming significant amounts of allylic bromide at temperatures above 120°C (Scheme 1.2 above). To avoid acid-catalyzed degradation, small amounts of non-nucleophilic acid scavengers, including epoxides and calcium

stearate, are added to BIIR to sequester HBr released from the polymer. Previous studies suggest BIIR dehydrobromination proceeds by an E1 mechanism involving deprotonation of allyl cation intermediates. In contrast, BIMS is more thermally stable than BIIR and has no reports of dehydrohalogenation.[5,9]

When exposed to tetra-N-alkylammonium bromide (TBAB) salts, the Exo-Br (**1**) functionality within BIIR becomes susceptible to nucleophilic rearrangement.[9] These isomerization reactions are highly selective for the *Z*-endo-bromomethyl (**2a**) isomer, due to the abnormal nucleophilic substitution (S_N2') mechanism. The S_N2' mechanism was postulated for a number of sterically hindered allylic halides similar to BIIR where bulky substituents direct the nucleophile to attack the allylic double bond with subsequent isomerization of the double bond and loss of the halide anion.[10] In cases where the nucleophilic species have a non-coordinating anion, observations indicated the reaction proceeded through an anti-configuration of nucleophiles and leaving groups in the transition state.[11]

In Scheme 1.3 on page 7, the diagram demonstrates two configurations for butyl rubber undergoing an S_N2' reaction by way of an anti-configuration of nucleophiles and leaving groups. The reaction proceeds either through one of two isomers (or their mirror images), the pro-(*Z*) conformer to produce the *Z*-endo-bromomethyl isomer (**2a**) or the pro-(*E*) conformer to produce the *E*-endo-bromomethyl isomer (**2b**). Computational studies of torsional energy profiles for the pro-(*E*) and pro-(*Z*) conformers indicate non-bonding interactions between R1 and R2 with the pro-(*E*) conformer making it less stable compared to the pro-(*Z*) conformer.[12] Selectivity for the Z-endo-bromomethyl isomer ((*Z*)-**1b**) is a consequence of the stability of the pro-(*Z*) conformer and the preference for the reaction to proceed through this lower energy transition state.

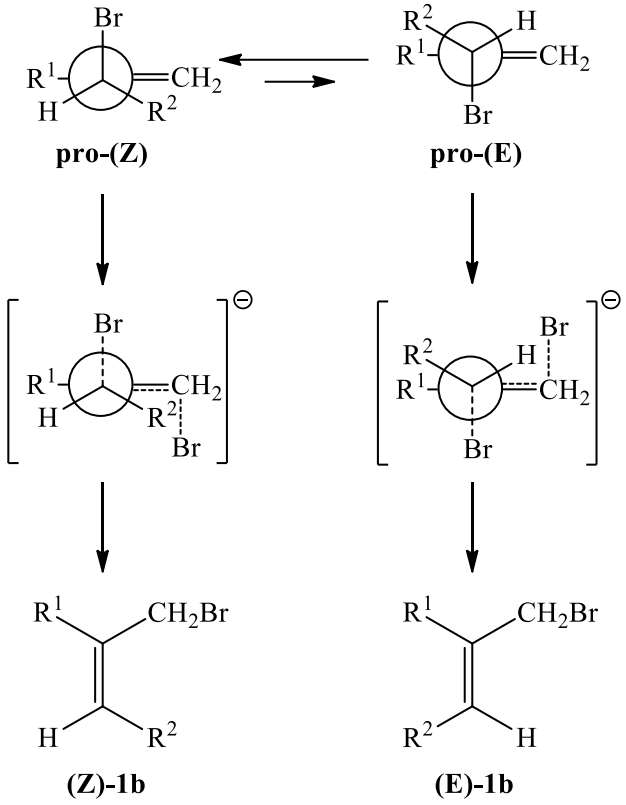

SCHEME 1.3 – An S_N2' rearrangement of Exo-Br functionality in BPMN[13]

Scheme 1.4 on page 8 illustrates the versatility of the allylic bromide functionality in BIIR to produce sulfide, ether, ester, thio-ether and amine derivatives via halide displacement. Sulfide (S_X) crosslinked derivatives of BIIR are industrially important reaction products found in the inner-liner of vehicle tires. The reaction of brominated pentamethylnonene (BPMN) with sulfur yields dimers containing either a single sulfur atom (monosulfide), two sulfur atoms (disulfide) or more than two sulfur atoms (polysulfide).[13] Sulfur-cured rubber articles contain weak sulfur-sulfur bonds that under stress may break and reform, consequently providing good dynamic properties. Unfortunately, in order to achieve fast curing rates and to prevent excessive degradation of polysulfide bonds, sulfur-cured articles require a multitude of toxic compounds in the rubber article that eventually leach over time.

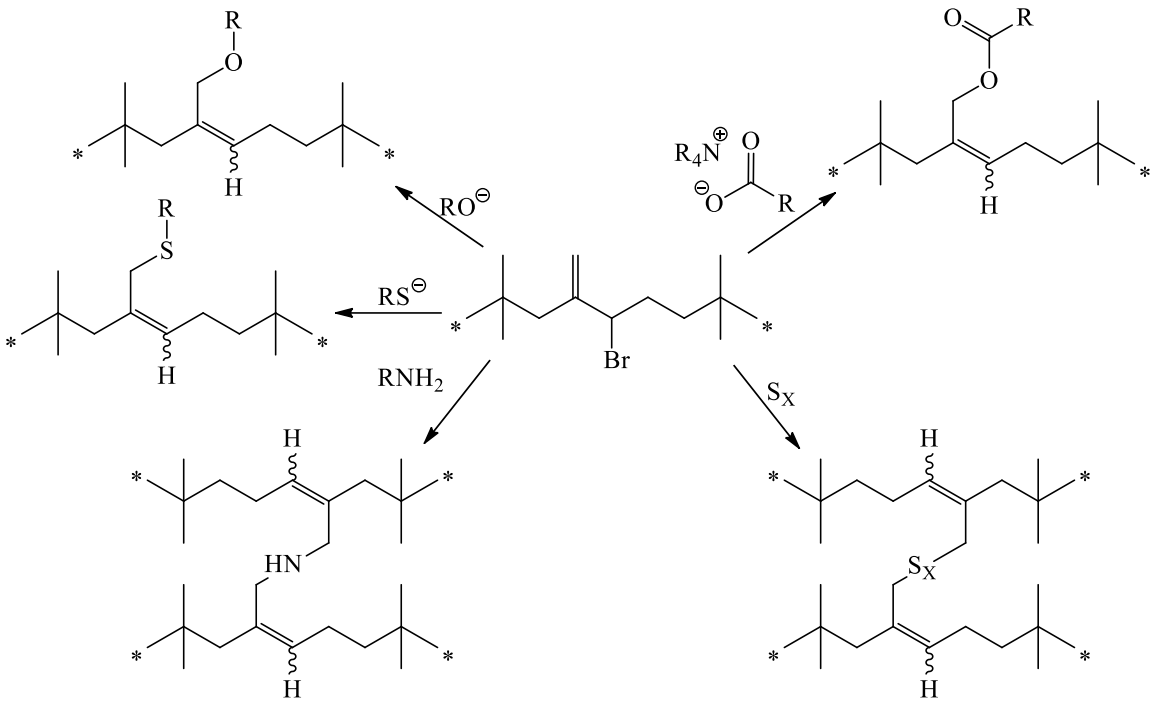

SCHEME 1.4 – Derivatization of the allylic bromide functionality in BIIR at elevated temperatures

BIIR and BIMS have the capability to undergo nucleophilic substitution by oxygen nucleophiles. For example, using the Williamson ether-synthesis method results in poly(ethylene oxide) and polybutadiene grafted BIIR.[14] Another method involves tetra-N-butylammonium carboxylate salts in a nucleophilic substitution reaction of BIIR and BIMS to synthesize, for example, polyisoprene and polystyrene grafted-copolymers of BIMS.[9,16] Grafted polybutadiene and polyisoprene modifies the polymer properties allowing the functional derivatives to crosslink through a wider range of crosslinking chemistry.

Thioether derivatives of BIIR bearing trialkoxysilane functionality are achievable using bromide displacement by thiolate nucleophiles.[15] This trialkoxysilane functionality develops a covalent bond between the polymer and filler by reacting with silanol groups on the surface of precipitated silica. This coupling reaction requires high surface energy fillers and may include silica and clay components typically difficult to disperse in non-polar isobutylene-based elastomers. The nucleophilic substitution of BIIR by mercaptopropyltrimethoxysilane provides the necessary compatibilization when mixing silica with the elastomer. This type of mixture yields a

well-dispersed filler compound with mechanical properties far superior to standard BIIR vulcanizates.

Nucleophilic substitution of BIIR and BIMS by primary, secondary and tertiary amines produces various products.[14] Primary amines undergo multiple N-alkylations generating crosslinked thermoset derivatives. Secondary amines undergo N-alkylation in low overall yields resulting from the reversibility of the reaction, producing polymer-bound tertiary amines. Tertiary amines undergo N-alkylations generating a polymer-bound quaternary ammonium bromide salt. These ion-containing polymers, or ionomers, have similar dynamic rheological properties as sulfur-cured rubber articles.

1.3 Ionomers

Ionomers are polymers containing less than 15 mole% of ionic functionality distributed uniformly along the polymer backbone, which solvate poorly in a non-polar matrix resulting in extensive ion pair aggregation and the formation of multiplets. Multiplets contain a small number (2-8) of ion pairs, however if the ionic content of the material is sufficient the multiplets may aggregate further to form clusters. The volume surrounding a multiplet restricts polymer chain mobility, illustrated in Figure 1.4 below, resulting in an extended rubbery plateau and occasionally the broadening of the glass-transition temperature or the appearance of a second glass-transition temperature.[16]

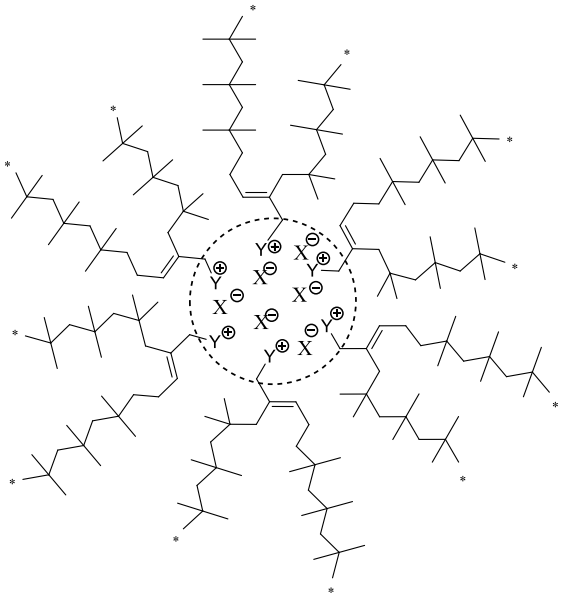

FIGURE 1.4 – Illustration of ion pair aggregation

The term “ionomer” first appeared in literature in 1965, defined as an olefin-based polymer containing ionic groups in relatively small amounts.[17] Prior to this, scientists did not recognize ionic crosslinks but did observe the incorporated ionic groups in elastomers as exerting a major influence on its properties. In the 1950’s, Goodrich Petroleum Corporation introduced a butadiene-acrylonitrile-acrylic acid terpolymer elastomer based on ionic interactions able to be neutralized with the oxide or salt of a polyvalent metal.[18] At the same time, the American chemical company DuPont introduced elastomers exhibiting a combination of ionic and covalent crosslinks. These sulphonated-based materials, produced from chlorinated polyethylene, had the ability to cure with various metal oxides.[19]

In 1965, two journals carried first-time articles on the subject of ionomers. The first, Modern Plastics[20], discussed the processibility of an ethylene-based plastic, while the second[17] introduced the term “ionomer”. In the mid-1960’s, DuPont introduced Surlyn® an ethylene-methacrylic acid copolymer partially neutralized with sodium or zinc (hydr)oxides. This modified polyethylene brought remarkable clarity and unique tensile properties to its products.[21,22]

In 1970, Eisenberg undertook the first comprehensive theoretical attempt to develop a meaningful understanding of salt group arrangements in ionomers. Eisenberg and MacKnight, among others, postulated various structures for ionic crosslinks and the resultant morphology, among which was the core-shell model of ionomers. In 1973, Marx et al, Binsbergen and Kroon introduced two additional models of ionomer morphology. In 1990, Eisenberg proposed a new multiplet-cluster model for the morphology of random ionomers.

The definition of multiplets are quadruplets, sextuplets and higher aggregates of ion pairs. Clusters, ion-rich regions, exist as a separate phase exhibiting a distinct glass-transition temperature. Governing the formation of multiplets in ionomers is the nature of the polymer, the ionic species and the strength of ion pair electrostatic interactions. Determining the interaction between ion pairs is the size of the ions and partial covalent character of the ionic bond. Determining the strength of ion pairs is by its electrostatic interactions, which if too weak to overcome the elastic forces of a polymer chain restricts the formation of multiplets.

Ion content determines the proximity of ion pairs, thus influencing multiplet formation. Ion pairs tend to not aggregate if sparse in number and if distanced sufficiently apart as to not

experience a significant electrostatic attraction. Polymers with a low dielectric constant and low glass-transition temperature favour ionic aggregation. Polymers with a high dielectric constant and/or high glass-transition temperature inhibit multiplet formation.

Steric factors limit the size of aggregates when ionic aggregation is energetically favorable, resulting in relatively small and rigid multiplets. However, less steric hindrance towards aggregation results in larger multiplets, an example being when ions situate at the ends of long flexible side-chains. Ion pairs within a multiplet anchor the polymer chain. At this point of attachment, the firmness of anchorage determines the extent of mobility restriction. Reduction in mobility occurs for neighboring non-anchored chains in the immediate vicinity of the multiplet surface. The flexibility of the polymer backbone determines the extent of the chain's restrictions in mobility surrounding each multiplet.

1.4 Ionomer Derivatives of Isobutylene-Rich Elastomers

Tensile properties of a non-polar elastomer can approach those of a covalently crosslinked rubber through the introduction of ion pairs. Ion-dipole interactions improve adhesion to high-energy surfaces (metals, glass and polar polymers) and disperse siliceous fillers during conventional rubber compounding operations. Interest exists in ionomers bearing organic cations, like phosphonium and ammonium functionality, owing to their anti-microbial activities. Since the ionic functionality is polymer bound it is possible to realize anti-microbial activity without any potential leaching problems typically associated with ionic liquid additives or metal nanoparticle technology.[23]

Initially prepared by Kennedy et al., isobutylene-based ionomers containing sulfonate functionality at both ends of the chain displayed an extended rubbery plateau with a tensile strength approaching covalently crosslinked vulcanizates, despite their low molecular weight.[24] However, the polymer network established by sulfonate group aggregation is labile resulting in excessive stress relaxation and permanent set when exposing the material to a static load, commonplace for all elastomeric ionomers. The lability of ionic bonds necessitates crosslinking in order to establish suitable physical properties required in any engineering application.

Parent et al. prepared numerous ionomer derivatives of BIIR through solvent-free alkylation of triphenylphosphine (PPh_3), tertiary amines (NR_3) and azoles (Figure 1.5 on page 12).

An example includes 1-butylimidazole (BuIm) by introducing allylic "onium" bromide functionality pendant to the polymer backbone. This method is similar to ionic liquid preparation[25], however the conditions required to produce the ionomers differ substantially from those used in small molecule systems.[26]

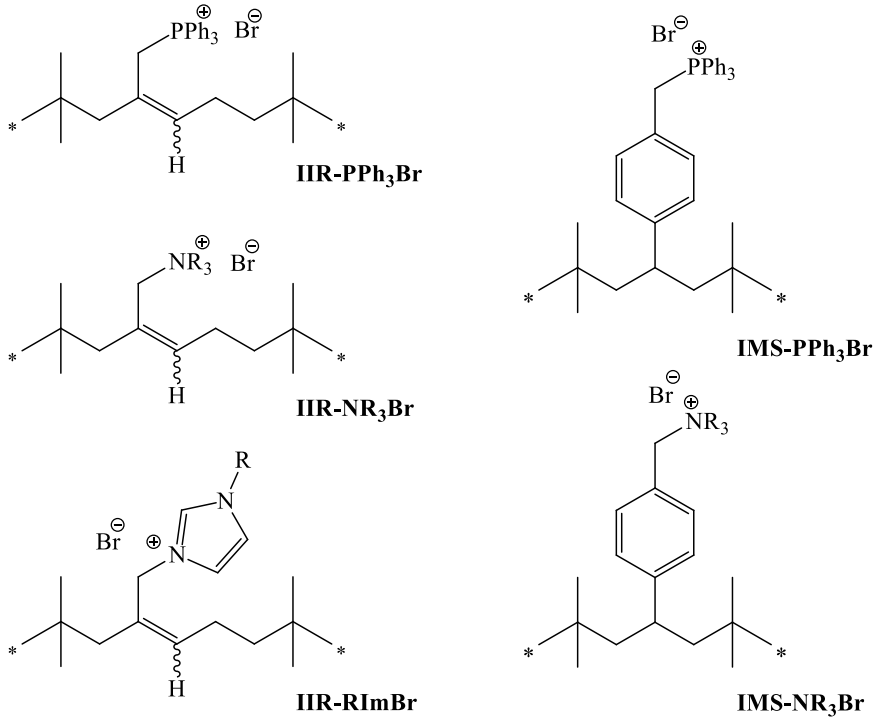

FIGURE 1.5 – Ionomer derivatives of BIIR and BIMS

The most extensively studied ionomer derivate is IIR-PPh_3Br (Figure 1.5 above) owing to its ease of preparation and thermal stability. Material preparation uses conventional polymer processing equipment under solvent-free conditions, whereas preparing its BIMS analogue (IMS-PPh_3Br) occurs in a tetrahydrofuran solution.[10] These isobutylene-based ionomers provide all of the aforementioned cationic ionomer properties and can undergo anion metathesis to alter its properties.[27]

Significant commercial interest also exists in mixing isobutylene-rich elastomers with reinforcing fillers. Difficulties persist in dispersing standard precipitated silicas within IIR, BIIR, IMS or BIMS. However, when using conventional mixing processes the corresponding phosphonium-bromide ionomer derivatives provide the necessary polymer-filler interactions essential for the dispersion of these materials.[10] Unfortunately, sulfur vulcanization rates for

IIR-PPh_3Br are slow based on the lack of residual allylic bromide functionality. An ionomer is capable of curing efficiently thus providing desirable dynamic and filler-dispersion properties, while not being susceptible to creep and stress relaxation.

Commercially available amines with their wide variety of functionalities led to an extensive study of tetraalkylammonium bromide ionomers, IIR-NR_3Br and IMS-NR_3Br (Figure 1.5 on page 12).[28] Unfortunately, N-alkylation of tertiary amines by BIIR is thermally reversible, attributed to the reverse Menschutkin reaction (Scheme 1.5 below)[29] in which the bromide displaces the amine from the ionomer. This requires a large excess of amine to push the allylic halide conversion to completion. In contrast, phosphonium and imidazolium halide derivatives of BIIR are relatively stable at temperatures commonly encountered by the elastomeric materials.[30]

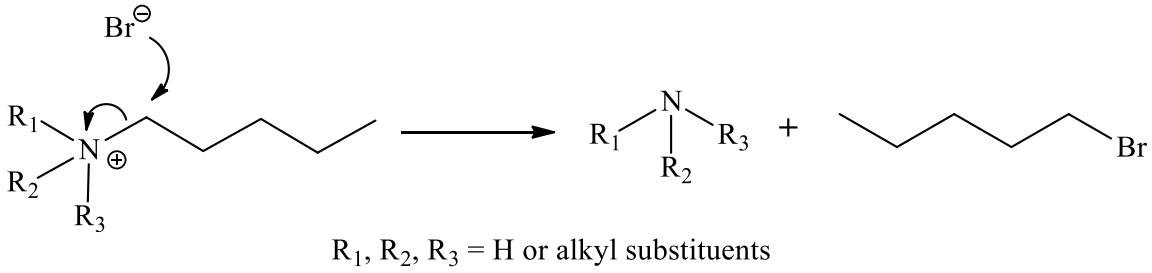

SCHEME 1.5 – A reverse Menschutkin reaction for a tetra-N-alkylammonium bromide

The wide variety of commercially available functional imidazoles makes attractive nucleophiles to functionalize BIIR and BIMS. Producing an isobutylene-based butylimidazolium bromide ionomer, IIR-BuImBr (Scheme 1.6 on page 14), is possible via N-alkylation of 1-butylimidazole by BIIR under both solvent-free conditions and in a toluene solution.[31] N-alkylation is the rate limiting-step as opposed to isomerization of the exomethylene allylic bromide to a more reactive isomer. Solvent-free reactions of N-butylimidazole containing both isomerized and "as-received" BIIR maintain similar reaction rates.[32]

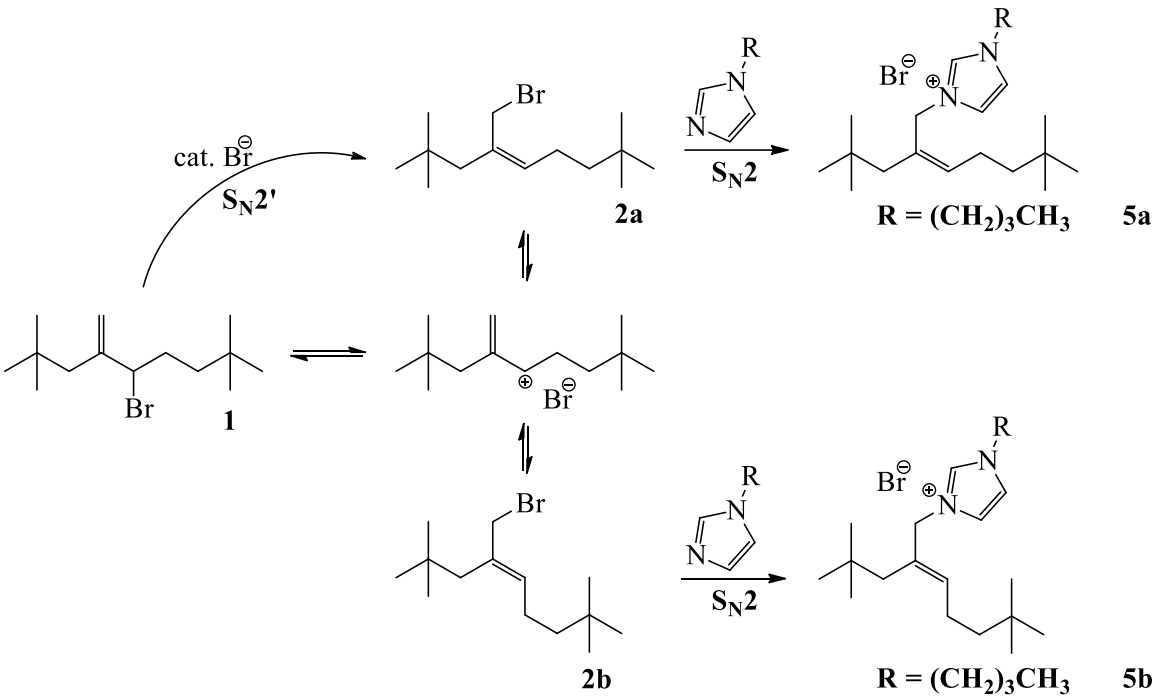

SCHEME 1.6 – Synthesis of an N-butylimidazolium bromide ionomer derivative of BIIR[31]

Reactions of BPMN with BuIm yielded 1-*N*-butyl-3-[(2*E,Z*)-6,6-dimethyl-2-neopentylhept-2-enyl] imidazolium bromide as a mixture of *E,Z*-isomers (**5a**, **5b**), with no exomethylene isomer analogous to **1** found among the reaction products. This is consistent with BIIR-derived products showing only evidence of *E,Z*-IIR-BuImBr functionality analogous to 1-*N*-butyl-3-[(2*E,Z*)-6,6-dimethyl-2-neopentylhept-2-enyl] imidazolium bromide. Based on this mechanism, the observed preference for the *Z* isomer over the *E* isomer is a result of the selective rearrangement of Exo-Br functionality within the BIIR starting material. IIR-BuImBr is comprised of a random distribution of imidazolium ion pairs whose concentration is limited to the 0.15 mmol of allylic bromide per gram of BIIR starting material.

Due to the versatile functionality and thermal stability of imidazolium halides, they have received considerable attention in the ionic liquid field. Unlike IIR-NR_3Br, IIR-BuImBr is stable to about 200°C without undergoing a reverse-Menschutkin reaction.[23,33] There is no nucleophile exchange observed after 2 hours of heating a toluene solution of IIR-BuImBr and tetra-N-butylammonium acetate. This robustness makes IIR-BuImBr suitable for processing at temperatures typically used for rubber compounding and crosslinking.

The action of crosslinking the imidazolium ionomer prevents creep and stress relaxation. However, the conversion of allylic or benzylic bromide to polymer-bound ion pairs consumes the reactive functionality needed for efficient sulfur vulcanization. Though isobutylene-rich ionomers bear functionality that engage in free radical crosslinking, peroxide-initiated curing becomes an attractive alternative.

1.5 Peroxide Curing Derivatives of Isobutylene-Based Elastomers

The rubber industry uses two main classes of crosslinking chemistry, sulfur-based and peroxide-based cure formulations.[33] Sulfur-based formulations provide superior dynamic properties like flex fatigue owing to the labile nature of their polysulfide crosslinks. However, sulfur-articles may compress irreversibly when subjected to sustained loading. Peroxide-based formulations provide high crosslink stability based on the strength of carbon-carbon bonds generated, and are thus less susceptible to compression set and stress relaxation.[34] Sulfur-based formulations typically contain amine bases and salts that may be harmful to health. Hence, if curative leaching is important peroxide formulations become desirable since the cure by-products result in simple ketones and alcohols.

INITIATION	ROOR	⟶	2RO•
HYDROGEN ABSTRACTION	RO• + PH	⟶	ROH + P•
TERMINATION			
Combination	2P•	⟶	P-P
Disproportionation	2P•	⟶	PH + P

SCHEME 1.7 – A simplified mechanism for peroxide-only crosslink formulations[33]

Scheme 1.7 above illustrates a stoichiometric free radical crosslinking process initiated by an organic-peroxide (ROOR). Thermolysis of the weak oxygen-oxygen bond yields reactive alkoxy radical intermediates by way of a relatively slow first-order decomposition process. The criterion for choosing initiators is their half-life at a desired curing temperature, since the rate of the

peroxide breakdown depends strongly on temperature. Dicumyl peroxide, commonly used as an initiator for rubber crosslinking has a half-life of approximately 5 minutes at 160°C.[35]

Polymer crosslinking involves the production of macroradicals through hydrogen atom abstraction from the polymer backbone using initiator-derived alkoxy radicals (Scheme 1.7 on page 15). Radical termination is extremely rapid with combination generating a crosslink and disproportionation having no immediate effect on the polymer's molecular weight. This hydrogen abstraction plus radical termination process is not auto-catalytic. Hence, the number of crosslinks cannot exceed the amount of initiator used in the formulation. In practice, these stoichiometric cures achieve less than quantitative yields given the effects of radical disproportionation as well as inefficiencies in producing macroradicals by hydrogen atom transfer.[36]

Peroxide cures are effective for most saturated elastomers such as hydrogenated nitrile-butadiene rubber and ethylene-propylene copolymers. However, due to the β-scission of polymer macroradicals (Scheme 1.8 below) peroxides do not cure isobutylene-rich elastomers.[37] Polyisobutylene degrades when treated with peroxides at conventional cure temperatures, since this unimolecular fragmentation lowers the material's molecular weight more than the radical combination increases the molecular weight. The 1-2 mole% of unsaturation within IIR lessens the extent of polymer degradation but does not support a free radical cure. Therefore, curing commercial grades of IIR occurs only by sulfur-based formulations.[38]

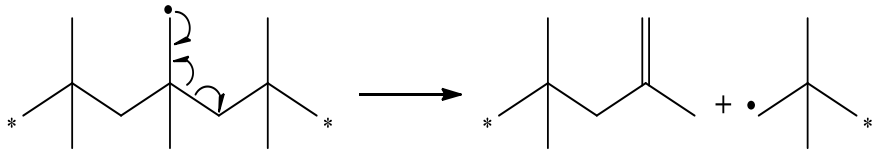

SCHEME 1.8 – A β-scission of primary polyisobutylene macroradicals

1.6 Macromonomer Derivatives of Isobutylene-Based Elastomers and Imidazole

Oxley and Wilson synthesized the first peroxide-curable isobutylene-rich elastomer by the co-polymerization of isobutylene, isoprene and divinylbenzene (Figure 1.6 on page 17).[41] When heated in the presence of peroxides the reactive unsaturation provided by the divinylbenzene monomer undergoes crosslinking rather than degradation. These types of materials known as

macromonomers do not cure by H-atom abstraction plus radical combination, but rather through the free radical oligomerization of pendant vinyl functionality. Since formation of polymer backbone macroradicals are avoidable in these cure systems, isobutylene-rich macromonomers crosslink to a high extent using relatively small amounts of peroxide. Unfortunately, the gel content of these materials can reach 85% since cationic polymerization of isobutylene with divinylbenzene produces a polymer already significantly crosslinked. This makes the material difficult to mix and process with other compound ingredients.

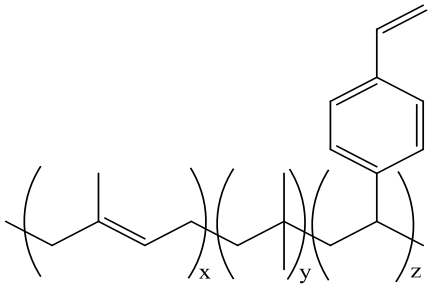

FIGURE 1.6 – Structure of an isobutylene, isoprene and divinylbenzene terpolymer

To produce gel-free macromonomers requires the exploitation of the allylic and benzylic bromide functionalities in BIIR and BIMS, respectively. A study introduced pendant acrylate functionality through nucleophilic substitution of both polymers.[39,40] Using tetra-N-butylammonium (TBA) acrylate successfully produced the desired macromonomer derivatives of BIIR shown in Scheme 1.9 on page 18. These materials are highly reactive and crosslink at high temperatures even in the absence of a radical initiator.[34] Additionally, the propensity of these macromonomers to oligomerize at room temperature makes storage stability challenging.

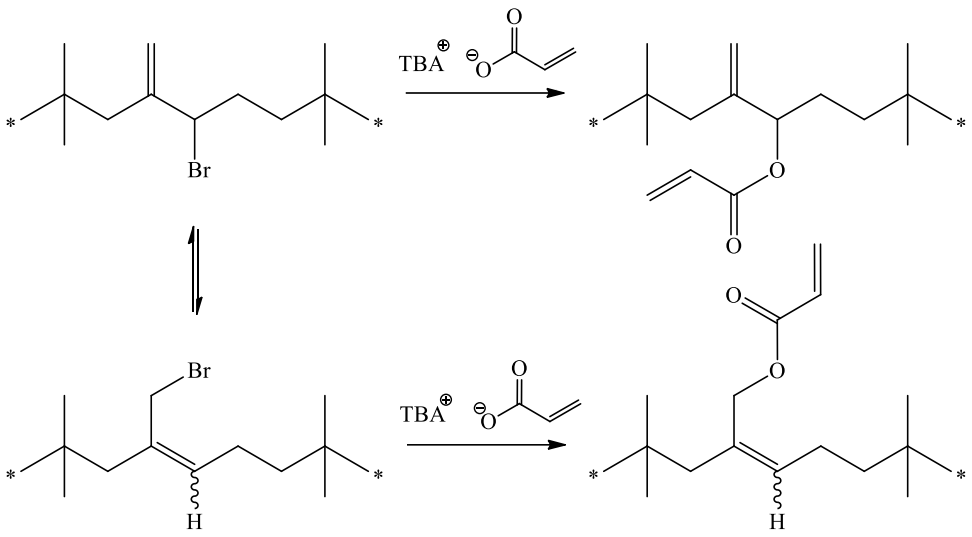

SCHEME 1.9 – The synthesis of acrylate derivatives of BIIR

Production of ionic liquids through the nucleophilic substitution of alkyl halides is analogous to nucleophilic substitution of BIIR and BIMS in forming ionomers. Worth noting nucleophiles include tertiary amines and triphenylphosphine, but ammonium bromide salts of BIIR and BIMS have stability problems in establishing equilibrium with the starting materials. Phosphonium bromide salts lack reactive functionality for subsequent crosslinking reactions and hence have stress relaxation problems. The ring-structure of azoles and azines allow incorporating functional groups capable of crosslinking the polymer and preventing stress relaxation. A comparison of the N-methylation of 1-methylimidazole, pyridine, oxazole and thiazole with methyl iodide, results in imidazoles having the fastest substitution rates among these heterocycles.[41]

It is necessary to consider the thermal stability of the previously discussed ammonium, phosphonium and imidazolium cations, since rubber mixing and compounding temperatures have the capability of reaching in excess of 100°C. Phosphonium halide derivatives of BIIR appear stable at elevated temperatures, unlike ammonium halides that undergo a reverse Menschutkin reaction.[29] Thermal stability studies, by thermogravimetric analysis (TGA) of imidazolium-based ionic liquids, indicated the onset of decomposition at between 280-300°C.[42] Isothermal TGA data on imidazolium bromide ionic liquids has shown a 1% weight loss occurring at 180°C after 10 hours.[43] Over 220°C the imidazolium halide ionic liquids undergo a reverse Menschutkin reaction where the halide anion acting as a nucleophile displaces the imidazolium group

producing an alkylimidazole and alkyl halide.[44] However, this should not occur for imidazolium bromide derivatives of BIIR and BIMS since rubber compounding processes and crosslinking reactions occur at temperatures below 200°C.

Vinylazoles and vinylazines produce peroxide-curable ionomer derivatives of BIIR and BIMS.[41] Fast N-alkylation rates reduce reaction times and prevent undesired gel formation during nucleophilic substitution. N-vinylimidazole provides one nitrogen atom for nucleophilic substitution reactions and a vinyl group unsaturation for crosslinking reactions with peroxide. Polymerization of N-vinylimidazolium halides is sufficiently slow, however this may impart storage stability not previously observed in macromonomer derivatives of BIIR or BIMS.[45,46]

1.7 Anti-microbial Polymer Technology

Infectious diseases kill more people worldwide than any other single cause and hence give great concern to many fields. In particular, medical devices, drugs, hospital work surfaces, surgery equipment, health care products, water purification systems, textiles, food packaging, appliances, aeronautics, and many more. Antimicrobial agents predominantly combat infection typically spread or transmitted through touching, eating, drinking and breathing. However, this method becomes problematic when microorganisms prove resistant, through rapid gene mutations, making neutralization or elimination virtually impossible.

Over the past decades, there has been a continuous effort to develop antibacterial polymers with the goal of replacing polymers impregnated with antibacterial agents. These agents are often low molecular weight compounds such as antibiotics, phenols, iodine, quaternary ammonium compounds or heavy metals such as silver, tin and mercury.[47]

Antibacterial additives are attractive but have limited or short-lived viable protection against infection owing to the difficulties in controlling the rate of diffusion of the antibacterial additive out of the polymer matrix. This leaching eventually renders the material ineffective, possesses a potential environmental risk and lends itself to the possible reaction of the leached material with other organic substances. As well, compounds released into the environment could lead to increased drug resistance throughout the microbial realm. Additionally, organic antibacterial agents have limited incorporability into polymeric compounds because organic

antibacterial agents typically have a vaporization point less than the temperatures involved during the formation of the polymer compositions.[47]

In comparison, polymeric compounds containing permanently bound antibacterial agents show better durability with or without low liberation of toxic products in the environment, thus reducing the losses associated with volatilization, photolytic decomposition, and transportation.[47] Additionally, they show increased efficiency, selectivity and handling safety. There are many strategies in designing synthetic antimicrobial polymers having a diverse manner of action over microorganisms. Their activity may be inherent in their original structure, due to chemical modification, or by the introduction of organic or inorganic antimicrobial agents to confer the resultant biocidal behavior. Most research has focused on polycationic systems because of their straightforwardness and synthetic flexibility.

Most antimicrobial polymers are positively charged since most bacterial cell walls are negatively charged, having a composition of 70% phosphatidylethanolamine. Hence, quaternary ammonium groups are the most explored polymeric biocide. The antibacterial activity of cationic species begins with its adsorption onto the bacterial cell surface, followed by diffusion through the cell wall to eventually bind to and disrupt the cytoplasmic membrane. Bridge formations, between adjacent phosphates of the membrane lipids, cause the release of cytoplasmic constituents such as potassium, DNA and RNA, which ultimately leads to the death of the cell.[48]

The biological activity of quaternary ammonium compounds depends on the nature of the organic groups attached to nitrogen, the number of nitrogen atoms present and the counterion.[49] Four organic substituents bond to nitrogen, which are either similar or different in their chemistry and structure and can be alkyl, aryl, or heterocyclic. At least one of the substituents should be a long alkyl chain to provide a hydrophobic segment compatible with the bilayer of the outer cell wall.[50] An increase in the alkyl chain length of an amphiphilic compound increases the hydrophobic interaction with the lipid bilayer of the cell wall, which in turn increases the antimicrobial activity of the compound. Quaternary ammonium compounds containing one long alkyl chain substituent of at least eight carbon atoms are very active biocides in water.[51] However, a drawback of permanent quaternary ammonium compound coatings is they generate a fouling surface, which can cause a negative immune response and chronic inflammation.

The imidazole ring is ubiquitous in nature. The imidazole functionality plays a critical role in many structures within the human body, notably in histamine and histadine, as well as biotin and imidazole alkaloids.[52] Imidazoles offer many biophysical interactions including the ability to hydrogen bond with proteins. In contrast, imidazolium salts lose their strong hydrogen-bonding ability through the alkylation of both nitrogens, but do aggregate electrostatically. Imidazolium salts have the ability to extract metal ions from aqueous solutions, dissolve carbohydrates, create polyelectrolyte brushes on a surface, coat metal nanoparticles, provide antimicrobial action and create oriented liquid crystals. Bioactive applications include imidazolium hydrogels, antiarrhythmics, and anti-metastic agents. Imidazole-based polymers readily associate with biological molecules through hydrogen bonding while imidazolium analogs offer electrostatic interactions, aggregation and self-assembly.[53]

Polysiloxanes bearing quaternary ammonium salt groups are highly flexible and increase the ease of contact of the quaternary groups with the microorganism.[47] Their amphiphilic character, with the hydrophilic inorganic part and the hydrophobic organic groups, augments the concentration of the quaternary groups near the microorganism cell wall.

Antimicrobial peptides, also known as host defense peptides, are an innate immune response produced by all living organisms. These peptides show effective antimicrobial activity against bacteria, viruses and fungi. They are usually positively charged and have both hydrophobic and hydrophilic sides, enabling the molecule to be soluble in aqueous environments while also passing through lipid-rich membranes.[47] Once in a target microbial membrane, the peptide kills cells through diverse mechanisms.

Fluorine-containing polymers are particularly attractive due to their water and oil repellency resulting from the low polarizability and strong electronegativity of the fluorine atom; high chemical, thermal, aging and weather resistance; low dielectric constant; and extremely low surface energy. The antimicrobial activity of the fluorine-containing polymers is associated with their surface activity and high hydrophophic character.[47]

N-halamines, compounds containing one or more nitrogen–halogen covalent bonds, provide a fast and total-kill against a wide-range of microorganisms without causing environmental concerns and the likelihood of establishing resistance by the microorganisms.[47]

Phenols, biocidal agents acting in the bacteria membrane, interact with the cell's surface causing its death through the disintegration of the cell membrane and release of intracellular constituents. Phenols also cause intracellular coagulation of cytoplasmic constituents, which can lead to cell death or inhibition of cell growth.[47]

Specific examples of antibacterial butyl polymers, as related to the work herein, include a resin-cured butyl rubber article incorporated with silver ions, US Patent 6,846,871 B2. The US Patent 6,238,575 demonstrates that the addition of Microban Additive B in a butyl diaphragm provides resistance to both gram-positive and gram-negative bacteria. US Patent 6420622 relates to a pressure sensitive butyl adhesive containing the antibacterial additive neomycin.

1.8 Research Objectives

A longstanding collaboration between the Parent Group and the Butyl Rubber Division of LANXESS Inc. has generated an improved understanding of BIIR chemistry, particularly with respect to the synthesis and properties of chemical derivatives. The research described in this thesis has several objectives related to the area of polymer chemistry.

- **a.** Synthesize and study the physical material properties of novel ionomeric elastomers bearing different imidazolium functionalities that are capable of peroxide-initiated crosslinking to provide hybrid ionic/covalent networked materials.
- **b.** Determine the antimicrobial properties of ionomeric elastomers.
- **c.** Characterize the cure reactivity of macromonomer derivatives of BIIR and BIMS that bear methacrylate, cinammate, crotonate and undecenoate functional groups, and compare each to the same material with additional imidazolium functionality.
- **d.** Develop a stable oil-in-water emulsion of an ionomeric elastomer with the use of a polymerizable imidazolium surfactant and study the physical properties of the final film/latex.
- **e.** Prepare a mixed alkylation BIMS product via a solvent-free compounding technique, and determine its ability to disperse conventional rubber fillers including carbon black and precipitated silica.
- **f.** Prepare a BIMS-clay nanocomposite with a polymerizable imidazolium surfactant and study its material properties.

REFERENCES

1. Coran, A.Y., Vulcanization, from *Science and Technology of Rubber*, 3rd Edition, 321 – 364, Mark, J.E., Erman, B., Eirich, F.R., Elsevier Academic Press, Boston (2005).

2. Brown, R., Dynamic Stress and Strain Properties, *Physical Testing of Rubber*, Springer, New York, USA, 2006, 173 – 180

3. Chu, C.Y., Vukov, R., Determination of the Structure of Butyl Rubber by NMR Spectroscopy, *Macromolecules*, **18**, 1423 – 1430 (1985).

4. Morrissey, R.T., Butyl Type Polymers Containing Bromine, *Industrial Engineering and Chemistry*, **47**, 1562 – 1569 (1955).

5. Powers, W.K., Wang, H.-C, Eur. Pat. 89305395.9 (1989).

6. Webb, R.N., Shaffer, T.D., Tsou, A.H., Butyl Rubber, Kirk Othmer Encyclopedia of Chemical Technology, DOI: 10. 1002/0471238961.0221202511180519.a01.pub2 (2003).

7. Parent, J.S., Thom, D.J., White, G., Whitney, R.A., Hopkins, W., Thermal Stability Studies of Brominated Poly(isobutylene-*co*-isoprene), *Journal of Polymer Science: Part A: Polymer Chemistry*, **39**, 2019 – 2026 (2001).

8. Nieuwenhuizen, P.J., Haasnoot, J.G., Reedjik, J., Model-compound Vulcanization – An Established Technique for the Next Century, *Raw Materials and Applications*, **53**, 144 – 152 (2000).

9. Parent, J.S., Malmberg, S., McLean, J.K., Whitney, R.A., Nucleophilic Catalysis of Halide Displacement from Brominated Poly(isobutylene-*co*-isoprene), *European Polymer Journal*, **46**, 702 – 708 (2010).

10. Magid, R.M., Nucleophilic and Organometallic Displacement Reactions of Allylic Compounds: Stereo- and Regiochemistry, *Tetrahedron*, **36**, 1901 – 1930 (1980). (b) Paquette, L.A., Stirling, C.J.M., The Intramolecular SN' Reaction, *Tetrahedron*, **48**, 7383 – 7423 (1992).

11. Streitwieser, A., Jayasree, E.G., Hasanayn, F., Leung, S.S.-H., A Theoretical Study of S_N2' Reactions of Allylic Halides: Role of Ion Pairs, *Journal of Organic Chemistry*, **73**, 9426 – 9434 (2008).

12. Malmberg, S., Parent, J.S., Pratt, D.A., Whitney, R.A., Isomerization and Elimination Reactions of Brominated Poly(isobutylene-*co*-isoprene), *Macromolecules*, **43**, 8456 – 8461 (2010).

13. Parent, J.S., White, G.D.F., Thom, D.J., Whitney, R.A., Hopkins, W., Sulfuration and Reversion Reactions of Brominated Poly(isobutylene-*co*-isoprene), *Journal of Polymer Science: Part A: Polymer Chemistry*, **41**, 1915 – 1926 (2003).

14. Guillen-Castellanos, S.A., Parent, J.S., Whitney, R.A., Synthesis and Characterization of Ether Derivatives of Brominated Poly(isobutylene-*co*-isoprene), *Journal of Polymer Science: Part A: Polymer Chemistry*, **44**, 983 – 992 (2006).

15. Parent, J.S., White, G.D.F., Whitney, R.A., Synthesis of Thioether Derivatives of Brominated Poly(isobutylene-*co*-isoprene): Direct Coupling Chemistry for Silica Reinforcement, *Journal of Polymer Science: Part A: Polymer Chemistry*, **40**, 2937 – 2944 (2002).

16. Eisenberg, A., Hird, B., Moore, R.B., A New Multiplet-Cluster Model for the Morphology of Random Ionomers, *Macromolecules*, **23**, 4098 – 4107 (1990).

17. Rees, R.W. and Vaughan, D.J., *Polym. Prepr.*, **6**, 287 (1965).

18. Brown, H.P. and Duke, N.G., *Rubber World*, **130**, 784 (1954).

19. Warner, R.R., *Rubber Age,* **71**, 205 (1952).

20. Rees, R.W., *Modern Plastics*, **42**, 209 (1964).

21. Ward, T.C. and Tobolski, A.V., *J. Appl. Polym. Sci.*, **11**, 2403 (1967).

22. MacKnight, W.J., McKenna, L.W., Read, B.E., Properties of Ethylene-Methacrylic Acid Copolymers and their Sodium Salts: Mechanical Relaxations. *Journal of Applied Physics*, **38**, 4208 (1967).

23. Adkinson, D., Ferrari, L.P., Parent, J.S., Whitney, R.A., PCT Int. Appl. WO 20100819 (2010).

24. Bagrodia, S., Tant, M.R., Wilkes, G.L., Kennedy, J.P., Sulphonated Polyisobutylene Telechelic Ionomers: 12. Solid-state Mechanical Properties, *Polymer*, **28**, 2207 – 2226 (1987).

25. Schleicher, J. C., Scurto, A.M., Kinetics and Solvent Effects in the Synthesis of Ionic Liquids: Imidazolium, *Green Chemistry*., **11**, 694-703 (2009).

26. Waterkamp, D.A., Heiland, M., Schlueter, M., Sauvageau, J.C., Beyersdorff, T., Thoeming, J., Synthesis of Ionic Liquids in Micro-reactors – A Process Intensification Study, *Green Chem.*, **9**, 1084-1090 (2007).

27. Arjunan, P., Wang, H-C., Olkusz, J.A., New Options via Chemical Modification of Polyolefins Part 1: Synthesis and Properties of Novel Phosphonium Ionomers from Poly(isobutylene-co-4-bromomethylstyrene), ACS Symposium Series 704 (Functional Polymers), Chapter 14, 199 – 216 (1998).

28. Tsou, A.H., Duvdevani, I., Agarwal, PK. Quaternary Ammonium Elastomeric Ionomers by Melt-state Conversion. *Polymer*, **45**, 3163-3173 (2004).

29. Gordon JE. J Org Chem 30, 2760-2763 (1965).

30. Parent, J.S., Malmberg, S.M., Whitney, R.A., Auto-catalytic Chemistry for the Solvent-free Synthesis of Isobutylene-rich Ionomers, *Green Chemistry*, **13**, 2818 – 2824 (2011).

31. Parent, J.S., Porter, A.M.J., Kleczek, M.R., Whitney, R.A., Imidazolium Bromide Derivatives of Poly(isobutylene-*co*-isoprene): A Novel Class of Elastomeric Ionomers, *Polymer*, **52**, 5410-5418 (2011).

32. Parent, J.S., Malmberg, S.M., Whitney, R.A., Auto-catalytic Chemistry for the Solvent-free Synthesis of Isobutylene-rich Ionomers, *Green Chemistry*, **13**, 2818 – 2824 (2011).

33. Dluzneski, P.R., Peroxide Vulcanization of Elastomers, *Rubber Chemistry and Technology*, **74**, 451 – 492 (2001).

34. Palys, L.H., Callais, P.A., Understanding Organic Peroxides to Obtain Optimal Crosslinking Performance, *Rubber World*, **229**, 35 – 41 (2003).

35. Dluzneski, P.R., The Chemistry of Peroxide Vulcanization, *Rubber World*, **224**, 34 – 37 (2001).

36 Gibian, M.J., Corley, R.C., Organic Radical-Radical Reactions. Disproportionation *vs.* Combination, *Chemical Reviews*, **73**, 441 – 464 (1973).

37. Thomas, D.K., The Degradation of Pölyisobutylene by Dicumyl Peroxide, *Transactions of the Faraday Society*, **57**, 511 – 517 (1961).

38. Loan, L.D., The Reaction Between Dicumyl Peroxide and Butyl Rubbers, *Journal of Polymer Science: Part A:Polymer Chemistry*, **2**, 2127 – 2134 (1964).

39. Xiao, S., Parent, J.S., Whitney, R.A., Knight, L.K., Synthesis and Characterization of Poly(isobutylene-*co*-isoprene)-derived Macro-monomers, *Journal of Polymer Science: Part A: Polymer Chemistry*, **48**, 4691 – 4696 (2010).

40. Merrill, N.A., Wang, H.-C., Dias, A.J., US 5824717 A 19981020 (1998).

41. Deady, L.W. Rates of N-Methylation of Azoles with Methyl Iodide and Dimethyl Sulphate, *Australian Journal of Chemistry*, **26**, 1949 – 1953 (1973).

42. Ngo, H.L., LeCompte, K., Hargens, L., McEwen, A.B., Thermal Properties of Imidazolium Ionic Liquids, *Thermochimica Acta*, **357 – 358**, 97 – 102 (2000).

43. Baranyai, K.J., Deacon, G.B., MacFarlane, D.R., Pringle, J.M., Scott, J., L., Thermal Degradation of Ionic Liquids at Elevated Temperatures, *Australian Journal of Chemistry*, **57**, 145 – 147 (2004).

44. Chan, B.K.M., Chang, N.-H., Grimmett, M.R., The Synthesis and Thermolysis of Imidazole Quaternary Salts, *Australian Journal of Chemistry*, **30**, 2005–2013 (1977).

45. Petrak, K.L., Reactivity of some Vinylimidazoles Towards Other Vinyl Monomers in Radical Copolymerization, *Journal of Polymer Science: Polymer Letters Edition*, **16**, 393 – 399 (1978).

46. Marcilla, R., Blazquez, J.A., Rodriguez, J., Pomposo, J.A., Mecerreyes, D., Tuning the Solubility of Polymerized Ionic Liquids by Simple Anion-Exchange Reactions, *Journal of Polymer Science: Part A: Polymer Chemistry*, **42**, 208 – 212, (2004).

47. Munoz-Bonilla, A., Fernandez-Garcia, M. Polymeric Materials with Antimicrobial Activity, *Progress in Polymer Science*, **37**, 281-339 (2012).

48. Kenawy, E.R., Abdel-Hay, F.I., El-Shanshoury. A.E.R.R., El-Newehy, M.H. Biologically Active Polymers. V. Synthesis and Antimicrobial Activity of Modified Poly(glycidyl methacrylate-co-2-hydroxyethyl methacrylate) Derivatives with Quaternary Ammonium and Phosphonium Salts, *Journal of Polymer Science Part A Polymer Chemistry*, **40**, 2384–93 (2002).

49. Li, G., Shen, J., Zhu, Y. A Study of Pyridinium-type Functional Polymers. III. Preparation and Characterization of Insoluble Pyridinium-type Polymers, *Journal of Applied Polymer Science*, **78**, 668–75 (2000).

50. Sauvet, G., Dupond, S., Kazmierski, K., Chojnowski, J.. Biocidal Polymers Active by Contact. V. Synthesis of Polysiloxanes with Biocidal Activity, *Journal of Applied Polymer Science*, **75**, 1005–12 (2000).

51. Abel, T., Cohen, J.I., Engel, R, Filshtinskaya, M., Melkonian, A., Melkonian, K. Preparation and Investigation of Antibacterial Carbohydrate-based Surfaces, *Carbohydrate Research*, **337**, 2495–9 (2002).

52. Anderson, E.B., Long, T.E. Imidazole- and Imidazolium-containing Polymers for Biology and Material Science Applications, *Polymer*, **51**, 2447–54 (2010).

53. Anderson, E.B., Long, T.E. Imidazole- and Imidazolium-containing Polymers for Biology and Material Science Applications, *Polymer*, **51(12)**, 2447-2454 (2010).

CHAPTER 2

ELASTOMERIC IONOMERS: PROPERTIES OF IMIDAZOLIUM BROMIDE DERIVATIVES OF POLY(ISOBUTYLENE-*CO*-ISOPRENE)

2.1 Introduction

Ionomers, or macromolecules containing small amounts of ionic functionality, are valued for their superior mechanical properties, adhesion to high surface energy fillers and as blend components.[1,2] The inability of the polymer matrix to solvate ion pairs leads to their aggregation in the solid-state. This generates an ionic network, which enhances material properties like dynamic storage modulus and melt elasticity. In addition, ion-dipole interactions with high surface energy solids promotes adhesion to siliceous fillers, polar materials and metals making ionomers particularly useful in adhesive, polymer blending, and polymer composite applications.

Ionomers bearing carboxylate and sulfonate functionality have thus far attracted extensive investigation. However, cationic ionomers have also attracted recent attention owing to their ability to inhibit the growth of microorganisms.[3] Interest rests in the derivatives of isobutylene-rich elastomers, since these materials provide exceptional impermeability, oxidative stability and vibration dampening characteristics. A simple route to cationic ionomer elastomers involves nucleophilic displacement of the halide from halogenated starting materials, such as brominated poly(isobutylene-*co*-isoprene) (BIIR).

While thermoplastic materials bearing unreactive carboxylate and sulfonate functionality have established widespread applications[4,5], ionomers with inert quaternary ammonium, phosphonium and imidazolium groups are also well recognized. This work is concerned with imidazole-derived ionomers that support a wider range of ionomer chemistry and further chemical modification. The expectation being that the reactivity of the functional group is alterable by concentrating groups within ionic aggregates and/or at the ionomer interface with high-energy surfaces.

The need for thermoset ionomer chemistry stems from the susceptibility of un-crosslinked elastomeric ionomers to creep and stress relaxation.[6] The resulting aggregation of ion pairs establishes a non-covalent network of polymer chains whose dynamic mechanical

properties approach those of conventional covalent thermosets comprising carbon-carbon and/or sulfide crosslinks. However, the lability of an ionic network leads to a poor response to static loads and thermoformable ionomers do not meet engineering material standards.

It is desirable to have a direct route to thermoset ionomers comprised of a network of stable covalent crosslinks and a labile network of aggregated ion pairs. These hybrid ionic/covalent networks are producible by a conventional polymer compounding approach. Wherein BIIR and an imidazole nucleophile are mixed together, shaped to a desired form and heated to accelerate N-alkylation. This work involved the direct preparation of imidazolium thermosets (Figure 2.1 below) by reacting BIIR with 1,1'(1,4-butanediyl)bis(imidazole) to yield IIR-(bis)ImidazoleBr, as well as the repeated alkylation of imidazole in the presence of a suitable base (IIR-ImidazoleBr).

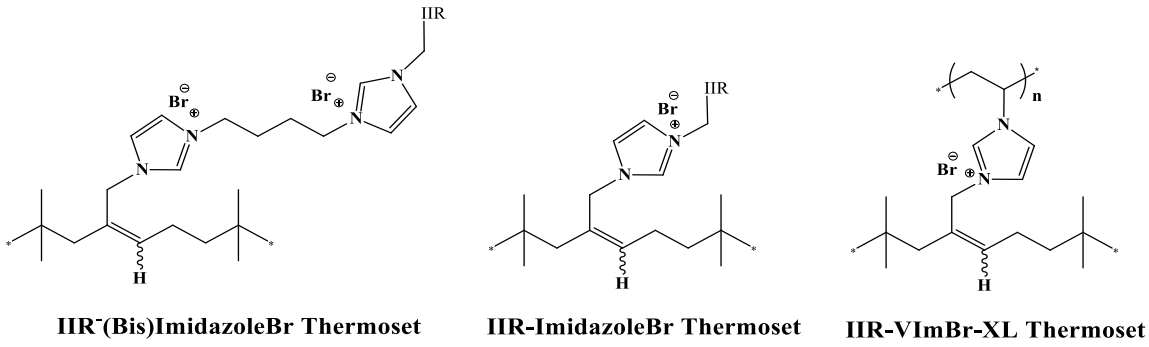

FIGURE 2.1 – Hybrid ionic/covalent imidazolium thermoset derivatives of BIIR

A third synthetic approach involved the preparation of a vinyl imidazolium bromide derivative of BIIR (IIR-VImBr), followed by radical oligomerization of pendant C=C groups to yield the desired thermoset (IIR-VImBr-XL, where XL indicates a crosslinked product). The two steps of this hybrid ionic/covalent network synthesis of IIR-VImBr are not necessarily orthogonal. Ion pair aggregates established during vinyl imidazole alkylation may affect the rate and yield of the subsequent vinylimidazolium oligomerization process. In addition, the transformation of IIR-VImBr into its thermoset derivative may alter the state of ion pair aggregation. These potential interdependencies differentiate IIR-VImBr oligomerization from the curing of conventional ionomers in which unreactive ionic functionality does not engage in polymer crosslinking.

The aim of this research is to examine the dynamics of these imidazolium ionomer thermoset preparations under a set of standard reaction conditions, and to provide insight into the resulting hybrid ionic/covalent networks (IIR-VImBr-XL, IIR-(bis)ImidazoleBr and IIR-ImidazoleBr). A dynamic oscillating rheometer probed the rate and yield of crosslinking. Afterwards, a comparison was made of the physical properties of the hybrid materials to appropriate benchmark materials. These include an uncured imidazolium bromide ionomer (IIR-BuImBr) and a non-ionic thermoset (IIR-Acrylate-XL). In testing the various materials, the following properties were determined: tensile strength of elastomer dog-bones, compression set of cured cylindrical elastomer pellets, contact angles, surface energies, adhesion to Mylar® film and anti-microbial activity against an E. coli bacterial culture.

2.2 Experimental

2.2.1 Materials

Poly(isobutylene-co-isoprene) (IIR or RB301) and brominated poly(isobutylene-co-isoprene)(BIIR or BB2030, M_n = 400 000 g/mol, polydispersity = 1.5, 0.15 mmol allylic bromide functionality/g BIIR) were used as supplied by LANXESS Inc. (Sarnia, Ontario). 1-Butylimidazole (BuIm, 98%), 1-vinylimidazole (VIm, ≥99%), imidazole (≥99%), tetra-N-butylammonium bromide (Bu_4NBr or TBAB, ≥98%), acrylic acid (anhydrous, 99%), tetra-N-butylammonium hydroxide (TBAOH, 1.0 M in methanol), tetra-N-butylammonium bromide (TBAB, 99%), tetra-N-butylammonium acetate (TBAAc, 97%), 1,4-dibromobutane (99%), sodium hydroxide (NaOH, ≥98%), zinc oxide (ZnO, ≥99%), stearic acid (≥98%), 1,8-bis(dimethylamino)naphthalene (Proton Sponge©, 98%), chloroform-d (99.8%D), methanol-d_4 (99.8%D), toluene-d_6 (99.6%D) and dicumyl peroxide (DCP, 98%) were used as received from Sigma-Aldrich (Oakville, Ontario). Bacteriological Agar (15 g/L, Marine BioProducts), Plate Levine EMB Agar (BD Becton Dickinson Canada Inc., Mississauga, Ontario), and E. coli (K12, 0.2 OD_{640}, supplied by Dorothy Agnew, Department of Microbiology and Immunology, Queen's University).

2.2.2 Synthesis of IIR-BuImBr

BIIR (120 g, 18.0 mmol allylic bromide) was dissolved in toluene (1200 mL, 10 wt%). Subsequently, BuIm (13.41 g, 108.0 mmol, 6 eq.) was added to the solution and reacted for 18 hours at 100 ± 2°C. The N-alkylation product was obtained by precipitation using excess acetone,

purified by dissolution/precipitation using tetrahydrofuran/acetone and dried *in vacuo*. The product IIR-BuImBr had a 95% conversion corresponding to an ion content of 0.14 mmol/g. The degree of N-alkylation was quantified by integrating the normalized ^{1}H NMR spectra, with respect to residual isoprene, to an estimated accuracy of ± 5%. ^{1}H NMR ($CDCl_3$ + 5 wt% CD_3OD): δ 4.89 (s, 2H, =C–C**H$_2$**–N$^+$–, *Z*-isomer), 4.82 (s, 2H, =C–C**H$_2$**–N$^+$–, *E*-isomer), 4.35 (t, 2H, N–C**H$_2$**–CH_2–CH_2–CH_3), see Appendix A for the ^{1}H NMR spectra.

2.2.3 Synthesis of IIR-VImBr

BIIR (120 g, 18.0 mmol allylic bromide) was dissolved in toluene (1200 mL, 10 wt%). Subsequently, VIm (10.16 g, 108.0 mmol, 6 eq.) was added to the solution and reacted for 50 hours at 100 ± 2°C. The N-alkylation product was obtained by precipitation using excess acetone, purified by dissolution/precipitation using tetrahydrofuran/acetone and dried *in vacuo*. The product IIR-VImBr had a 75% conversion corresponding to an ion content of 0.11 mmol/g. The degree of N-alkylation was quantified by integrating the normalized ^{1}H NMR spectra, with respect to residual isoprene, to an estimated accuracy of ± 5%. ^{1}H NMR ($CDCl_3$ + 5 wt% CD_3OD): δ 11.53 (s, 1H, –N$^+$–C**H**–N–), 7.61 (s, 1H, –N$^+$–CH=C**H**–N–), 7.42 (dd, 1H, –N–C**H**=CH_2), 5.80 (dd, 1H, N–CH=CH–**H$_{trans}$**), 5.41 (dd, 1H, N-CH=CH–**H$_{cis}$**), *Z*-isomer: δ 7.16 (s, 1H, *Z*, –N$^+$–C**H**=CH–N–), 5.69 (t, 1H, *Z*, CH_2–C=C**H**–CH_2), 4.91 (s, 2H, –C–C**H$_2$**–N$^+$), *E*-isomer: δ 7.20 (s, 1H, *E*, –N$^+$–C**H**=CH–N–), 5.68 (t, 1H, *E*, CH_2–C=C**H**–CH_2), 4.84 (s, 2H, *E*, –C–C**H$_2$**–N$^+$). Conjugated dienes: δ 5.98 (d, 1H, exo-diene), 5.92 (d, 1H, endo-diene). Residual isoprene: δ 5.04 (t, 1H, CH_3–C=C**H**–CH_2-), see Appendix A for the ^{1}H NMR spectra.[7]

2.2.4 Synthesis of 1,1'(1,4-Butanediyl)Bis(Imidazole)

NaOH (12.50 g) was dissolved in water (12.50 g) and mixed with toluene (60 mL). Imidazole (1.31 g, 19.8 mmol) and Bu_4NBr (0.606 g, 1.98 mmol) were added to the solution at 25°C until all solids were dissolved. Afterwards, 1,4-dibromobutane (2.02 g, 9.32 mmol) was added and the solution heated to 60°C for 16 hours. Upon cooling to 25°C, water (80 mL) was added to the mixture before recovering crystals by vacuum filtration (1.48 g, 84% yield). ^{1}H NMR ($CDCl_3$) δ 1.76 (t, -CH_2-C**H$_2$**-C**H$_2$**-CH_2-, 4H), 3.93 (m, N-C**H$_2$**-CH_2-, 4H), 6.86 (s, 2H), 7.07 (s, 2H), 7.44 (s, 2H), m.p. = 83-86°C.[6]

2.2.5 Solid-State Reaction of BIIR and 1,1'(1,4-Butanediyl) Bis(Imidazole)

BIIR (40.0 g, 6.00 mmol allylic bromide) was mixed with 1,1'(1,4-butanediyl)bis(imidazole) (0.58 g, 3 mmol, 6 eq.) at 90°C and 60 rpm using a Haake Polylab R600 internal batch mixer equipped with Banbury blades.[6]

2.2.6 Synthesis of Tetra-N-Butylammonium Acrylate

Acrylic acid (0.29 mL, 4.0 mmol) was mixed with TBAOH (1.25 mL, 1.0 M in MeOH, 4.0 mmol) and stirred for 30 minutes at room temperature. Methanol removed by Kugelrohr distillation (80 Pa, room temperature) yielded white crystals.

2.2.7 Synthesis of IIR-Acrylate

BIIR (20 g, 3.0 mmol allylic bromide) was dissolved in toluene (200 mL, 10 wt%). Subsequently, tetra-N-butylammonium bromide (0.48 g, 0.5 mmol, 0.5 eq.) was added to the solution and the mixture isomerized for 1 hour at 85 ± 2°C. Next, tetra-N-butylammonium acrylate (1.03g, 3.3 mmol, 1.1 eq.) was added to the solution and allowed to react for 2 hours at 85 ± 2°C ensuring allylic bromide conversion. The esterification product was obtained by precipitation in excess acetone, purified by dissolution/precipitation using tetrahydrofuran/acetone and dried *in vacuo*. IIR-Acrylate was produced in 100% conversion, corresponding to an acrylate content 0.15 mmol/g. The degree of esterification was quantified by integrating the normalized ^{1}H NMR spectra, with respect to residual isoprene, to an estimated accuracy of ± 5%. ^{1}H NMR ($CDCl_3$) for IIR-Acrylate: δ 6.41 (d, 1H, –O–C(=O)–CH=CH–$\mathbf{H_{trans}}$), δ 6.15 (m, 1H, –O–C(=O)–C**H**=CH_2), δ 5.82 (d, 1H, –O–C(=O)–CH=CH–$\mathbf{H_{cis}}$), δ 4.68 (s, 2H, =C–C$\mathbf{H_2}$–O–C(=O)–, Z-ester), δ 4.61 (s, 2H, =C–C$\mathbf{H_2}$–O–C(=O)–, E-ester). ^{1}H NMR for residual isoprene: δ 5.07 (t, 1H, CH_3–C=CH–CH_2).

2.3 Instrumentation and Analysis

2.3.1 Structural Analysis by NMR

^{1}H NMR analysis was conducted with a Bruker AM500 spectrometer with chemical shifts (δ) reported relative to tetramethylsilane in ppm.

2.3.2 Rheological Characterization

Rheological characterization used an Alpha Technologies Advanced Polymer Analyzer 2000 equipped with biconical disks. Crosslinking time sweeps were conducted at 160°C with a 3° oscillation arc (30% applied strain) and 1 Hz frequency. Subsequently, stress relaxation measurements were made at 100°C and 2° strain. Temperature sweeps from 100°C to 200°C and back to 100°C were set to a 3° oscillation arc and 1 Hz frequency.

2.3.3 Preparation of Cured Macrosheets for Tensile Measurements

A dried elastomer sample (40.0 g batch) coated with a measured amount of DCP in acetone was dried and passed through a two-roll mill approximately ten times. Approximately 35.0 g of the mixture was sheeted with a two-roll mill and compression molded [160°C, 20 MPa, 25 min ($5t_{1/2}$ for DCP)[8]] providing a final sheeted product of 2.00 ± 0.05 mm thickness. Specimens for tensile testing were prepared as described in ASTM D4482[9] and analyzed using an INSTRON Series 3360 universal testing instrument operating at a crosshead speed of 500 mm/min at 23 ± 1°C.[10] Reported results are the average of five replicate measurements.

2.3.4 Preparation of Cured Macrosheets for Adhesion Measurements

A Teflon sheet was placed initially atop a rectangular cavity of a compression mold, followed by an elastomeric sample (15 g, milled into a rectangular shape) and then a small Teflon strip atop one of the rectangular edges of the sample. Finally, a Mylar® sheet was placed atop of everything and overtop this the upper plate of the compression mold. The sample, within the mold, was cured in a Wabash press at 160°C for 25 min. Upon completion, the sample while still adhering to the Mylar® sheet and Teflon strip was slowly detached from the bottom Teflon rectangular sheet. The sheet, now divided into rectangular strips (25 mm in width), was tested for peel strength (N) utilizing the INSTRON Series 3360 universal testing instrument operating at a crosshead speed of 500 mm/min at 23 ± 1°C.

2.3.5 Preparation of Cured Cylinders for Compression Set Measurements

Four samples (2.5 g each), from the main batch, were placed inside individual cylindrical molds (14.0 mm diameter, 12.5 mm height) and cured (160°, 25 min) to give final sample dimensions of 14 ± 0.1 mm in diameter and 12.5 ± 0.2 mm in height. Each sample had its height

measurement recorded before placing it between stainless steel plates with stainless steel spacers in a pneumatic press. The spacer height was 6.44 mm and corresponded to an applied strain of approximately 45%. Compression was set at 3.5 MPa and remained in place for 18 hours. After removal, the samples settled for 0.5 hours before recording the final height of each cylinder. This procedure was adapted from ASTM D395 – 03 (2008).[11]

2.3.6 Determination of Surface Energy of Cast Elastomer Films

The sessile drop method aids in the measurement of contact angles. Elastomers dissolved in an appropriate solvent or combination of solvents were cast as films, with minimal roughness, on varying substrates (glass slides, Teflon and aluminum sheets). The contact angles created by five liquids (octane, dodecane, tetradecane, hexadecane, and cyclohexane), on the different films, were determined utilizing digital imagery of the sessile drop (VCA Optima, AST Products, Inc.) between 5 and 10 seconds after the drop made contact with the surface. The average contact angle value, of ten trials, was then used in a Zisman plot where the X-axis plots the surface tension of the test liquids[12] and the Y-axis plots the cosine of the corresponding contact angle. The extrapolation of the cosθ vs. γ curve to cosθ = 1 (corresponding to the zero contact angle, or the complete wetting limit) provided the value of the critical surface energy of the material tested.

2.3.7 Anti-Microbial Studies of Cast Elastomer Films

Films (5-wt% solution in THF) of IIR, IIR-BuImBr, and IIR-VImBr were cast in separate sterilized glass Petri dishes. The Petri dishes were air dried for a day, then dried in an oven (50°C) to remove any remaining solvents and finally autoclaved (Steris-Amsco Century, SG-120 Scientific Gravity Sterilizer). A suspension (1 mL) of E. coli (K12) was added to 40 mL Tryptic Soy Broth (TSB) in a sterile 125 mL Erlenmeyer flask. The incubated suspension, at 37°C, was shaken for 2 hours at 180 rpm (Innova™ 4400, Incubator Shaker, New Brunswick Scientific). After the bacterial suspension (1 mL) achieved an absorption of approximately 0.250 (Ultrospec 3000 UV/Visible Spectrophotometer, Biochrom) the bacterial suspension (0.1 mL) was added to deionized and autoclaved water (5 mL). Next, the cell/water solution was poured over a cellulose acetate filter (0.45 µm pore size, Sartorius GmbH) using vacuum filtration. The membrane, once placed into a Petri dish containing Levine EMB Agar, was covered with an elastomer film, or with nothing for the control sample. The Petri dishes, sealed with parafilm, were incubated for 48-72 hours at 37°C (Forma Scientific model 3956 reach-in incubator). All samples, or Petri dishes, had photographs

taken and their anti-microbial properties/levels determined. These activities took place in a laminar flow hood (Class II A/B3 Biological Safety Cabinet, Forma Scientific).

2.4 Results and Discussion

2.4.1 Cure Dynamics and Yields

The following is a comparative study of three hybrid ionic/covalent network materials, IIR-(Bis)ImidazoleBr, IIR-ImidazoleBr and IIR-VImBr-XL (Figure 2.2 on page 35). The first two materials were prepared by mixing BIIR with a nucleophile and required base to give a relatively low viscosity compound, and subsequently heating in a compression mold to produce the ionomer thermoset. This simple compounding approach is convenient and solvent-free. However, imidazolium bromide functionality is generated in the compression mold and is hence not present during the compounding process. As such, the bis-imidazole and imidazole + base processes cannot provide enhanced adhesion during compound mixing, which is often beneficial when filler dispersion is desired. Moreover, the desired N-alkylation reactions must compete with dehydrohalogenation of allylic bromide functionality and may result in a lower ultimate state of cure.

On the other hand, IIR-VImBr-XL involves processing a pre-made ionomer of high viscosity and good adhesion to high-energy surfaces. Therefore, this approach can facilitate the dispersion of fillers, such as precipitated silica. Furthermore, the radical oligomerization of vinyl imidazolium groups proceeds to a very high conversion, allowing all 0.15 mmole/g of curable functionality to contribute to the covalent network formation.

An ideal thermoset formulation is inactive at 100°C to facilitate compound mixing, provides a short induction period at 160°C to permit the compound to conform to the dimensions of the compression mold and then crosslinks quickly to a high final modulus that does not revert to a lower crosslink density over time. Quantifying the dynamics of a crosslinking reaction (Figure 2.2 on page 35) requires an oscillating biconical disc rheometer operating at a fixed temperature, strain and frequency. The rheometer encloses a polymer/curative mixture between two biconical disks and measures the torque required to oscillate the bottom disc relative to the top disc as a function of time. The dynamic storage (G`) and loss (G``) moduli, a standard for

measuring polymer stiffness and elasticity, provide insight into the influences of ion pair aggregation on the solid-state rheological properties of ionomers.[13]

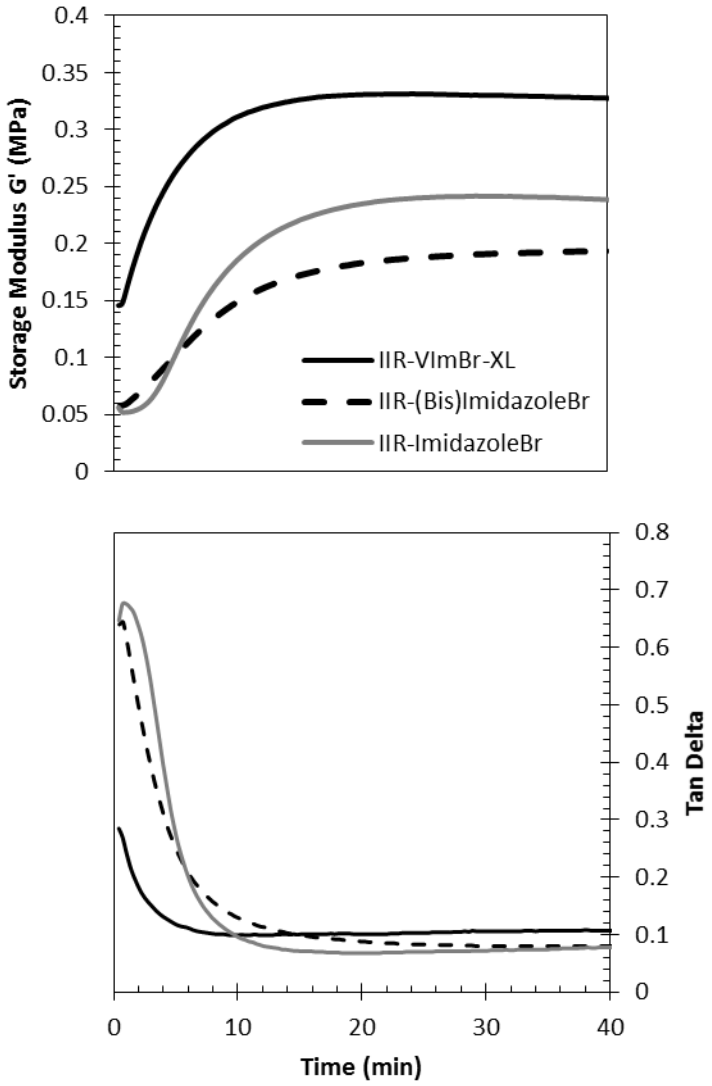

FIGURE 2.2 – Dynamics of thermoset ionomer crosslinking

Scheme 2.1 on page 36 illustrates the synthesis of a bis-imidazolium thermoset by the reaction of BIIR with 1,1'(1,4-butanediyl)bis(imidazole).[6] A 1:2 molar ratio of nucleophile to electrophile is ideal from the standpoint of reaction stoichiometry. However, HBr elimination competes with the desired nucleophilic substitution and dehydrohalogenation can be significant at temperatures above 120°C, leading not only to the loss of electrophile but also to the potential protonation of alkyl imidazole. Both processes are expected to reduce crosslink

yields. Note that BIIR contains a small amount of non-nucleophilic acid scavengers such as epoxides and calcium stearate that sequester HBr released by the polymer. Limited studies of BIIR dehydrobromination suggest it proceeds by an E1 mechanism involving deprotonation of allyl cation intermediates. Hence, imidazole-based nucleophiles should not accelerate HBr elimination rates.

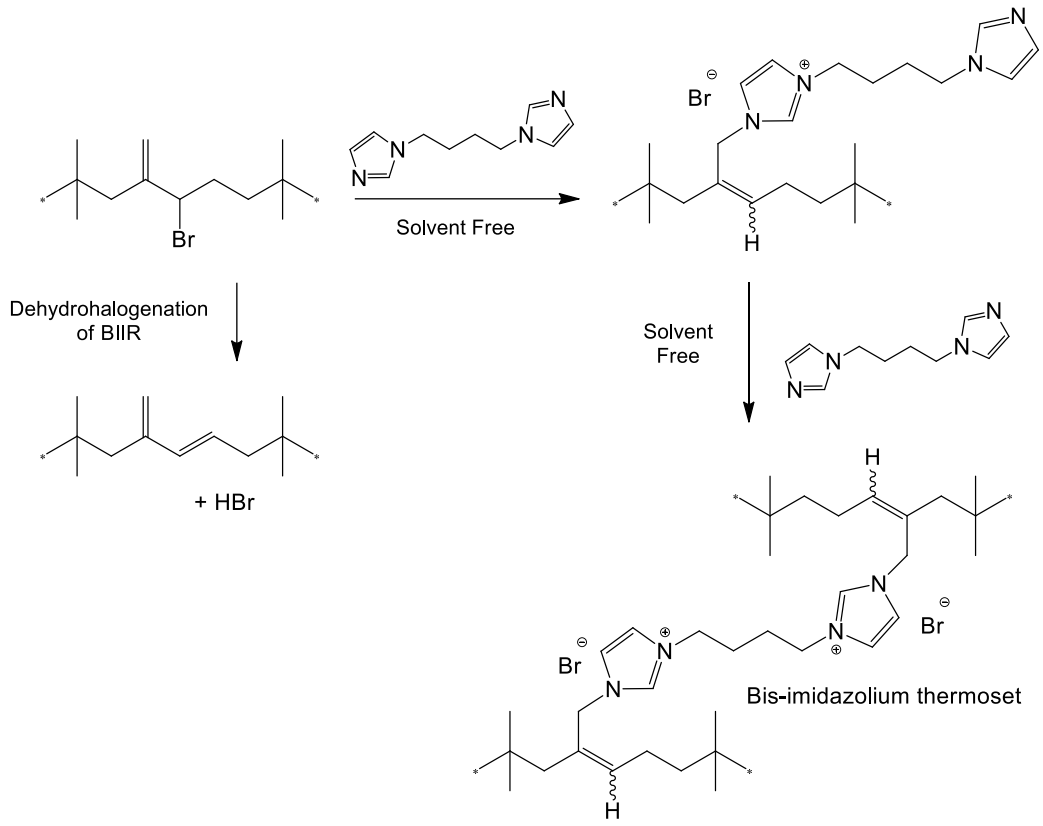

SCHEME 2.1 – Bis-imidazolium thermoset synthesis and dehydrohalogenation of BIIR

The rheometry data plotted in Figure 2.2 on page 35 illustrate the dynamics of a BIIR + bis-imidazole formulation containing 0.5 molar equivalents of 1,1'(1,4-butanediyl)bis(imidazole) relative to the 0.15 mmoles of allylic bromide functionality per gram of polymer. Crosslinking began from the outset, proceeding at a moderate rate to a final change in storage modulus $\Delta G'$=0.13 MPa. This ultimate modulus value did not decline significantly throughout the 40 min duration of the experiment, indicating the hybrid ionic/covalent network established in the thermoset is thermally stable at 160 °C. However, this crosslink density fell significantly short of those provided by the other two thermoset ionomer preparations.

An alternate synthetic route involves the repeated alkylation of imidazole by BIIR in the presence of a suitable base (Scheme 2.2 below). Nucleophilic displacement of bromide from the elastomer yields an imidazolium salt, whose deprotonation by a moderate base gives an imidazole-functionalized polymer intermediate.[6] Alkylation of this intermediate by a second allylic halide generates the desired ionomer crosslink. Note that the ideal stoichiometry for this process is a 1:2 ratio of nucleophile to electrophile, yielding an imidazolium bromide functional group concentration of 0.075 mmole/gram, or one-half of the allylic bromide content of BIIR. However, as described above for the bis-imidazole system, BIIR dehydrohalogenation can reduce this yield significantly where HBr elimination competes effectively with the N-alkylation of free and polymer-bound imidazole nucleophiles.

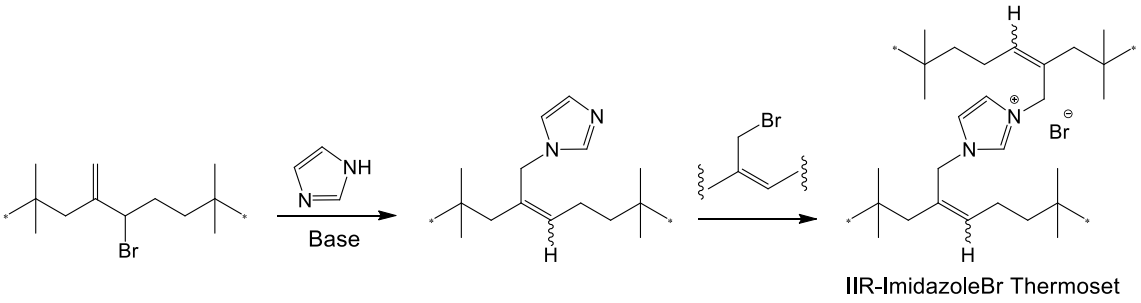

Scheme 2.2 – Bis-alkylation of imidazole

Figure 2.2 on page 35 illustrates the progress of a BIIR cure formulation containing 0.5 equivalents of imidazole and 0.5 equivalents of Proton Sponge©, relative to the allylic bromide functionality within BIIR. Additional base was provided to sequester the HBr released through BIIR dehydrohalogenation, thereby minimizing the potential for imidazole protonation. It is interesting to note crosslinking did not occur immediately, as the onset of the G' increase is delayed by several minutes. This induction delay can be of significant practical importance, since thermoset articles must be first molded and/or extruded into a desired shape before crosslinking renders them incapable of being processed. Presumably, differences in the alkylation rate of free imidazole and polymer-bound imidazole underlies this induction phenomenon. The ultimate state of cure is reflected by a ΔG'=0.18 MPa, which is significantly greater than its counterpart IIR-(bis)ImidazoleBr and yet considerably less than the vinylimidazolium bromide cure yield.

IIR-VImBr is a macromonomer derivative of butyl rubber that may contain 0.15 mmoles of vinyl functionality per gram of elastomer when the material is prepared at temperatures below which BIIR dehydrohalogenation is operative. Since N-vinylimidazolium halide salts are relatively unreactive towards homopolymerization,[14] storage stability problems reported for other macromonomer systems can be avoided[15,16] and IIR-VImBr can be stored under ambient conditions for weeks without the need for stabilizing additives. Crosslinking of this functional ionomer is accomplishable by mixing with a suitable radical initiator whose decomposition upon heating leads to oligomerization of the pendant vinyl functionality (IIR-VImBr-XL, Scheme 2.3 below). By avoiding complications associated with BIIR dehydrohalogenation, this approach is expected to yield the highest imidazolium bromide functionality of the three methods tested. Additionally, the thermoset should be free of residual HBr salts, activated epoxides and calcium stearate by-products.

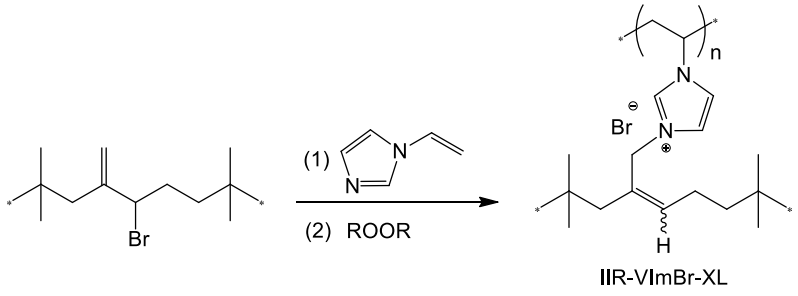

SCHEME 2.3 – Synthesis of a vinyl-imidazolium bromide hybrid network

Figure 2.2 on page 35 demonstrates the cure activity of an IIR-VImBr formulation containing 7.5 µmole of dicumyl peroxide per gram of elastomer. Thermolysis of the initiator (half-life of 5.4 min at 160 °C) resulted in radical oligomerization of aggregated vinylimidazolium bromide functionality, increasing the ionomer's storage modulus to a final value of $\Delta G'$=0.32 MPa. The final modulus was stable beyond the 20 min mark of the cure process and suffered none of the cure reversion incurred by macromonomer systems employing excessive peroxide loadings. Assuming conversion of the 0.11 mmol/g of vinyl functionality within IIR-VImBr-XL by the 7.5 µmol DCP/g charged to the formulation, the peroxide yield of this crosslinking reaction is 14 mmol vinyl /mmol DCP. This is a clear indication of a chain reaction nature of the process as the conversion of the multiple vinyl groups occur through each radical generated by peroxide thermolysis.

2.4.2 Rheological Properties of Hybrid Ionic/Covalent Thermosets

Insight into the unique balance of material properties provided by thermoset ionomers is possible through the study of dynamic storage and loss moduli as a function of temperature, and the investigation of the thermoset's stress-relaxation response to a constant applied strain.

Temperature sweep and stress relaxation data were acquired for the IIR-(bis)ImidazoleBr, IIR-ImidazoleBr, IIR-VImBr-XL thermosets and two additional benchmark materials. IIR-BuImBr is an un-crosslinked ionomer containing 0.15 mmole/g of butylimidazolium bromide functionality and, as such, provides insight into a purely ionic network. IIR-Acrylate-XL is a peroxide-cured acrylate ester derivative of BIIR containing no ionic functionality, thereby providing information on the response of a purely covalent thermoset. All materials share the same polymer backbone and random distribution of pendant functional groups, by virtue of their common origin.

Temperature sweeps, Figure 2.3 on page 40, took place from 100°C to 200°C then back to 100°C, traversing almost identical paths in both directions. Similar to other elastomeric ionomers[2], the storage modulus of IIR-BuImBr declined with a temperature increase, owing to the reduction in ionic network strength. The non-ionic thermoset IIR-Acrylate-XL behaved contrary to that of IIR-BuImBr, as its storage modulus increased significantly over the recorded temperature range. This is consistent with the standard models of covalent thermoset behaviour, whose entropically driven elasticity responds with a greater restorative force as the temperature increases. The response of IIR-VImBr-XL, IIR-ImidazoleBr and IIR-(bis)ImidazoleBr-XL to the increase in temperature is remarkable in terms of its relative insensitivity. The near constant value of 0.32 MPa for IIR-VImBr-XL clearly differentiates itself from IIR-BuImBr and IIR-Acrylate-XL. The assumption being that a loss in ionic network strength counterbalances with an increase in covalent network strength as the temperature rises.

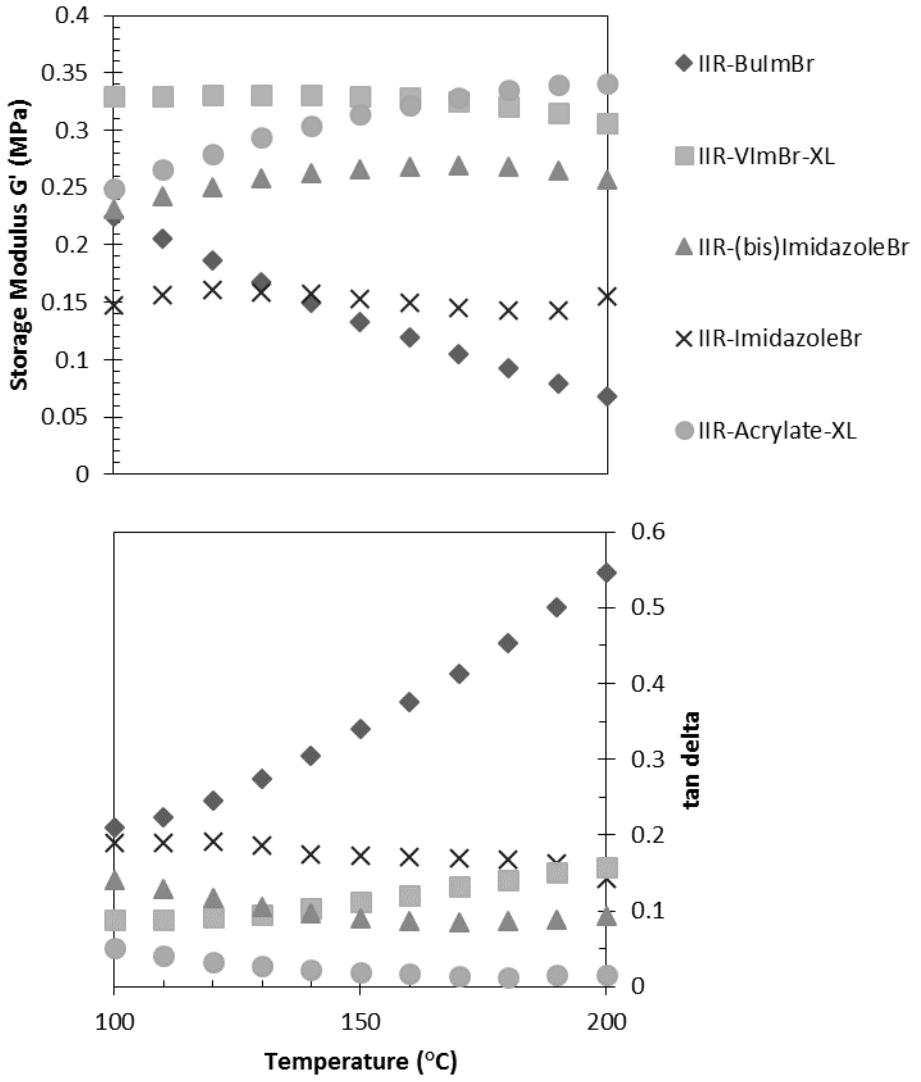

FIGURE 2.3 – Dynamics of various BIIR derivatives at temperature sweeps of 100-200°C at a 2° strain and 1 Hz frequency

Figure 2.4 on page 41 is a stress relaxation plot illustrating the evolution of the static modulus of materials at 100°C when subjected to constant shear strain. As expected, the un-crosslinked polymer IIR-BuImBr demonstrated a high degree of stress relaxation, a result of its labile nature, brought on by the movement of its chain segments. Unstable polymer networks can relax completely giving a static modulus (measured stress / applied strain) of zero, while tight covalent networks can provide a stable static modulus, since the relaxation of chain segments is restricted. Without a covalent crosslink network preventing polymer chains from flowing through

their entanglements, the modulus of the IIR-BuImBr declined continuously practically reaching zero stress.

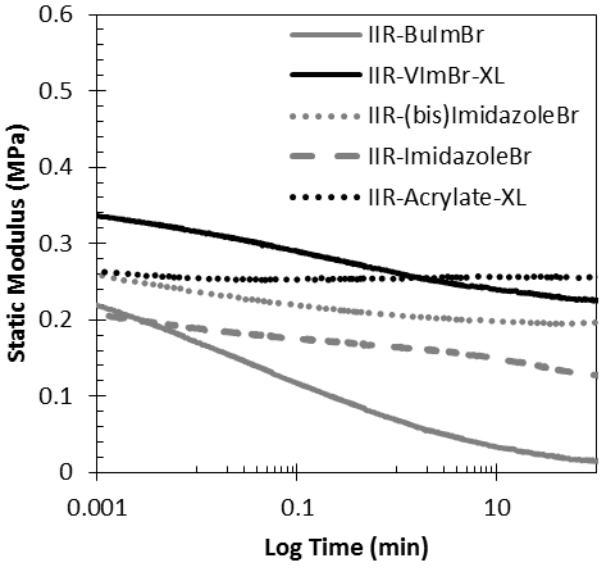

FIGURE 2.4 – Stress-relaxation of various BIIR derivatives at 100°C and fixed strain at 2° arc

In contrast, the covalent network of IIR-Acrylate-XL prevented the flow of polymer chain segments resulting in a near constant modulus. In keeping with its hybrid structure, the response of IIR-VImBr-XL, IIR-ImidazoleBr and IIR-(bis)ImidazoleBr to a constant strain was intermediate between that of IIR-BuImBr and IIR-Acrylate-XL. Demonstrating a slight relaxation followed by a stable plateau, which is evidence of ionic network relaxation as well as covalent network stability. The modulus of IIR-VImBr-XL declined throughout the measurement approaching that of IIR-Acrylate-XL, an indication that the relaxation of imidazolium bromide ion pair aggregates led to a condition where maintaining the shear stress is attributable to the entropic response of the covalent network.

The observations for the three hybrid ionic/covalent network materials (specifically referring to the temperature sweeps and stress relaxation data) indicate that despite the differences in cure rate, final modulus and compounding technique all three materials provided the same trends. In particular, the loss in ionic network strength counterbalances with an increase in covalent network strength as the temperature rises, and the network of ion pair aggregates are subject to relaxation while the covalent network maintains a stable response to an applied strain.

As such, a hybrid ionic/covalent network provides material performance with the benefits of conventional ionomers and covalent thermosets. However, the cure rate, final modulus and compounding technique do present different physical properties for these hybrid materials.

2.4.3 Physical Properties

The development of a compound for a target application is typically a trial and error process involving the measurement of a wide range of rheological properties. While the selection of test methods depends on the target application, physical measurements of common interest to ionomer formulations include tensile properties, compression set, surface energy and adhesive strength. Each of these measurements will be described in turn for the three ionomer thermosets of present interest, as well as the IIR-BuImBr and IIR-Acrylate-XL control materials.

Compression set measurements are complimentary to stress relaxation data, in that both tests measure a material's response to a static applied strain. Compression of cylindrical samples for 18 hours resulted in permanent deformation, reported as a percentage of the applied strain. Therefore, a low compression set value reflects a heightened resistance to permanent deformation under a static load. The data listed in Table 2-1 on page 43 demonstrates the superior performance of the peroxide-cured thermosets, with IIR-acrylate-XL and IIR-VImBr-XL providing the lowest compression sets owing to the stability of their covalent networks. As expected, the labile nature of ion pair aggregates resulted in a significant permanent deformation in the case of IIR-BuImBr. However, the IIR-(bis)ImidazoleBr produced a surprising result, in that a compression set of just 7% was obtained despite the relatively low $\Delta G'$ recorded during its crosslinking dynamics experiment (Figure 2.2 on page 35).

TABLE 2.1 – Tensile, Compression, Surface Energy and Adhesion Data

Elastomer	Compression Set (%)	Young's Modulus (MPa)	Tensile Strain at Break (%)	Tensile Stress at Maximum Load (MPa)	Surface Energy (mJ/m^2)	Peal Strength (N)
IIR	–	–	–	–	20 ± 1	6.1 ± 2.7
IIR-BuImBr	60 ± 2.0	0.72 ± 0.05	2300 ± 190	8.1 ± 1.1	19 ± 1	10 ± 0.22
IIR-VImBr-XL	6 ± 0.2	0.78 ± 0.04	300 ± 70	2.1 ± 0.2	20 ± 1	7.2 ± 0.50
IIR-(bis)ImidazoleBr	7 ± 0.4	0.64 ± 0.02	900 ± 90	1.9 ± 0.3	20 ± 2	23 ± 1.7
IIR-ImidazoleBr	30 ± 1.0	0.64 ± 0.03	690 ± 40	1.4 ± 0.4	19 ± 2	19 ± 2.1
IIR-Acrylate-XL	2 ± 0.2	0.45 ± 0.03	250 ± 20	0.7 ± 0.1	20 ± 1	5.6 ± 1.3

Tensile analysis involves measuring a material's resistance to a constant tensile strain rate with results typically summarized by Young's modulus, tensile strain at break and elongation at break values. The Young's modulus data presented in Table 2-1 above is remarkable, in that all four ionomer samples, including the un-vulcanized IIR-BuImBr material, were stiffer at low elongation than IIR-Acrylate-XL. This is a consequence of the unique stiffness provided by an ionic network at low elongation. By virtue of its hybrid ionic/covalent network, IIR-VImBr-XL provided the highest modulus value. The aggregation of butyl-imidazolium bromide functionality within IIR-BuImBr was sufficient to provide a Young's modulus of 0.72 MPa, while the low ion pair content, generated by a bis-imidazole and an imidazole cure, gave correspondingly low stiffness values. Failure properties were consistent with expectations based on polymer network densities, with elongation and tensile strength at break values declining with increasing crosslink density. Where a high crosslink density is related to a large change in storage modulus.

Given the widespread interpretation of adhesive strength in terms of surface energy phenomena, the effect of polymer-bound imidazolium bromide functionality on the critical surface energy of an isobutylene-rich elastomer is of considerable fundamental interest. The critical surface energies, determined by extrapolating to $\cos\theta=1$, did not differ significantly among the derivatives nor with the varying substrates (Table 2-1 above and Figure 2.5 on page 44). A likely indication that the concentration of ionic functionality (< 0.15 mmol/g) in contact with the

drop was too low to affect its wetting properties. Nevertheless, imidazolium bromide functionality had a clear influence on elastomer adhesion and anti-microbial activity, as described below.

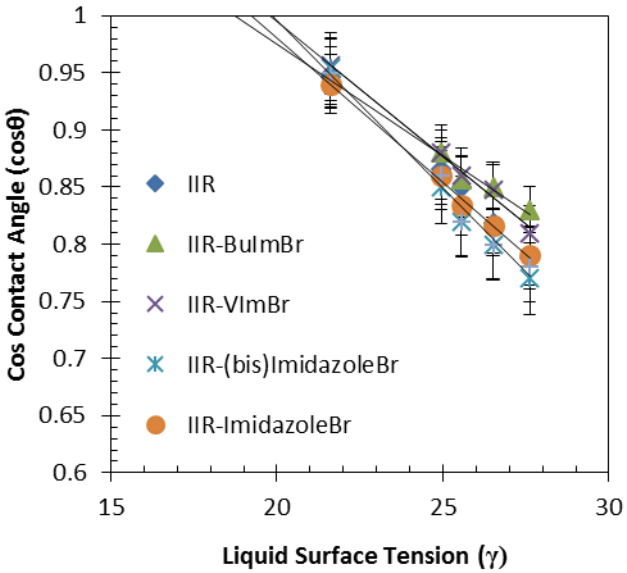

FIGURE 2.5 – Contact angle measurement results

Peel strength tests for different BIIR derivatives studied adherence to Mylar®, a polyester sheet. The findings reported in Table 2-1 on page 43 indicate superior adhesion for all four ionomeric materials compared to un-vulcanized IIR and IIR-Acrylate-XL. The superior performance of IIR-(bis)ImidazoleBr and IIR-ImidazoleBr may be due to the differences in crosslinking dynamics and material viscosity. Recall that IIR-VImBr-XL is a high viscosity ionomer that cures rapidly at 160°C (Figure 2.2 on page 35) making it difficult for the elastomer to wet a polyester film efficiently. On the other hand, IIR-(bis)ImidazoleBr and IIR-ImidazoleBr are low viscosity formulations that crosslink comparatively slowly, thereby allowing the material to produce an adhesive bond with lower residual strain. As such, ionomer thermosets prepared by compounding techniques may provide superior peel strength compared to those generated by a macromonomer approach.

2.4.4 Anti-Microbial Properties

Materials with a broad spectrum of anti-bacterial properties are necessary to improve current technologies in order to stay at the forefront of the fight against drug-resistant bacteria.[17] Bactericidal properties prevent the proliferation of harmful microorganisms by reducing or

eliminating the need for antiseptic treatment of surfaces people regularly touch, since pathogens easily spread through contact. Materials able to prevent bacterial growth or survival would significantly reduce human infections. Studies of imidazolium ionic liquids and other small molecules point to cytotoxicity as highly dependent on the counter-anion and length of the alkyl chain on the nitrogen of the imidazole ring, where extended alkyl chains increase anti-microbial contributions.[18]

The investigation of anti-microbial activity against E. coli focused on IIR, IIR-BuImBr and IIR-VImBr, since these materials did not contain any potentially toxic cure residue derived from un-alkylated nucleophile and/or HBr elimination. The setup for the anti-microbial test consisted of a cellulose acetate filter coated with E. coli laid face-up in an agar Petri dish. The size of the membrane's pores, 0.45 μm, permits the cells to absorb agar nutrients from below, yet prohibits cell migration down through the pores, preventing any direct contact with the agar. After covering the E.coli coated membrane with an elastomeric film, sealing the Petri dish and incubating the systems for 48-72 hours, an examination of the bacterial colony growth on the membrane surface was performed.

Figure 2.6 on page 46 illustrates four independent experiments involving different elastomeric films. Figure 2.6A is a control experiment in which no elastomer film covered the membrane. These conditions produced the greatest extent of bacteria cell growth. Figure 2.6B is a sample produced under an IIR film and shows significant cell proliferation on the membrane, as well as the polymer film (not shown). Figures 2.6C and D for IIR-BuImBr and IIR-VImBr films, respectively, demonstrate no evidence of bacteria colony growth.

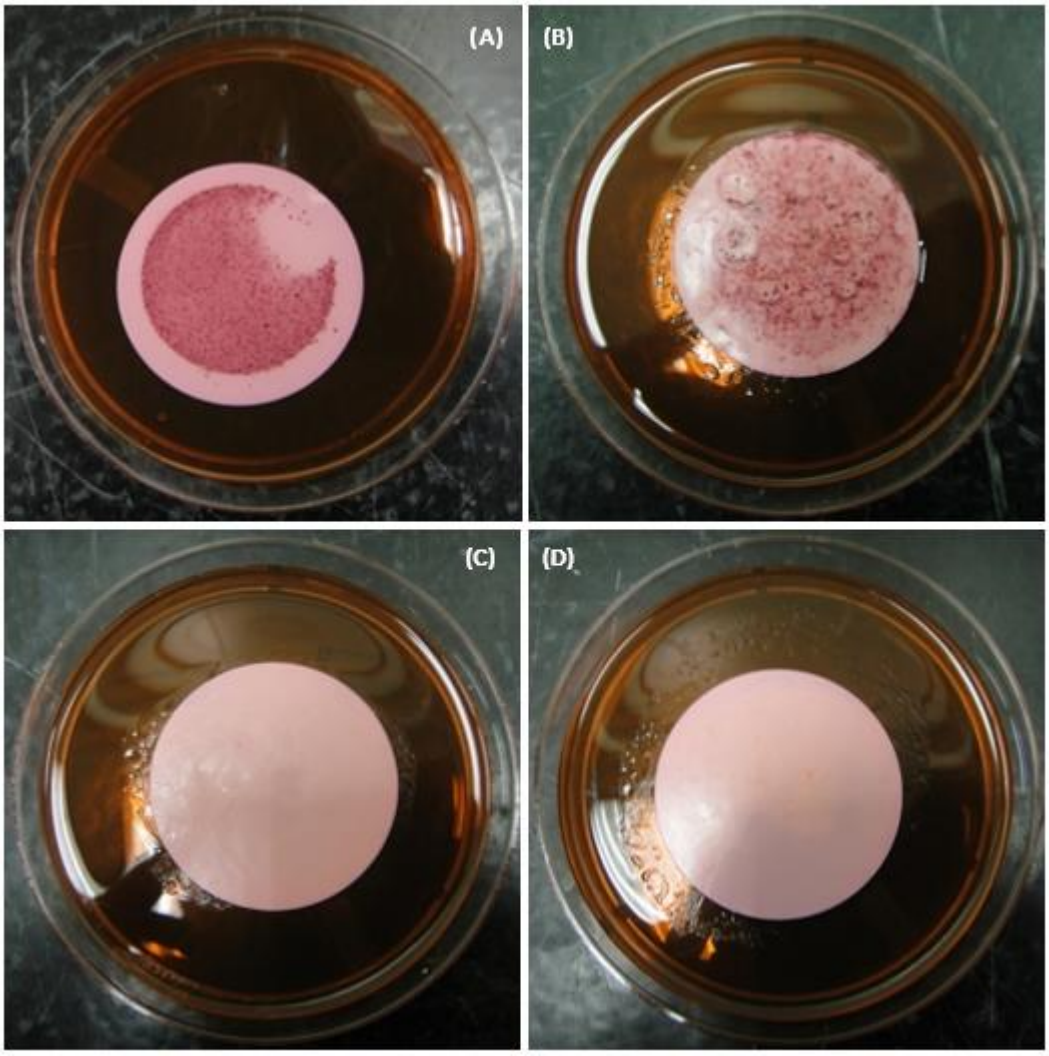

FIGURE 2.6 – Images showing extent of bacterial growth of a (A) control sample, and under an (B) IIR film, (C) IIR-BuImBr film, and (D) IIR-VImBr film

Antibacterial activity of related ionomer systems reports adsorption of the ionic moieties onto the bacterial cell surface, diffusion through the cell wall and binding to the cytoplasmic membrane resulting in its disruption. Bridge formations between adjacent phosphates of the membrane lipids cause the release of cytoplasmic constituents (like potassium, DNA and RNA) which ultimately lead to cell death.[3] In all cases, it is desirable to limit the loss of anti-microbial reagents into the environment, resulting from leaching and/or extraction.[3] Having the ionic group covalently bound to the polymer backbone negates these issues and potentially increases efficiency, selectivity and handling safety

2.5 Conclusions

A series of isobutylene-rich imidazolium bromide ionomers were prepared through the N-alkylation of a range of imidazole nucleophiles by the allylic halide functionality within BIIR. Exploiting the versatility of imidazole chemistry produced ionomer thermosets with properties originating from both a network of covalent crosslinks and network of ion pair aggregates. These solid-state reactions were amenable to standard compounding and crosslinking methods yielding unconventional thermosets with dynamic rheological properties akin to those generated by sulfur and peroxide cure formulations.

REFERENCES

1. Halliday, L. Ionic polymers. 1st ed. New York: Wiley; 1975.

2. Eisenberg, A., Kim, J.S. Introduction to Ionomers. 1st ed. New York: Wiley; 1998.

3. Munoz-Bonilla, A., Fernandez-Garcia, M. Polymeric Materials with Antimicrobial Activity. *Progress in Polymer Science*, **37**, 281-339 (2012).

4. MacKnight, W.J., Earnest, T.R. The Structure and Properties of Ionomers. *Journal of Polymer Science: Macromolecular Reviews*, **16**, 41-122 (1981).

5. Fitzgerald, J.J., Weiss, R.A. Synthesis, Properties, and Structure of Sulfonate Ionomers. *Journal of Macromolecular Science – Review in Macromolecular Chemistry & Physics*, **C28**, 99-185 (1988).

6. Parent, J.S., Porter, A.M.J., Kleczek, M.R., Whitney, R.A., Imidazolium Bromide Derivatives of Poly(isobutylene-co-isoprene): A Novel Class of Elastomeric Ionomers, *Polymer*, **52**, 5410-5418 (2011).

7. Ozvald, A.M. Reactive Ionomers: N-vinyliidazolium Bromide Derivatives of Poly(isobutylene-co-isoprene) and Poly(isobutylene-co-para-methylstyrene). Master of Applied Science Thesis, Queen's University (2012).

8. ASTM Standard D3182 – 07, Standard Practice for Rubber – Materials, Equipment and Procedures for Mixing Standard Compounds and Preparing Standard Vulcanized Sheets, *ASTM International*, West Conshohocken, PA, 2007, DOI: 10. 1520/D03182 - 07, www.astm.org.

9. ASTM Standard D4482 – 11, Standard Test Method for Rubber Property – Extension Cycling Fatigue, *ASTM International*, West Conshohocken, PA, 2007, DOI: 10. 1520/D4482-11, www.astm.org

10. ASTM Standard D412 – 06a^{E2}, Standard Test Methods for Vulcanized Rubber and Thermoplastic Elastomers – Tension, *ASTM International*, West Conshohocken. PA. 2006, DOI: 10. 1520/D0412-06AE02, www.astm.org

11. ASTM Standard D395 – 03 (2008), Standard Test Methods for Rubber Property – Compression Set, *ASTM International*, West Conshohocken, PA, 2008, DOI: 10. 1520/D0395-03R08, www.astm.org

12. Surface tension values of some common test liquids for surface energy analysis. Data Physics. Accessed: December 10 2013. http://www.surface-tension.de/

13. Capek I. Dispersion of Polymer Ionomers: I, *Advances in Colloid Interface Science*, **112**, 1-29 (2004).

14. (a) Petrak, K.L., Reactivity of some Vinylimidazoles Towards Other Vinyl Monomers in Radical Copolymerization, *Journal of Polymer Science: Polymer Letters Edition*, **16**, 393 – 399 (1978). (b) Marcilla, R., Blazquez, J.A., Rodriguez, J., Pomposo, J.A., Mecerreyes, D., Tuning the Solubility of Polymerized Ionic Liquids by Simple Anion-Exchange Reactions, *Journal of Polymer Science: Part A: Polymer Chemistry*, **42**, 208 – 212, (2004).

15. Oxley, C.E., Wilson, G.J., A Peroxide Curing Butyl Rubber, *Rubber Chemistry and Technology*, **42**, 1147 – 1154 (1969).

16. Gronowski, A., Osman, A., Crockett, T., PCT Int. Appl., WO 2006060896 A1 20060615 (2006).

17. Levy, S.B., Marshall, B. Antibacterial Resistance Worldwide: Causes, Challenges and Responses. *Nature Medicine*, **406**, 122-129 (2004).

18. Frade, R.F.M., Rosatella, A.A., Marques, C.S., Branco, L.C., Kulkarni, P.S., Mateus, N.M.M.. Afonso, C.A.M., and Duarte, C.M.M. Toxicological Evaluation on Human Colon Carcinoma Cell Line (CaCo-2) of Ionic Liquids Based on Imidazolium, Guanidinium, Ammonium, Phosphonium, Pyridinium and Pyrrolidinium Cations. *Green Chemistry*, **11**, 1660-1665 (2009).

CHAPTER 3

FUNCTIONAL GROUP REACTIVITY AND ION PAIR AGGREGATION OF BIIR AND BIMS

3.1 Introduction

Elastomeric ionomers, comprised of a small amount of ion pairs distributed within a non-polar polymer backbone, provide physical properties that differ substantially from those of non-ionic analogues.[1] Previous work has demonstrated the influence of imidazolium bromide functionality on ionomers derived from brominated poly(isobutylene-*co*-isoprene), or BIIR, and brominated poly(isobutylene-*co*-*para*-methylstyrene), or BIMS. The inability of the polymer matrix to solvate ion pairs leads to their aggregation in the solid-state, generating an ionic network that enhances material properties like dynamic storage modulus and melt elasticity.[2]

Ozvald et al. have demonstrated the ability of isobutylene-rich ionomers bearing vinylimidazolium bromide functionality to crosslink extensively when activated by standard peroxide initiators.[3] These multifunctional macromonomers cure through radical homopolymerization of pendant vinyl groups, yielding thermosets that contain both a covalent network of C-C bonds and an ionic network of aggregated ion pairs. A description of the unique physical properties provided by these network structures is included in Chapter 2.

The current chapter concerns the structure/reactivity of peroxide-curable derivatives of BIIR and BIMS. This study involves dual comparisons: non-ionic versus imidazolium macromonomers and BIIR versus BIMS derivatives. Comparisons of macromonomers bearing simple ester functionality (crotonate, cinnamate, methacrylate, acrylate; Scheme 3-1 on page 52) to analogues bearing imidazolium bromide functionality (Scheme 3.2 on page 61) explore the effects of ion pair aggregation on macromonomer crosslinking dynamics and yields. Given that imidazolium bromide aggregation may concentrate macromonomer functionality within multiplets, a potential exists for these ionomers to provide unique cure characteristics.

Comparative studies of BIIR and BIMS derivatives provide an insight into the effects of polymer backbone reactivity on peroxide-cure outcomes. BIIR contains 0.15 mmoles of allylic bromide functionality per gram of polymer, and 0.15 mmoles/g of unbrominated isoprene mers,

both of which distribute more or less randomly within the polymer chains. In contrast, BIMS contains 0.22 mmole/g of benzylic bromide functionality and 0.51 mmole/g of unbrominated para-methylstyrene mers that tend to group together within polymer chains. This subtle difference in chemical functionality and composition distribution may produce different cure characteristics, particularly for macromonomers bearing relatively unreactive oligomerizable functionality.

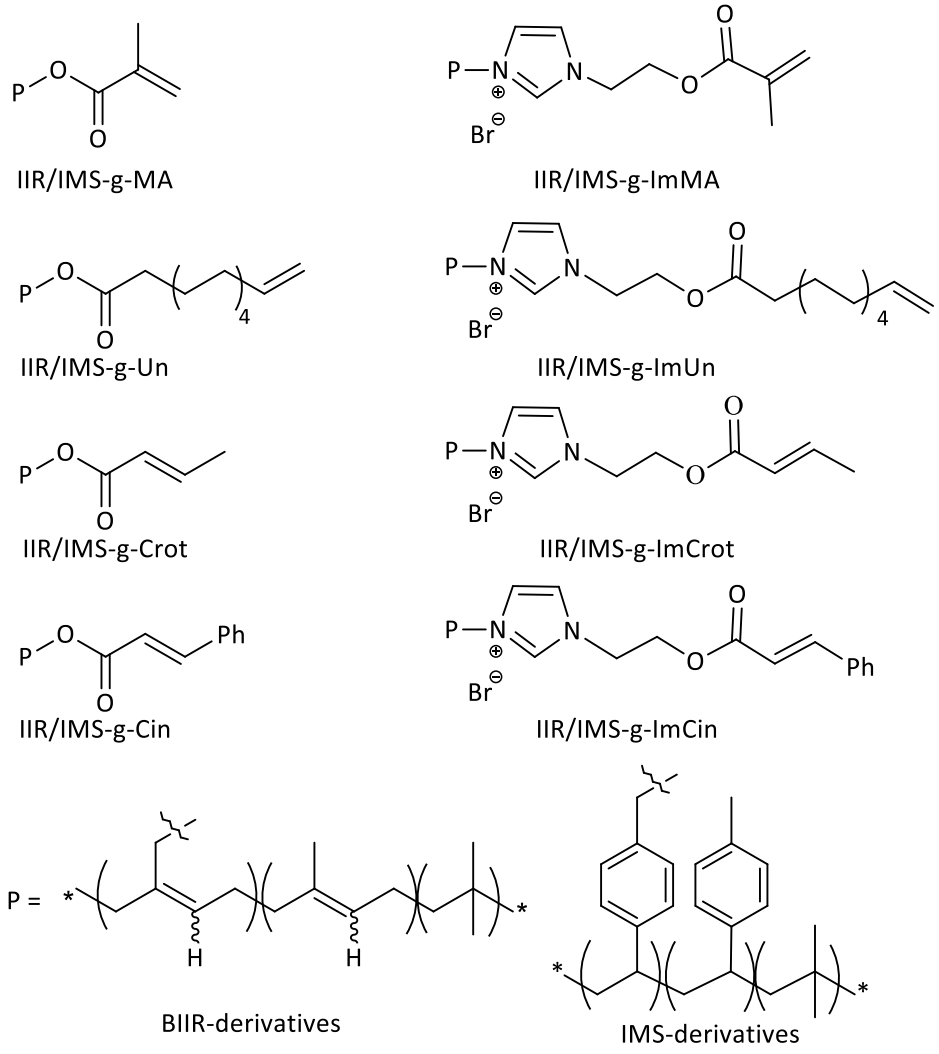

SCHEME 3.1 – Macromonomer derivatives of BIIR and BIMS

3.2 Experimental

3.2.1 Materials

Brominated poly(isobutylene-co-isoprene)(BIIR or BB2030, M_n = 400 000 g/mol, polydispersity = 1.5, 0.15 mmol allylic bromide functionality/g BIIR) were used as supplied by LANXESS Inc. (Sarnia, Ontario). Brominated poly(isobutylene-*co*-*para*-methylstyrene) (BIMS, Exxpro 3745, 0.22 mmol benzylic bromide functionality / g BIMS) was used in the form supplied by Exxon Mobil Chemical (Baytown, Texas). Crotonic acid (98%), *trans*-cinammic acid (≥99%), crotonoyl chloride (90%), cinnamoyl chloride (98%), 10-undecenoyl chloride (97%), methacryloyl chloride (purum, dist., ≥ 97% (GC), contains 0.02% 2,6-di-tert-butyl-4-methylphenol as stabilizer), 10-undecenoic acid (98%), methacrylic acid (99%), tetrabutyl ammonium acetate (97%), 3,3-dimethyl butyric acid (98%), 1-(2-hydroxyethyl)imidazole (97%), potassium hydroxide (KOH, reagent grade, ≥90%), tetrabutylammonium bromide (TBAB), sodium hydroxide (NaOH, ≥98%) and sodium carbonate (Na_2CO_3, ≥99%) were used as received from Sigma-Aldrich (Oakville, Ontario). Oxalic acid ($C_2O_4H_2$, 0.1N Standardized Solution) was used as received from Alfa Aesar.

3.2.2 Synthesis of 2-(1*H*-Imidazol-1-yl)Ethyl Cinnamate

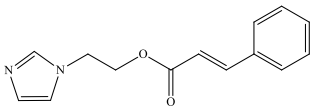

Cinnamoyl chloride (1.8g, 10.80mmol, 1.2eq.) and 1-(2-hydroxyethyl)imidazole (1.0g, 8.92mmol, 1eq.) were individually dissolved in dichloromethane (DCM). Dissolved cinnamoyl chloride was added drop-wise to the dissolved 1-(2-hydroxyethyl)imidazole and stirred overnight at room temperature. DCM was removed by vacuum and the residual oil dissolved in H_2O. The solution was acidified using oxalic acid and washed with ethyl acetate. Subsequently, sufficient sodium hydroxide (NaOH) was added to basify the solution and the product extracted with ethyl acetate. Yellow crystals were removed by Kugelrohr and dried *in vacuo*. The product 2-(1*H*-Imidazol-1-yl)ethyl cinnamate had a 56% yield. ^{1}H NMR ($CDCl_3$, δ, ppm): 7.69 (s, 1H, -N-C**H**=N-), 7.65 (m, 2H, -C**H**-CH-CH-CH-C**H**-), 7.52 (m, 1H, -C**H**=CH-CO-O-), 7.40 (m, 2H, -CH-C**H**-CH-C**H**-CH-), 7.07 (m, 1H, -CH-CH-C**H**-CH-CH-), 6.97 (d, 1H, -N-C**H**=CH-N-), 6.42 (d, 1H, N-CH=C**H**-N), 6.38 (d, 1H, -CH-C**H**-CO-O-), 4.45 (t, 2H, -N-CH_2-C**H_2**-O-), 4.25 (t, 2H, -N-C**H_2**-CH_2-O-). Mass Spec: 242.1055, $C_{14}H_{14}N_2O_2$.

3.2.3 Synthesis of 2-(1*H*-Imidazol-1-yl)Ethyl But-2-Enoate

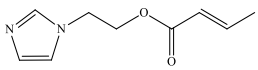

Crotonoyl chloride (2.75g, 26.31mmol, 1.2eq.) and 1-(2-hydroxyethyl)imidazole (2.5g, 22.30mmol, 1eq.) were dissolved individually in dichloromethane (DCM). In an isopropanol bath, dissolved crotonoyl chloride was added drop-wise to the dissolved 1-(2-hydroxyethyl)imidazole and allowed to stir overnight at room temperature. DCM was removed by vacuum and the residual oil dissolved in H_2O. The solution was acidified with oxalic acid and washed with ethyl acetate. Subsequently, the solution was basified with sodium hydroxide and extracted with ethyl acetate. The off-white crystals were removed by Kugelrohr and dried *in vacuo*. The product 2-(1*H*-Imidazol-1-yl)ethyl but-2-enoate had a 52% yield. ^{1}H NMR ($CDCl_3$, δ, ppm): 7.70 (s, 1H, -N-C**H**=N-), 7.00 (d, 1H, -N-C**H**=CH-N-), 6.52 (d, 1H, N-CH=C**H**-N), 6.90 (m, 1H, -CH_3-C**H**=CH-), 5.78 (d, 1H, -CH_3-CH=C**H**-), 4.45 (t, 2H, -N-CH_2-C**H$_2$**-O-), 4.25 (t, 2H, -N-C**H$_2$**-CH_2-O-), 1.95 (3H, dd, C**H$_3$**-). Mass Spec: 180.1027, $C_9H_{12}N_2O_2$.

3.2.4 Synthesis of 1-(undec-10-en-1-yl)-1*H*-Imidzole

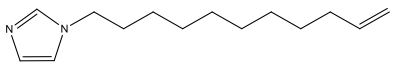

Imidazole (1.31g, 19.8mmol) and Bu_4NBr (0.606g, 1.98mmol) were added to a solution of NaOH (12.50g, 312.5mmol), water (12.50g) and THF (60mL). Then 1-bromoundecene (4.35g, 18.64mmol) was added and allowed to react for 16 hours at 60°C. Upon cooling, THF was removed by rotary evaporation and the product extracted three times with DCM. The organic layer was dried with magnesium sulfate and the filtrate concentrated by rotary evaporation to obtain a pale yellow oil. The product 1-(undec-10-en-1-yl)-1*H*-Imidzole had a 98% yield. ^{1}H NMR ($CDCl_3$, δ, ppm): 7.40 (s, 1H, -N-C**H**-N-), 7.00 (s, 1H, -N-C**H**=CH-N-), 6.85 (s, 1H, -N-CH=C**H**-N-), 5.75 (ddt, 1H, -CH_2-C**H**=CH_2), 4.90 (dd, 2H, -CH_2-CH=C**H$_2$**), 3.86 (t, 2H), 1.98 (dd, 2H), 1.71 (t, 2H), 1.22-1.32 (m, 12H).

3.2.5 Synthesis of 2-(1*H*-Imidzole-1-yl)Ethyl Methacrylate

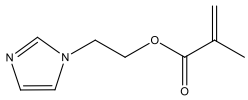

1-(2-Hydroxyethyl)imidazole (0.121g, 1.076mmol) was dissolved in dichloromethane (5mL) and purged of oxygen with nitrogen gas. Methacryloyl chloride (0.169g, 1.614mmol, 1.5eq.) dissolved in dichloromethane (5mL) was added drop-wise to the flask and stirred overnight at room temperature. DCM was removed by rotary evaporation and the resulting imidazolium chloride salt dissolved in water. The solution was then acidified with oxalic acid and washed with ethyl acetate. The solution was then basified

with sodium carbonate and the pale yellow oil product extracted with excess toluene and recovered after distillation of the toluene solvent. The product 2-(1*H*-Imidzole-1-yl)ethyl methacrylate had a 42% yield. ^{1}H NMR ($CDCl_3$, δ, ppm): 7.50 (s, 1H, -N-C**H**-N-), 7.07 (s, 1H, -N-C**H**=CH-N-), 6.95 (s, 1H, -N-CH=C**H**-N-), 6.08 (s, 1H, -OOC-C(CH_3)=CH-**H_{trans}**), 5.60 (s, 1H, -OOC-C(CH_3)=CH-**H_{cis}**), 4.38 (t, 2H, -N-C**H_2**-CH_2-COO-), 4.23 (t, 2H, -N-CH_2-C**H_2**-COO-), 1.92 (s, 3H, -OOC-C(C**H_3**)=CH_2).

3.2.6 Synthesis of IMS-g-Cinnamate (IMS-g-Cin)

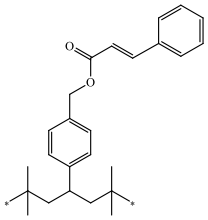

BIMS (20g, 0.22 mmol/g benzylic bromide) dissolved in THF (250mL) was reacted with *trans*-Cinammic acid (1.3038g, 8.80mmol, 2eq.), KOH (3eq., 0.7406g) and TBAB (0.7092g, 0.5g) for 24 hours at 65°C. The product was obtained by precipitating the solution in excess acetone, purifying by dissolution/precipitation using THF/acetone and drying *in vacuo*. ^{1}H NMR ($CDCl_3$, δ, ppm): 7.75 (d, 2H, Ph-C**H_2**-O-), 7.50-6.90 (m, 5H, C_6**H_5**), 6.50 (d, 1H, -CO-C**H**=CH-), 5.20 (s, 2H, Ph-C**H_2**-O-), and the residual brominated *para*-methylstyrene mer: 4.49 (s, 2H), 4.45 (s, 2H).

3.2.7 Synthesis of IMS-g-Crotonate (IMS-g-Crot)

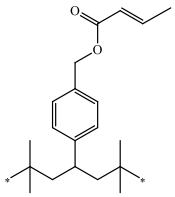

BIMS (20g, 0.22 mmol/g benzylic bromide) dissolved in THF (250mL) was reacted with crotonic acid (0.7576g, 8.80mmol, 2eq.), KOH (0.7406g, 3eq.) and TBAB (0.7092g, 0.5eq.) for 24 hours at 65°C. The product was obtained by precipitating the solution in excess acetone, purifying by dissolution/precipitation using THF/acetone and drying *in vacuo*. ^{1}H NMR ($CDCl_3$, δ, ppm): 6.70 (d, 2H, Ph-C**H_2**-O-), 5.87 (d, 1H, -CO-C**H**=CH–CH_3), δ 5.10 (s, 2H, Ph-C**H_2**-O-), and the residual brominated *para*-methylstyrene mer: 4.49 (s, 2H), 4.45 (s, 2H).

3.2.8 Synthesis of IMS-g-Undecenoate (IMS-g-Un)

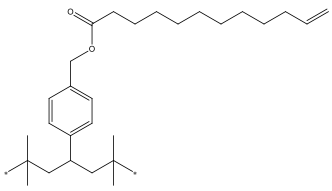

10-Undecenoic acid (0.88g, 3.7mmol) was reacted with a 1M solution of Bu_4NOH in methanol (4.8mL, 4.8mmol Bu_4NOH) to yield the desired Bu_4Ncarboxylate salt, and isolated by removing methanol under vacuum. BIMS (10g, 0.22 mmol/g benzylic bromide) dissolved in toluene (100mL) was reacted with the Bu_4Ncarboxylate salt (1.955g, 4.6mmol, 2eq.) at 100 °C for 5 hours. The product was obtained by precipitating the solution in

excess acetone, purifying by dissolution/precipitation using THF/acetone and drying *in vacuo*. ^{1}H NMR ($CDCl_3$, δ, ppm): 5.73 (ddt, 1H, -CH_2-C**H**=CH_2), 4.99 (s, 2H, Ph-**CH_2**-OOC-), 4.88 (dd, 2H, -CH_2-CH=C**H_2**), 3.68 (t, 2H, -OOC-C**H_2**-CH_2-), and the residual brominated *para*-methylstyrene mer: 4.49 (s, 2H), 4.45 (s, 2H).

3.2.9 Synthesis of IMS-g-Methacrylate (IMS-g-MA)

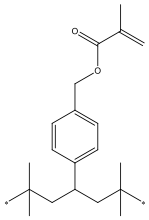

BIMS (20g, 0.22 mmol/g benzylic bromide) dissolved in THF (250mL) was reacted with methacrylic acid (0.76g, 8.83mmol, 2eq.), KOH (0.7406g, 3eq.) and TBAB (0.7092g, 0.5eq.) for 24 hours at 65°C. The product was obtained by precipitating the solution in excess acetone, purifying by dissolution/precipitation using THF/acetone and drying *in vacuo*. ^{1}H NMR ($CDCl_3$, δ, ppm): 6.08 (s, 1H, -C(CH_3)=CH-**H_{trans}**), 5.50 (s, 1H, -C(CH_3)=CH-**H_{cis}**), 5.01 (s, 2H, -Ph-C**H_2**-O-), and the residual brominated *para*-methylstyrene mer: 4.49 (s, 2H), 4.45 (s, 2H).

3.2.10 Synthesis of IMS-g-Acetate (IMS-g-Ac)

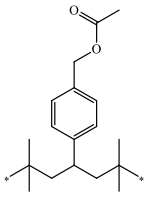

BIMS (12g, 0.22 mmol/g benzylic bromide) dissolved in THF (140mL) was reacted with tetrabutylammonium acetate (1.592g, 5.28mmol, 2eq.) for 24 hours at 65°C. The product was obtained by precipitating the solution in excess acetone, purifying by dissolution/precipitation using THF/acetone and drying *in vacuo*. ^{1}H NMR ($CDCl_3$, δ, ppm): 5.01 (s, 2H, -Ph-C**H_2**-O-), and the residual brominated *para*-methylstyrene mer: 4.49 (s, 2H), 4.45 (s, 2H).

3.2.11 Synthesis of IMS-g-3,3-Dimethylbutyrate (IMS-g-*t*BuAc)

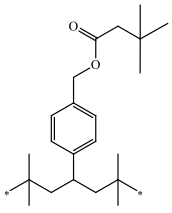

BIMS (12g, 0.22 mmol/g allylic bromide) dissolved in THF(140 mL) was reacted with 3,3-dimethyl butyric acid (0.6133g, 5.28mmol, 2eq.), KOH (0.4444g, 3eq.) and TBAB (0.5eq, 0.4255g) for 24 hours at 65°C. The product was obtained by precipitating the solution in excess acetone, purifying by dissolution/precipitation using THF/acetone and drying *in vacuo*. ^{1}H NMR ($CDCl_3$, δ, ppm): 5.01 (s, 2H, -Ph-C**H_2**-O-), 2.25 (m, 2H, -CO-C**H_2**-), and the residual brominated *para*-methylstyrene mer: 4.49 (s, 2H), 4.45 (s, 2H).

3.2.12 Synthesis of IIR-g-Cinnamate (IIR-g-Cin)

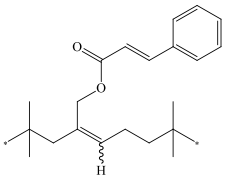

BIIR (20g, 0.15 mmol/g allylic bromide) dissolved in toluene (200mL) was reacted with *trans*-cinammic acid (0.8890g, 6.00mmol, 2eq.), KOH (0.5050g, 3eq.) and TBAB (0.4836g, 0.5eq.) for 24 hours at 100°C. The product was obtained by precipitating the solution in excess acetone, purifying by dissolution/precipitation using THF/acetone and drying *in vacuo*. ^{1}H NMR ($CDCl_3$, δ, ppm): 7.70 (d, 1H, Ph-C**H**=CH-CO-), 7.60-7.10 (m, 5H, C_6**H**$_5$), 6.40 (d, 1H, Ph-CH=C**H**-CO-), 4.72 (s, 2H, E-ester, =CH-C**H**$_2$-OCO-), 4.62 (s, 2H, Z ester, =CH-C**H**$_2$-OCO-).

3.2.13 Synthesis of IIR-g-Crotonate (IIR-g-Crot)

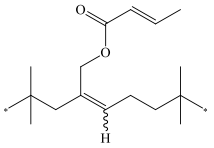

BIIR (20g, 0.15 mmol/g allylic bromide) dissolved in toluene (200mL) was reacted with crotonic acid (0.5165g, 6.00mmol, 2eq.), KOH (3eq., 0.5050g) and TBAB (0.5eq, 0.4836g) for 24 hours at 100°C. The product was obtained by precipitating the solution in excess acetone, purifying by dissolution/precipitation using THF/acetone and drying *in vacuo*. ^{1}H NMR ($CDCl_3$, δ, ppm): 6.92 (m, 1H, -CH=C**H**-CH_3), 5.95 (d, 1H, -CO-C**H**=CH-), 4.65 (s, 2H, E-ester, =CH-C**H**$_2$-OCO-), 4.60 (s, 2H, Z ester, =CH-C**H**$_2$-OCO-).

3.2.14 Synthesis of IIR-g-Undecenoate (IIR-g-Un)

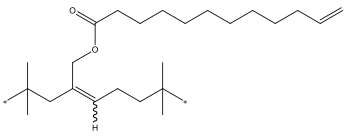

10-Undecenoic acid (0.88g, 3.7mmol) was reacted with a 1M solution of Bu_4NOH in methanol (4.8ml, 4.8mmol Bu_4NOH) to yield the desired Bu_4Ncarboxylate salt, and isolated by removing methanol under vacuum. BIIR (16g, 0.15 mmol/g allylic bromide) dissolved in toluene (160 mL) was reacted with Bu_4NBr (0.77g, 2.4mmol) at 85 °C for 3 hours. The solution was then reacted with the Bu_4Ncarboxylate salt (2.04g, 4.8mmol) for another hour at 85 °C. The product was obtained by precipitating the solution in excess acetone, purifying by dissolution/precipitation using THF/acetone and drying *in vacuo*. ^{1}H-NMR ($CDCl_3$, δ, ppm): 5.68 (m, 1H, -CH_2=C**H**-CH2-, 1H), 4.85 (d, 1H, C**H**$_2$=CH-), 4.79 (d, 1H, C**H**$_2$=CH-), 4.56 (s, 2H, Z ester, =CH-C**H**$_2$-OCO-), 4.51 (s, 2H, E-ester, =CH-C**H**$_2$-OCO-).

3.2.15 Synthesis of IIR-g-Methacrylate (IIR-g-MA)

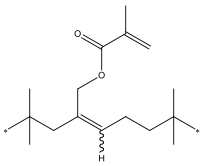

Methacrylic acid (0.322g, 3.7mmol) was treated with a 1M solution of Bu_4NOH in methanol (3.7ml, 3.7mmol Bu_4NOH) to yield the desired Bu_4Ncarboxylate salt, and isolated by removing methanol under vacuum. BIIR (11g, 0.15 mmol/g allylic bromide) dissolved in toluene (100 mL) was reacted with Bu_4NBr (0.53g, 1.65mmol) at 85 °C for 3 hours. The Bu_4Ncarboxylate salt (1.2g, 3.7mmol) was added before heating the reaction mixture to 85 °C for an hour. The product was obtained by precipitating the solution in excess acetone, purifying by dissolution/precipitation using hexanes/acetone and drying *in vacuo*. ^{1}H-NMR ($CDCl_3$, δ, ppm): 6.03 (s, 1H, C**H**$_2$=C(CH_3)-COO-, 1H), 5.47 (s, 1H, C**H**$_2$=C(CH_3)-COO-, 1H), 4.56 (s, 2H, Z ester, =CH-C**H$_2$**-OCO-), 4.51 (s, 2H, E-ester, =CH-C**H$_2$**-OCO-, 2H, s), 3.36 (s, 3H, (CH_2=C(C**H$_3$**)-COO-, 3H).

3.2.16 Synthesis of IMS-g-2-(1H-Imidazol-1-yl)Ethyl Cinnamate (IMS-g-ImCin)

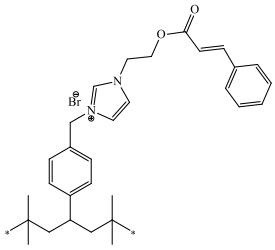

BIMS (20g, 0.22 mmol/g benzylic bromide) dissolved in $CHCl_3$ (250mL) was reacted with 2-(1-H-imidazol-1-yl)ethyl cinnamate (2.13g, 8.79mmol, 2eq.) for 72 hours at 60°C. The product was obtained by precipitating the solution in excess methanol, purifying by dissolution/precipitation using THF/methanol and drying *in vacuo*. ^{1}H NMR ($CDCl_3$ + 5 wt% CD_3OD, δ, ppm): 6.83 (d, 1H, -CO-C**H**=CH-Ph), 5.46 (s, 2H, Ph-**CH$_2$**-N$^+$-), 4.70 (t, 2H, -N-C**H**$_2$-CH_2-COO-), 4.56 (t, 2H, -N-CH_2-C**H**$_2$-COO-), and the residual brominated *para*-methylstyrene mer: 4.49 (s, 2H), 4.45 (s, 2H).

3.2.17 Synthesis of IMS-g-2-(1-H-Imidazol-1-yl)Ethyl But-2-Enoate (IMS-g-ImCrot)

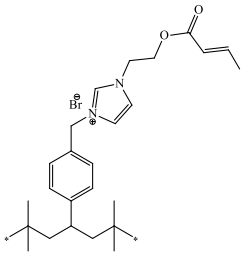

BIMS (20 g, 0.22 mmol/g benzylic bromide) dissolved in $CHCl_3$ (250mL) was reacted with 2-(1-H-imidazol-1-yl)ethyl but-2-enoate (1.58g, 8.80mmol, 2eq.,) for 72 hours at 60°C. The product was obtained by precipitating the solution in excess methanol, purifying by dissolution/precipitation using THF/methanol and drying *in vacuo*. ^{1}H NMR ($CDCl_3$ + 5 wt% CD_3OD, δ, ppm): 5.83 (m, 1H, -CO-C**H**=CH-CH_3), 5.45 (s, 2H, Ph-**CH$_2$**-N$^+$-), 4.65 (t, 2H, -N-C**H**$_2$-CH_2-COO-), 4.48 (t, 2H, -N-CH_2-C**H**$_2$-COO-), and the residual brominated *para*-methylstyrene mer: 4.49 (s, 2H), 4.45 (s, 2H).

3.2.18 Synthesis of IMS-g-1-(Undec-10-En-1yl)-1H-Imidzole (IMS-g-ImUn)

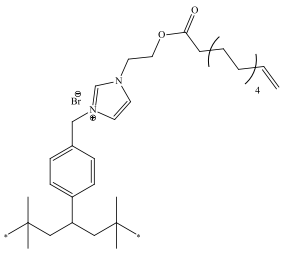

BIMS (40g, 0.22 mmol/g benzylic bromide) was mixed with 1-(undec-10-En-1yl)-1H-Imidazole (2.230g, 10.12mmol, 1.1eq.) at 100 °C and 30 rpm using a Haake Polylab R600 internal batch mixer. ^{1}H NMR ($CDCl_3$ + 5 wt% CD_3OD, δ, ppm): 10.22 (s, 1H, -N^+-C**H**-N-), 5.80 (ddt, 1H, -CH_2-C**H**=CH_2), 5.48 (s, 2H, Ph-**CH_2**-N^+-), 4.95 (dd, 2H, -CH_2-CH=C**H_2**), 4.30 (dd, 2H, -N-C**H_2**-CH_2-O-), and the residual brominated *para*-methylstyrene mer: 4.49 (s, 2H), 4.45 (s, 2H).

3.2.19 Synthesis of IMS-g-2-(1H-Imidzole-1-yl)Ethyl Methacrylate (IMS-g-ImMA)

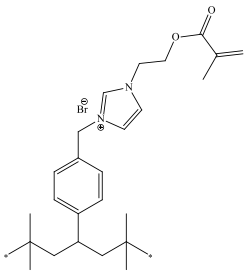

BIMS (10g, 0.22 mmol/g benzylic bromide) dissolved in chlorobenzene (100mL) was reacted with 2-(1H-imidazol-1-yl)ethyl methacrylate (0.829g, 4.6mmol, 2eq.) for 7 hours at 100 °C. The product was obtained by precipitating the solution in excess acetone, purifying by dissolution/precipitation using THF/acetone and drying *in vacuo*. ^{1}H NMR ($CDCl_3$ + 5 wt% CD_3OD, δ, ppm): 9.94 (s, 1H, -N^+-C**H**-N-), 6.08 (s, 1H, -OOC-C(CH_3)=CH-**H_{trans}**), 5.60 (s, 1H, -OOC-C(CH_3)=CH-**H_{cis}**), 5.39 (s, 2H, Ph-C**H_2**-N^+-), 4.70 (t, 2H, -N-C**H_2**-CH_2-COO-), 4.54 (t, 2H, -N-CH_2-C**H_2**-COO-), and the residual brominated *para*-methylstyrene mer: 4.49 (s, 2H), 4.45 (s, 2H).

3.2.20 Synthesis of IIR-g-2-(1H-Imidazol-1-yl)Ethyl Cinnamate (IIR-g-ImCin)

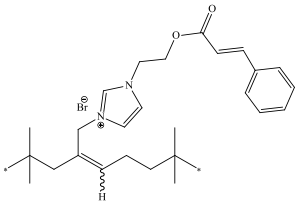

BIMS (20g, 0.15 mmol/g allylic bromide) dissolved in $CHCl_3$ (250mL) was reacted with 2-(1-H-imidazol-1-yl)ethyl cinnamate (2.13g, 8.79mmol, 2eq.) for 6 days at 60°C. The product was obtained by precipitating the solution in excess acetone, purifying by dissolution/precipitation using THF/acetone and drying *in vacuo*. ^{1}H NMR ($CDCl_3$ + 5 wt% CD_3OD, δ, ppm): 6.83 (d, 1H, -CO-C**H**=CH-Ph), 5.44 (s, 2H, Ph-**CH_2**-N^+-), 5.10 (t, 2H, -N-C**H_2**-CH_2-COO-), 4.90 (t, 2H, -N-CH_2-C**H_2**-COO-), 4.56 (s, 2H, Z ester, =CH-C**H_2**-OCO-), 4.51 (s, 2H, E-ester, =CH-C**H_2**-OCO-).

3.2.21 Synthesis of IIR-g-2-(1-*H*-Imidazol-1-yl)Ethyl But-2-Enoate (IIR-g-ImCrot)

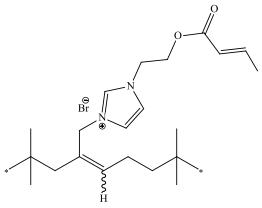

BIMS (20 g, 0.15 mmol/g allylic bromide) dissolved in $CHCl_3$ (250mL) was reacted with 2-(1-*H*-imidazol-1-yl)ethyl but-2-enoate (1.58g, 8.80mmol, 2eq.,) for 6 days at 60°C. The product was obtained by precipitating the solution in excess acetone, purifying by dissolution/precipitation using THF/acetone and drying *in vacuo*. ^{1}H NMR ($CDCl_3$ + 5 wt% CD_3OD, δ, ppm): 7.53 (m, 1H, -CO-C**H**=CH-CH_3), 7.10 (d, 1H, N^+-C**H**=CH-N-), 6.90 (d, 1H, N^+-CH=C**H**-N-), 5.45 (s, 2H, Ph-**CH_2**-N^+-), 4.56 (s, 2H, Z ester, =CH-C**H_2**-OCO-), 4.51 (s, 2H, E-ester, =CH-C**H_2**-OCO-), 4.38 (t, 2H, -N-C**H_2**-CH_2-COO-), 3.90 (t, 2H, -N-CH_2-C**H_2**-COO-).

3.2.22 Synthesis of IIR-g-1-(Undec-10-en-1-yl)-1*H*-Imidzole (IIR-g-ImUn)

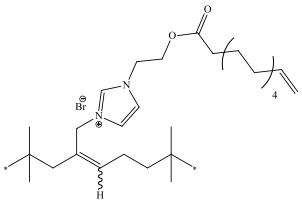

BIIR (20g, 0.15 mmol/g allylic bromide) dissolved in $CHCl_3$ (250mL) was reacted with 1-(undec-10-En-1yl)-1*H*-Imidazole (1.12g, 5.06mmol, 1.1eq.) for 5 days at 60 °C. The product was obtained by precipitating the solution in excess acetone, purifying by dissolution/precipitation using THF/acetone and drying *in vacuo*. ^{1}H NMR ($CDCl_3$ + 5 wt% CD_3OD, δ, ppm): 10.20 (s, 1H, -N^+-C**H**-N-), 5.80 (ddt, 1H, -CH_2-C**H**=CH_2), 4.90 (s, 2H, -C**H_2**-N^+-), 4.95 (dd, 2H, -CH_2-CH=C**H_2**), 4.30 (dd, 2H, -N-C**H_2**-CH_2-O-), 4.50 (s, 2H, E-ester, =CH-C**H_2**-OCO-), 4.55 (s, 2H, Z ester, =CH-C**H_2**-OCO-).

3.2.23 Synthesis of IIR-g-2-(1*H*-Imidzole-1-yl)Ethyl Methacrylate (IIR-g-ImMA)

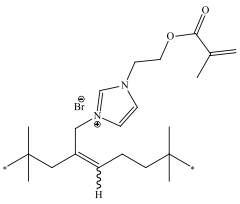

BIMS (20g, 0.15 mmol/g allylic bromide) dissolved in $CHCl_3$ (250mL) was reacted with 2-(1*H*-imidazol-1-yl)ethyl methacrylate (1.658g, 9.2mmol, 2eq.) for 5 days at 60 °C. The product was obtained by precipitating the solution in excess acetone, purifying by dissolution/precipitation with THF/acetone and drying *in vacuo*. ^{1}H NMR ($CDCl_3$ + 5 wt% CD_3OD, δ, ppm): 9.90 (s, 1H, -N^+-C**H**-N-), 6.15 (s, 1H, -OOC-C(CH_3)=CH-**H_{trans}**), 5.80 (s, 1H, -OOC-C(CH_3)=CH-**H_{cis}**), 4.95 (s, 2H, -C**H_2**-N^+-), 4.60 (t, 2H, -N-C**H_2**-CH_2-COO-), 4.45 (t, 2H, -N-CH_2-C**H_2**-COO-).4.50 (s, 2H, E-ester, =CH-C**H_2**-OCO-), 4.55 (s, 2H, Z ester, =CH-C**H_2**-OCO-).

3.2.24 Instrumentation and Analysis

^{1}H-NMR spectra were acquired on a Bruker AM500 spectrometer. The peaks were sharpened by adding deuterated methanol to the ionomer solutions in chloroform, by extending T_2 relaxation times.

Dynamic shear-modulus measurements were obtained using an Alpha Technologies Advanced Polymer Analyzer 2000, operating in a parallel plate configuration. An uncured sample (5.0 g) coated with a measured amount of DCP (0.5 wt %) in acetone was dried then passed through a two-roll mill approximately ten times. This mixed compound was then cured in a rheometer cavity for an hour at 160°C, 3° oscillation arc (30% applied strain) and 1 Hz frequency.

3.3 Results and Discussion

3.3.1 Peroxide-Initiated Crosslinking Dynamics and Yields

It is well understood that polyisobutylene does not cure under the action of peroxides, but degrades through β-scission of alkyl macro-radical intermediates.[4] The extent of degradation reduction in isobutylene-rich copolymers, containing 2-8 mole% isoprene, results from the differences in reactivity of allylic functionality within the unsaturated mers. Xiao et al. have shown that acetate ester derivatives of BIIR also incur significant losses in dynamic storage modulus (G') when treated with dicumyl peroxide (DCP) at 160 °C.[5] The acetate and *t*-butyl acetate derivatives of BIMS (Scheme 3.2 below) demonstrate similar behaviour, as indicated by a decline of G' when compounded with DCP and reacted under identical conditions (Figure 3.1 on page 62). These results confirm that allylic and benzylic ester derivatives of BIIR and BIMS are not cure reactive, and that oligomerizable functionality is required to produce a crosslinkable elastomer.

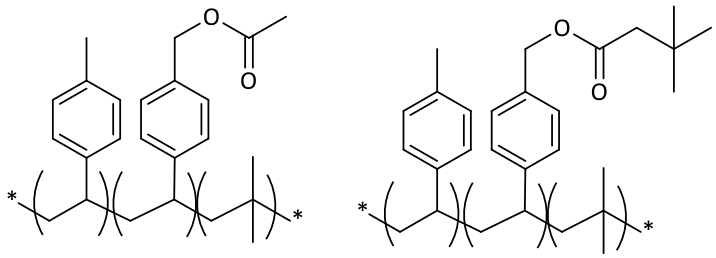

SCHEME 3.2 – Acetate ester derivatives of BIMS

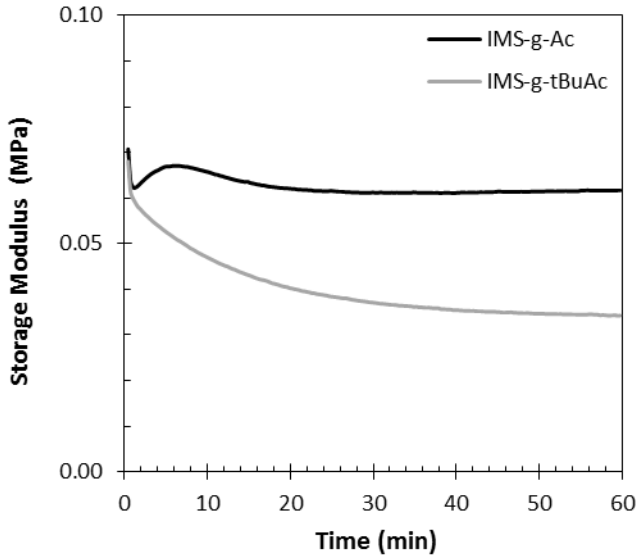

FIGURE 3.1 – Dynamics of peroxide-initiated degradation for acetate and t-butyl acetate derivatives of BIMS (T = 160°C; [DCP] = 18 µmol/g)

Scheme 3-1 on page 52 lists the various synthesized macromonomers, prepared through bromide displacement of BIIR and BIMS by the appropriate carboxylate salt or N-substituted imidazole nucleophile. Produced in quantitative yields, the desired functional groups had no complications from dehydrohalogenation of the starting material. As a result, each material contained 0.15 mmoles or 0.22 mmoles of reactive functionality per gram of BIIR or BIMS derivative, respectively. Note that an efficient macromonomer converts all pendant functional groups into a covalent polymer network when initiated by 0.5 wt% of dicumyl peroxide (DCP) at 160°C. Crosslinking dynamics can be monitored by measuring the dynamic storage modulus (G'), which increases in proportion to covalent network density.

Figure 3.2 on page 63 illustrates the dynamics of peroxide-initiated crosslinking for methacrylate-functionalized macromonomers. Yamazaki and Seguchi[6] have previously demonstrated the cure reactivity of methacrylate ester derivatives of BIMS, while Vikram[7] described the DCP-initiated crosslinking of the corresponding BIIR derivative. Both IMS-g-MA and IIR-g-MA started with a comparatively low storage moduli, and crosslinked to an ultimate G' over similar timescales. However, IMS-g-MA cured to a higher extent, owing to the higher functional group content provided by the BIMS starting material. With 0.22 mmoles of methacrylate functionality per gram of rubber in the BIMS derived elastomer compared to just 0.15 mmoles/g

in the BIIR derivative, expectations were for a more extensive covalent network for the IMS-g-MA system.

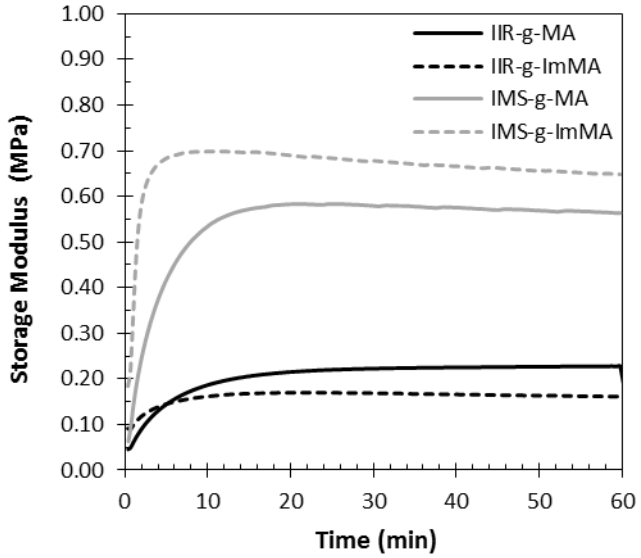

FIGURE 3.2 – Dynamics of peroxide-initiated macromonomer crosslinking for methacrylate-based macromonomer derivatives of BIIR and BIMS (T = 160°C; [DCP] = 18 μmol/g)

The methacrylate functionalized ionomers, IMS-g-ImMA and IIR-g-ImMA, demonstrated higher initial G' values than their non-ionic analogues, owing to the aggregation of imidazolium bromide groups establishing an ionic network. It is reasonable to assume that ion pair aggregation will concentrate methacrylate functionality within the ionomer multiplets, since the oligomerizable groups are covalently bound to imidazole moieties. However, it is difficult to predict how this aggregation might affect crosslinking dynamics and yields, since relatively little is known about the kinetic chain length of macromonomer cures and how many oligomerizable groups comprise a crosslink node in a non-ionic thermoset. The data plotted in Figure 3.2 above reveals a higher initial cure rate for both imidazolium-functionalized macromonomers. This higher crosslinking rate persists in the IMS-g-ImMA system, as the ionomer progresses to a higher ultimate cure extent than IMS-g-MA. However, the initial cure reactivity in IIR-g-ImMA was not sustained and the ionomer reaches a lower crosslink density than IIR-g-ImMA.

Stark differences in the chemistry of BIMS and BIIR derivatives are apparent in the cure performance of undecenoate esters. Unlike methacrylate monomers, unactivated α-olefins are not readily homopolymerized, owing to relatively low propagation rate constants as well as

degradative hydrogen atom transfer arising from hydrogen atom abstraction from the allylic position. As such, the simple undecenoate-based elastomers, IMS-g-Un and IIR-g-Un were not expected to provide exceptional cure activity. Indeed, Vikram[7] has previously demonstrated the meagre crosslinking rate and yield for the BIIR derivative. The data plotted in Figure 3.3 below is consistent with the previous report on IIR-g-Un, showing little evidence of substantial crosslinking when activated with DCP. Interestingly, the IIR-g-ImUn ionomer demonstrated improved cure performance, possibly due to the positive effects of undecenoate ester aggregation within imidazolium bromide multiplets.

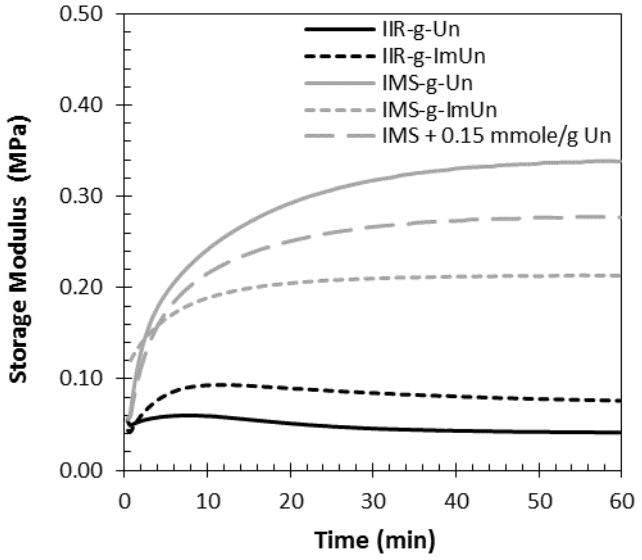

FIGURE 3.3 – Dynamics of peroxide-initiated macromonomer crosslinking for undecenoate-based derivatives of BIIR and BIMS (T = 160°C; [DCP] = 18 µmol/g)

It is clear, however, the undecenoate esters of IMS crosslink with remarkably different efficiencies. The IMS-g-Un system is the most surprising, given its ability to reach a final modulus of G'=0.34 MPa, which is comparable to that attained by the methacrylate-based macromonomers (Figure 3.3 above). The improved cure performance of IMS-g-Un relative to IIR-g-Un was not solely a result of differences in functional group concentration. An IMS-g-Un sample containing 0.15 mmoles undecenoate / g polymer and 0.07 mmoles acetate / g polymer crosslinked extensively, albeit with a slightly lower yield than that observed for the fully functionalized BIMS derivative. Therefore, the inherent reactivity of the IMS-g-Un system is greater than that of its IIR analogue.

The response of the IMS system to the introduction of imidazolium bromide functionality also differed from that of the IIR-based elastomers. Whereas the isobutylene-*co*-isoprene based material containing undecenoate groups benefited from ionic functionality, the cure rate and yield provided by IMS-g-ImUn was substantially lower than that generated by IMS-g-Un. In this case, aggregation of macromonomer functionality retarded the intrinsic reactivity of an IMS polymer backbone coupled to undecenoate ester groups.

These differences persisted in the cinnamate and crotonate ester systems. The IIR derivatives demonstrated poor cure performance while the BIMS derivatives cured to high extent but suffered a loss in reactivity when functionalized with ion pairs (Figure 3.4 below). Note that crotonate and cinnamate monomers are not readily homopolymerized and, as such, their reactivity is expected to mirror that of the undecenoate materials as previously described.

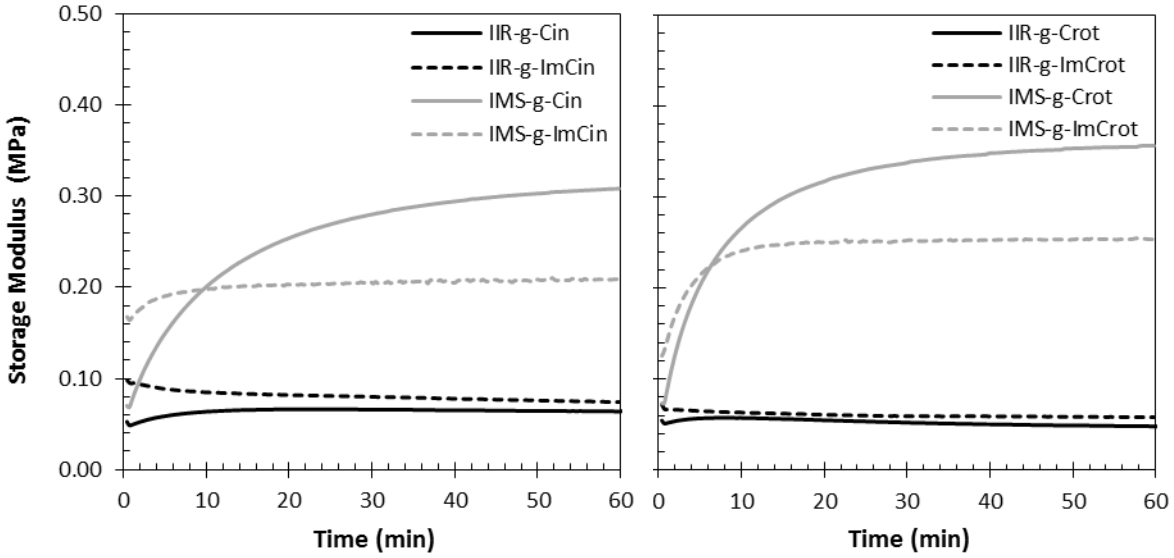

FIGURE 3.4 – Dynamics of peroxide-initiated macromonomer crosslinking for less reactive functional groups on BIIR and BIMS (T = 160°C; [DCP] = 18 µmol/g)

The intention of the synthesis and characterization of the macromonomers illustrated in Scheme 3-1, on page 52, was to generate insight into the effects of ion pair aggregation on cure activity, and assess the differences derived from an IMS-based polymer backbone versus an IIR-based polymer backbone. With respect to the influences of ion pair aggregation, the data clearly demonstrates where cure reactivity is concerned; little technological benefit is realized in moving from a non-ionic macromonomer to an imidazole-functionalized analogue. It appears that the crosslink density a methacrylate-functionalized macromonomer attains through

homopolymerization of its pendant groups does not improve through ion pair aggregation. Less reactive functional groups such as unactivated α-olefins, crotonates and cinnamates are not activated by ionic functionality, and in some cases their cure performance worsens. However, the imidazolium-based macromonomers may have promise where a requirement exists for material properties such as adhesion, filler dispersion and anti-microbial activity.

The reactivity of IMS-g-Un was unexpected, given that α-olefins cannot be homopolymerized with high kinetic chain lengths, and previous studies of IIR-g-UA confirmed little cure activity. The performance of IMS-g-Un is not solely due to higher functional group contents, as demonstrated in Figure 3.3 on page 64. Clearly, since ester derivatives of IMS not bearing C=C bonds do not crosslink (Figure 3.1 on page 62), there exists a particular synergy between the backbone of IMS and α-olefin functionality. The obvious difference between the two starting materials, BIMS and BIIR, is the amount and structure of unhalogenated comonomer groups. Whereas BIIR contains 0.15 mmole/g of unbrominated isoprene mers, BIMS contains 0.51 mmole/g of unbrominated para-methylstyrene mers.

It should be noted that the radical crosslinking of an isobutylene-rich macromonomer is a competitive process between the crosslinking of pendant C=C groups and fragmentation of activated isobutylene-mers. Introducing isoprene unsaturation or para-methylstyrene benzylic sites mitigate the extent of polymer degradation. By directing radical populations away from the primary alkyl radicals that cleave and toward relatively low energy allylic/benzylic radicals that terminate exclusively by combination. Note that both IMS-g-Ac and IMS-g-*t*BuAc did not undergo significant degradation when treated with 0.5 wt% of DCP at 160 °C (Figure 3.1 on page 62). This indicates all ester derivatives of IMS are less susceptible to chain scission than their IIR analogues. This observation does not account for the unique reactivity of IMS-g-UA, only that the "baseline" reactivity of IMS-derivatives is more favourable than that of IIR-derivatives.

A complete understanding of the IMS-g-Un system requires thorough knowledge of the mechanism through which an α-olefin is activated during a peroxide cure. This information is not presently available. However, it is known that allylic monomers such as 1-undecene, propylene and isobutylene engage in radical intermediates through C=C addition (homopolymerization) and allylic hydrogen atom abstraction (degradative chain transfer). Both processes can ultimately yield crosslinks, since macro-radical addition to pendant C=C functionality produces a crosslink point,

as do macro-radical combination with allylic macro-radical intermediates. Note these addition/abstraction pathways of undecenoate esters are operative in the IIR-g-Un system, which do not cure extensively.

The superior reactivity of IMS-g-Un may be attributed to the large concentration of tertiary and primary benzylic sites provided by a high para-methylstyrene content. When only 0.51 mmole/g of unbrominated para-methylstyrene mers are provided, as in the case of IMS-g-Ac, the material is cure neutral (neither degrading nor crosslinking extensively). When an additional 0.22 mmole/g of undecenoate functionality is provided, as in the case of IMS-g-Un, the population of resonance stabilized allylic and benzylic radicals is greatly increased, thereby suppressing polymer backbone fragmentation and heightening the extent of macro-radical combination. This assumes that IMS-g-Un cures essentially through a stoichiometric cure mechanism involving hydrogen atom abstraction from the polymer by peroxide-derived radicals, followed by macro-radical combination to yield the desired covalent crosslinks. Further experimental work is required to test this proposed reaction mechanism.

3.4 Conclusions

Various macromonomers were synthesized and characterized to gain insight into the effects of ion pair aggregation on cure activity, and assess the differences derived from an IMS-based polymer backbone versus an IIR-based polymer backbone. The crosslink density of a methacrylate-functionalized macromonomer does not improve through ion pair aggregation, and less reactive functional groups are not activated by ionic functionality and in some cases, their cure performance worsens. Preparing an imidazole-functionalized macromonomer provides little technological benefit when cure reactivity is concerned, unless material properties such as adhesion, filler dispersion and anti-microbial activity are required.

The subtle differences in chemical functionality and composition distribution of BIIR and BIMS produced substantially different cure characteristics, particularly for macromonomers bearing relatively unreactive oligomerizable functionality. Much is to be learnt from the effects of the tertiary and primary benzylic sites, provided by the high para-methylstyrene content in BIMS, on cure reactivity.

REFERENCES

1. Halliday, L. Ionic polymers. 1st ed. New York: Wiley; 1975.

2. Eisenberg, A., Kim, J.S. Introduction to Ionomers. 1st ed. New York: Wiley; 1998.

3. Ozvald, A., Parent, J.S., Whitney, R.A., Hybrid Ionic/Covalent Polymer Networks Derived from Functional Imidazolium Ionomers, *Journal of Polymer Science Part A: Polymer Chemistry*, **51(11)**, 2438-2444 (2013).

4. Loan, L.D., The Reaction Between Dicumyl Peroxide and Butyl Rubbers, *Journal of Polymer Science: Part A: Polymer Chemistry*, **2**, 2127 – 2134 (1964).

5. Xiao, S., Parent, J.S., Whitney, R.A., Knight, L.K., Synthesis and Characterization of Poly(isobutylene-co-isoprene)-derived Macro-monomers, *Journal of Polymer Science: Part A: Polymer Chemistry*, **48**, 4691 – 4696 (2010).

6. Yamazaki, T. and Seguchi, T., ESR Study on Chemical Crosslinking Reaction Mechanisms of Polyethylene Using a Chemical Agent. IV. Effect of Sulfur- and Phosphorous-type Antioxidants, *Journal of Polymer Science: Part A: Polymer Chemistry*, **38**, 3092–3099 (2000).

7. Vikram, K. "Peroxide Curable Butyl Rubber Derivatives", Ph.D. Thesis, Queen's University, 2012.

CHAPTER 4

PROPERTIES OF A VINYLIMIDAZOLIUM BROMIDE DERIVATIVE OF POLY(ISOBUTYLENE-CO-ISOPRENE) O/W EMULSION

4.1 Introduction

Due to environmental concerns, the development of waterborne coatings continues to be of primary interest to industry. Coatings with zero volatile organic compounds (VOC), external weather durability, good block resistance, fast curing at relatively low temperatures, good adhesion to a variety of substrates and low water sensitivity are just some of the required properties of such coatings. During the past 60 years, emulsion polymerization has been a versatile process in the preparation of a wide variety of water-based coatings.[1] However, high molecular weight, isobutylene-rich elastomers can only be synthesized by cationic polymerization processes that are highly sensitive to moisture. Therefore, emulsions containing this elastomer must be prepared by the post-polymerization approach described in this report. The objective of this phase of the project was to prepare a novel ionomeric emulsion capable of providing the aforementioned coating properties.

Emulsions are colloidal systems consisting of discrete dispersions of droplets of one liquid phase within another immiscible liquid phase, where one is referenced as the oil and the other water. To achieve different characteristics in an emulsion depends on which liquid is in the dispersed phase, commonly present in the form of spherical drops. The classic emulsion types include oil-in-water (O/W) for oil droplets dispersed in water, and water-in-oil (W/O) for water droplets dispersed in oil. Formulating an emulsion (or emulsification) requires a device like a turbine blender, ultrasonicator or the two phases flowing through a membrane, static mixer or porous medium. Another formulation technique is spontaneous emulsification where the two phases make contact through the initiation of a chemical reaction or the nucleation of one phase within another due to a temperature reduction.[2]

Emulsions form by the intimate mixing of an oil and water phase, often in the presence of a surfactant. Surfactants, molecules with polar and non-polar chemical groups in their structure, control the size of the dispersed particles and confer stability on the emulsion. The

surfactant absorbs at the interface between the two phases and lowers the interfacial tension between the phases, hence facilitating the formation of the emulsion (usually by the input of mechanical energy). Subsequently, the surfactant stabilizes droplets against coalescence by providing electrostatic and steric barriers.[2] Note, however, that most surfactants are not reactive and not covalently bound to a particle surface. This can result in a lack of stability of the latex under some specific constraints such as high ionic strength, freezing or high shearing. When exposed to water or high humidity, the formed films lack high water rebound adhesivity and low-dimensional stability. These phenomena result when surfactants desorb from the particle surface under these constraints, migrate towards the film surface or give rise to hydrophilic domains within the film upon phase separation.[1]

One means of avoiding these difficulties is to use a polymerizable surfactant that chemically binds to latex particles. The surfmer employed in this work was 3-dodecyl-1-vinylimidazolium bromide, with a chemical structure similar to the functionalized ionomer rendered into the emulsion, vinylimidazolium bromide grafted poly(isobutylene-co-isoprene).[3] This surfmer can plasticize the ionomer, increase the extent of a free radical cure, provide additional ionic functionality to the material, deliver a reactive anion to the formulation through anion metathesis and, most importantly, stabilize the emulsion against coagulation. An advantage for this class of surfactants is its engagement of the polymer in co-curing and eliminating the potential for leaching from the vulcanizate.

Since butyl rubber shows no natural hydrophilic propensity, brute mechanical dispersion is needed to convert the solid polymer into an aqueous dispersion. Lord Corporation is the sole manufacturer of Aqualast® BL-100 aqueous butyl elastomer emulsion. Production of this emulsion begins by rendering the butyl polymer into a workable cement phase. Subsequently, while in an aqueous phase, surfactants and additional stabilizers assist in the emulsification process during which time the raw components convert to a submicron-size, homogeneous raw latex. The raw latex is stripped and concentrated, providing a stable aqueous emulsion of butyl rubber.

The objective of this work is to formulate an O/W emulsion from a vinylimidazolium bromide derivative of poly(isobutylene-*co*-isoprene) (IIR-VImBr) with the use of a (3-dodecyl)-1-vinylimidazolium bromide polymerizable surfmer. The final emulsion targets adhesive surface-coating applications requiring interfacial bonding or curing and anti-microbial

properties in various conditions and environments. This report describes the preparation of this emulsion, and provides details of its particle size distribution, zeta potential, viscosity, solids content, pH, resistance to centrifugation, stability towards freeze/thaw cycles and the critical micelle concentration of the surfmer. Latex-derived ionomer films are characterized via solid-state rheology, tensile analysis, resistance to adsorption and deformation when immersed in water, and gravimetric analysis of leachables/extractables.

4.2 Experimental

4.2.1 Materials

Brominated poly(isobutylene-co-isoprene) (BIIR or BB2030, MN = 400 000 g/mol, polydispersity = 1.5, 0.15 mmol allylic bromide functionality/g BIIR) was used as supplied by LANXESS Inc. (Sarnia, Ontario). The 1-vinylimidazole (Vim, ≥ 99%), 1-bromododecane (98%), ethyl acetate (spectrophotometric grade), hexanes (anhydrous, 95%), hexyl alcohol (≥98%), chloroform-d (99.8%D), methanol-d4 (99.8%D), DMSO-d6 (99.9%D) and dicumyl peroxide (DCP, 98%) were used as received from Sigma-Aldrich (Oakville, Ontario).

4.2.2 Synthesis of IIR-VImBr

BIIR (120 g, 18.0 mmol allylic bromide) dissolved in toluene (1200 mL, 10 wt%) was reacted with VIm (10.16 g, 108.0 mmol, 6 eq.) for 50 hours at 100°C. The N-alkylation product was obtained by precipitation using excess acetone, purified by dissolution/precipitation using tetrahydrofuran/acetone and dried *in vacuo*. The product IIR-VImBr had a 75% conversion corresponding to an ion content of 0.11 mmol/g. The degree of N-alkylation was quantified by integrating the normalized ^{1}H NMR spectra to an estimated accuracy of ± 5%. ^{1}H NMR ($CDCl_3$ + 5 wt% CD_3OD): δ 11.53 (s, 1H, –N^+–C**H**–N–), 7.61 (s, 1H, –N^+–CH=C**H**–N–), 7.42 (dd, 1H, –N–C**H**=CH_2), 5.80 (dd, 1H, N–CH=CH–$\mathbf{H_{trans}}$), 5.41 (dd, 1H, N–CH=CH–$\mathbf{H_{cis}}$), *Z*-isomer: δ 7.16 (s, 1H, *Z*, –N^+–C**H**=CH–N–), 5.69 (t, 1H, *Z*, CH_2–C=C**H**–CH_2), 4.91 (s, 2H, –C–C$\mathbf{H_2}$–N^+), *E*-isomer: δ 7.20 (s, 1H, *E*, –N^+–C**H**=CH–N–), 5.68 (t, 1H, *E*, CH_2–C=C**H**–CH_2), 4.84 (s, 2H, *E*, –C–C$\mathbf{H_2}$–N^+). Conjugated dienes: δ 5.98 (d, 1H, exo-diene), 5.92 (d, 1H, endo-diene). Residual isoprene: δ 5.04 (t, 1H, CH_3–C=CH–CH_2-).[4]

4.2.3 Synthesis of 3-Dodecyl-1-Vinylimidazolium Bromide

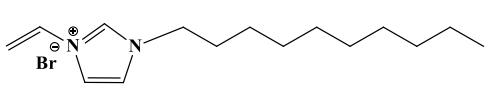

After combining 1-vinylimidazole (2.000 g), 1-bromododecane (6.582 g) and ethyl acetate (5.0 mL, spectrophotometric grade) the solution was stirred at room temperature for 12 hours. Subsequently, the solution was reacted at 55°C for 24 hours. After a cool-down, the white precipitate was filtered-off and washed several times with ethyl acetate (spectrophotometric grade) and the solid product dried *in vacuo*. ^{1}H NMR (DMSO-d_6, δ, ppm): 9.53 (s, 1H, -N^+-C**H**-N-), 8.21 (d, 1H, CH_2=C**H**-N^+-), 7.94 (d, 1H, -N^+-C**H**=CH-N-), 7.30 (d, 1H, -N^+-CH=C**H**-N-), 5.96 (dd, 1H, C**H**$_2$=CH-N^+-), 5.42 (dd, 1H, C**H**$_2$=CH-N^+-), 4.19 (t, 2H, -N-C**H$_2$**-CH_2-), 1.80 (m, 2H, N-CH_2-C**H$_2$**-), 1.24 (m, 14H, -N-CH_2-CH_2-(C**H$_2$**)$_7$-CH_3), 0.85 (t, 3H, -CH_2-C**H$_3$**). Mass Spec: 263.2487(M^+), $C_{17}H_{31}N_2$, mp: 47°C.[5]

4.2.4 IIR-VImBr Emulsion Formulation

IIR-VImBr (5 g) and dicumyl peroxide (DCP, 0.2 wt% organic content, 0.01 g) were dissolved in hexanol (5 g) and hexanes (20 g). The 3-dodecyl-1-vinylimidazolium bromide surfmer (15 wt% ionomer content, 0.75 g) was dissolved in distilled water (25.0 g) and added to the ionomer solution. The emulsion was sonicated (3 minutes, 50 – micro-tip limit power output) to achieve a white milky solution. The solvents and water (10%) were removed under vacuum without allowing the rubber to precipitate.

4.2.5 Preparation of Film

The emulsion solution was poured into a glass dish (20 cm x 14 cm), in thin layers, allowed to dry in a fume hood and then additional layering followed until consuming the solution. This procedure prevents bubble formation and limits non-uniformities in the film.

4.2.6 Preparation of Cured Film

The film was placed on a metal plate (sprayed with silicone oil) in a compression mold apparatus [0.2 wt% organic content, 160°C, 25 min ($5t^{1/2}$ for DCP)] with the top plate 2 millimetres from the surface of the film, providing a final cured sheet with a thickness of 0.32 ± 0.05 mm.

4.3 Analysis

NMR characterization utilized the Bruker AM500 instrument with chemical shifts (δ) reported relative to tetramethylsilane in ppm. The peaks for the ^{1}H NMR were sharpened by adding deuterated methanol to the ionomer solutions in chloroform, by extending T^2 relaxation times. A Waters/Micromass GC-T TOF mass spectrometer, operating in electron impact mode, was utilized in acquiring high-resolution mass spectrometry data needed in this study.

Conductivity of the surfactant was measured with a potentiometer (CDM210 Conductivity Meter, Radiometer analytical MeterLab). Measurements began with a concentrated stirred solution of surfactant and deionized water at 25°C. The solution was diluted (5mL deionised water) and conductivity measured each time. This continued until observing an abrupt change in the conductivity (mS/cm) vs. concentration (mol/L) plot. In dilute solutions, ionic surfactants act as individual ions. At a concentration above the critical value, known as the critical micelle concentration (CMC), surfactant molecules aggregate forming micelles. An abrupt change in conductivity, surface tension, and osmotic pressure occurs at the CMC of a surfactant due to micelle formation.

Measuring particle size and distribution of the colloidal particles requires the employment of a Dynamic Light Scattering (DLS) instrument (Zetasizer Nano Series by Malvern Instruments). A few drops of the final emulsion product were diluted by filling the disposable plastic cuvette with deionized water to the maximum limit. The contents were inserted into the DLS instrument for analysis, in triplicate. The DLS measures Brownian motion by illuminating the particles with a laser and analyzing the fluctuation intensity of the scattered light. Brownian motion occurs when liquid dispersed particles undergo random movements caused by liquid molecule bombardment, where smaller particles diffuse through the fluid faster than larger particles. Particle size with the respective standard deviation value was measured with an auto-correlator and mathematical algorithms directly by the instrument.

To produce a stable emulsion an emulsifying agent is added to alter the rate of coalescence by creating an interfacial film, which acts as a barrier or produces repulsive electrical forces between approaching droplets. A monolayer of surfactant is absorbed and a double-layer of ionic emulsifiers build around the droplets. The double layer consists of the charged portion of the emulsifier at the water interface and of the surrounding counterions. If the counterion

concentration is low and the thickness of the electrical double layer is large, long-range repulsive forces form causing droplets to repel one another on approach. The potential produced by the double-layer creates a repulsive effect between the oil droplets, hindering coalescence. The repulsive electrical-potential at the emulsion interface is indirectly calculable and the related quantity, or zeta potential, is directly determined.[6] Zeta potential is predominantly determined by measuring the electrophoretic mobility of the dispersed particles in a charged field. Other instruments used in determining this value include an electrophoretic mass transport analyzer, streaming current detector and electrokinetic sonic amplitude device. The Zetasizer Nano series calculates the zeta potential by determining the electrophoretic mobility and then applying the Henry equation. A few drops of the final emulsion product were diluted using deionized water in a disposable 'dip' cell then placed into the instrument with sample analysis taken in triplicate. The 'dip' cell had electrodes at either end to which a potential was applied. To obtain the electrophoretic mobility an electrophoresis experiment [using Laser Doppler Velocimetry (LDV)] was performed on the sample to measure the velocity (expressed in unit field strength) of the moving particles towards the electrode of the opposite charge.

Measurement of the viscosity is important since Stoke's law asserts that the rate of phase separation (v) between liquid 1 (ρ_1 $\boldsymbol{\rho_1}$) and liquid 2 (ρ_2 $\boldsymbol{\rho_2}$) depends on the gravity (g $\mathbf{g}$), radius of the particles (r $\mathbf{r}$) and viscosity (η $\boldsymbol{\eta}$) of the medium.

$$v = \frac{2r^2(\rho_1 - \rho_2)g}{9\eta} \qquad (1)$$

The viscosity of the emulsion (20 mL) was measured with a rotating spindle viscometer (PV-E Viscometer, Brookfield, spindle no. 62) at a stirring rate of 100 rpm. Latex is a non-Newtonian fluid where the viscosity becomes shear-dependent. In practice, the viscosity of an emulsion limits the solids content of a latex. For a monodisperse latex, viscosity approaches infinity as the volume fraction of the polymer particles approaches 0.64. Alternately, a polydisperse latex displays a low viscosity since small particles fit within the voids of the array of big particles.

Gravimetric analysis measured the solids content of the final latex.[7] The emulsion (2 g), after cast in a petri dish, was dried in an oven at 110°C until achieving a constant weight. The solids content (%) was calculated using the following formula:

$$\text{solids content (\%)} = \frac{W_2 - W_0}{W_1 - W_0} \text{x} 100\% \qquad (2)$$

where W_0 is the weight of the petri dish, and W_1 and W_2 the weight of the emulsion before and after drying to a constant weight, respectively.

The pH (Accumet Basic AB15 pHmeter, Fisher Scientific) of the emulsion was determined at room temperature (25°C).

The resistance of an emulsion to centrifugation depends on the difference of densities between the oily and aqueous phases. The stability under centrifugation reflects the strength of the interfacial film.[8] A centrifugation tube filled with 20 mL of emulsion underwent a centrifugal acceleration of 5000 m/s^2 (2850 RCP) for 5 min (Thermo IEC 21000; International Equipment Company). The centrifugal acceleration γ (m/s^2) is given as $\gamma = 110N^2R$, where N is the rotation speed and R is the radius of gyration (cm) measured from the axis of the centrifuge to the bottom of the tube in the horizontal position.

To subject an emulsion to freeze/thaw cycles, a hermetically closed test tube filled with the emulsion (15 mL) was vertically stored for 16 h in a freezer at -21°C and then for 8 h at room temperature (21°C ± 2). Observations of any physical changes taking place were recorded during the four-cycle process.

To acquire data for tensile strength requires an INSTRON Series 3360 universal testing instrument operating at a crosshead speed of 500 mm/min at 23 ± 1°C.[9] The Young's modulus was determined using the slope of the stress (MPa) vs. strain (mm/mm) curve from 0 mm to 0.2 mm of extension. To cut the dog-bones necessitated a specimen cutter, described in ASTM D4482.[10] Each sample had five replicate measurements to test the precision of the compounding and physical testing procedures.

Rheological characterization utilized an oscillatory rheometer (Advanced Polymer Analyzer 2000, Alpha Technologies) operating in a parallel plate configuration. A sample (5.0 g) of

the elastomer was passed through a two-roll mill approximately ten times. The compound cured in the rheometer cavity at 160°C for an hour, 3° oscillation arc (30% applied strain) and 1 Hz frequency. Measurements for stress relaxation were at 100°C with a 2° strain for an hour, and temperature sweeps from 100°C to 200°C, at a 3° oscillation arc and 1 Hz frequency.

To study water adsorption and deformation of the prepared film required immersion in water for a month. The films were weighed each week, to compare with the initial measurements, and photographed before and after immersion of the 30-day period to note any visual differences.

A study was made of leachables and extractables of the cured latex film. A sample refluxed in both toluene and chloroform for 6 h was then dried *in vacuo* to achieve a constant weight. The value obtained was compared to the original mass prior to the test to determine a change in mass, also known as gel content.

4.4 Results and Discussion

4.4.1 Surfmer Characterization

Although the ionomer contains multiple imidazolium bromide groups per polymer chain, the ion pair content of the material could not support a surfactant-free emulsion. Given that an additional stabilizing agent was required, a polymerizable surfactant, or surfmer, with similar functionality as the IIR-VImBr polymer was employed. The surfmers 3-dodecyl-1-vinylimidazolium bromide, 3-hexadecyl-1-vinylimidazolium bromide and 3-octadecyl-1-vinylimidazolium bromide were synthesized and tested, with only the C_{12}-based surfmer being effective. A minimum required concentration of 15 wt% surfmer relative to the ionomer was above the critical micelle concentration (CMC) for this surfmer, allowing the emulsion to withstand sonication, heat build-up and removal of the solvents by vacuum without incurring coagulation.

Conductivity measurements determined the CMC of 3-dodecyl-1-vinylimidazolium bromide as approximately 0.0090 M. By comparison, the common anionic surfactant, sodium dodecyl sulfate (SDS, found in many cleaning and hygiene products), has a CMC of 0.0082 M in pure water at 25°C. In dilute solutions (below the CMC) ionic surfactants act as individual ions, however at a concentration above the CMC surfactant molecules aggregate and form micelles.

4.4.2 Emulsion Characterization

Rendering the IIR-VImBr into an aqueous dispersion required dissolving the material to produce a polymer cement of relatively low viscosity. Pure solvents such as tetrahydrofuran, acetone, hexanes, chloroform, benzene, chlorobenzene and dichloromethane could not dissolve the ionomer. However, mixtures comprised of a majority of non-polar solvent and a minority of polar solvent proved capable of solvating both the polymer backbone and imidazolium bromide ion pairs. The most effective solvent mixture contained 10 wt% ionomer, 80 wt% hexanes and 10 wt% hexanol. Removal of hexanes from the emulsified cement was achieved readily by rotary evaporation, while hexanol removal required additional time.

The minimum water content for this system to achieve a stable emulsion was determined to be a 1:1 ratio of water to organics content. Sonication at a power output of 50 for 3 minutes formed particles of a consistent size and a relatively similar polydispersity index that could disperse in the water media. Subjecting the final emulsion to vacuum for approximately one hour removed the hexanes, hexanol and 10% of the water content.

The resulting IIR-VImBr emulsion was a milky white liquid, following sonication and the removal of organic solvents (Figure 4.1 below), with a bimodal particle size distribution (Table 4-1 on page 78) comprising a population with a mean diameter of 250 nm and a population with a mean diameter of 1650 nm.

FIGURE 4.1 – IIR-VImBr emulsion following sonication and the removal of organic solvents

The properties of emulsions can change through a number of processes, including creaming, coalescence, flocculation, phase separation, rupture and Ostwald ripening. Analysis of emulsion stability often relates to the zeta potential of the system, with values reflecting the

stability of the dispersed system in a chosen environment. The zeta potential is the difference in potential between the surface of the tightly bound layer of ions on the particle surface and the electro-neutral region of the solution. When the zeta potential is 25mV or more, absolute value, the repulsive forces exceed the attractive London forces, the particles disperse and the system is deflocculated. When the zeta potential is less than 25mV, absolute value, the attractive forces exceed the repulsive forces and the particles come together leading to flocculation.6 The zeta potential measured, for the emulsion of interest, was strongly negative in value at -41.4 ± 1.5 mV (Table 4-1 below), indicating good stability.

TABLE 4.1 – Measurement Values for IIR-VImBr Emulsion

Physical Properties	IIR-VImBr Emulsion
Median Size ± S.D. (nm)	422 ± 10
Zeta Potential (Peak Value ± S.D.) (mV)	-41.4 ± 1.5
Creaming Volume (%) After Centrifugation	85
Viscosity ± S.D. (mPa s)	5.1 ± 0.3
pH	7.20 ± 0.05
Solids Content (%)	8 ± 1

Creaming, the migration of the dispersed phase under the influence of buoyancy, will cause particles to float or sink depending on their density and the viscosity of the continuous phase. Creaming is undesirable since it causes difficulties in storage and handling. The creaming volume percentage[12] reflects the stability with time of the emulsion formulation as determined by centrifugation and was 85% for the IIR-VImBr formulation, Table 4-1 above. Additionally, Table 4-1 reports the emulsion viscosity, pH and solids content.

This emulsion demonstrated intrinsic stability, indicating no phase separation or sedimentation after positioned vertically for several months at room temperature. The emulsion underwent three freeze/thaw cycles undergoing only moderate damage. The emulsion phase separated after the first cycle in the freezer and ruptured after four cycles.

4.4.3 Bulk Material Characterization

Intermolecular ion pair interactions of the imidazole-based functionality provide the polymer chain network of BIIR with improved modulus and elasticity for both the IIR-VImBr bulk-material thermoset and latex film. Observing the dynamics of a crosslinking reaction is

possible with an oscillating biconical disc rheometer operating at a fixed temperature, strain and frequency.

Figure 4.2 below illustrates the cure dynamics for both the IIR-VImBr thermoset and latex film. The bulk material properties of the latex film were compared to those of the thermoset to observe if they were affected by the emulsification procedure. The latex film, with dicumyl peroxide, was dried, folded and placed into a biconical disk rheometer.

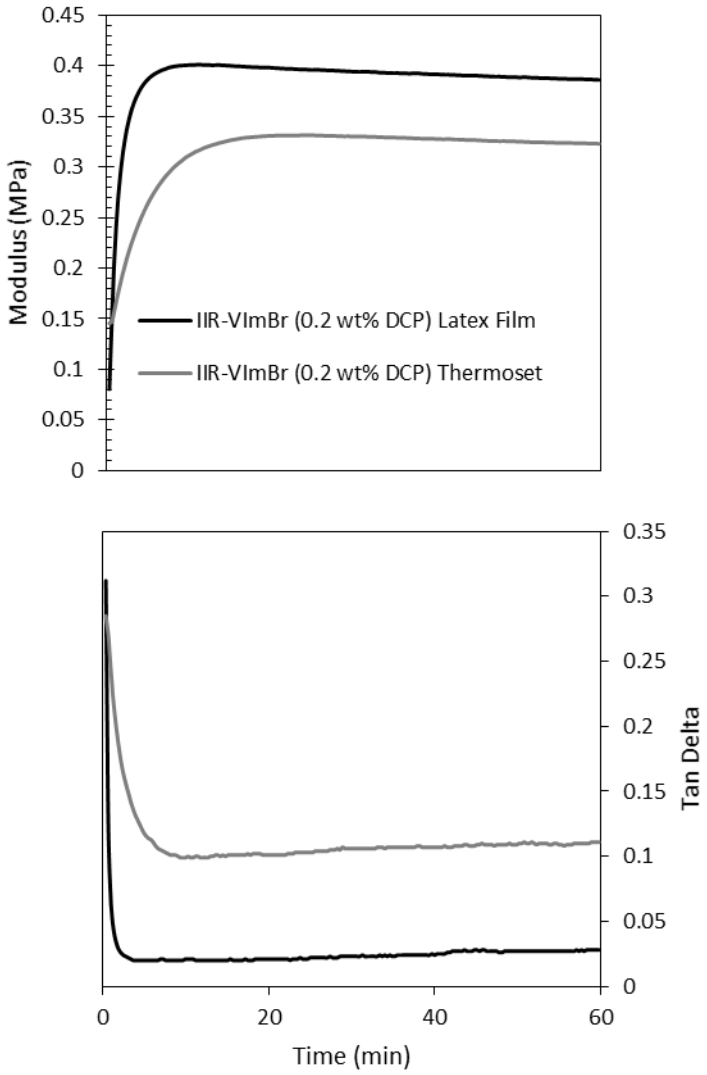

FIGURE 4.2 – Comparison of storage moduli (G') for the IIR-VImBr latex film (0.2 wt% DCP) and thermoset (0.2 wt% DCP)

The increase in storage modulus, for both materials, is indicative of covalent crosslinking. The high initial storage moduli values indicate the presence of an ionic crosslink network comprised of N-vinylimidazolium bromide multiplets that existed prior to crosslinking. Initiation of the radical oligomerization of aggregated vinylimidazolium bromide functionality increased the ionomer's storage modulus. However, the additional ionic content via the added surfmer resulted in a higher extent of cure and final storage modulus for the latex film, despite a lower initial storage modulus. No cure reversion was observed for both materials, which would result due to polymer backbone fragmentation often observed upon consumption of the pendant macromonomer functionality.

Monitoring the response of a sample subjected to a constant strain-deformation provides insight on relaxation properties. Figure 4.3 below provides modulus measurements as a function of time for samples held at 100°C and a fixed strain of 2° arc. The stable covalent network prevents the polymer chain segments from flowing, resulting in a less severe decline of modulus throughout the measurement. The network of ion pair aggregates is subject to relaxation while the covalent network maintains a stable response to the applied strains, preventing the polymer chains from flowing through their entanglements. The latex shows a superior response to applied stress, as compared to its thermoset counterpart, showing zero degradation over the course of the experiment. Despite the presence of greater ionic content in the latex film, ionic relaxation is not observed but instead the covalent or entropic strength is greater than in the bulk material.

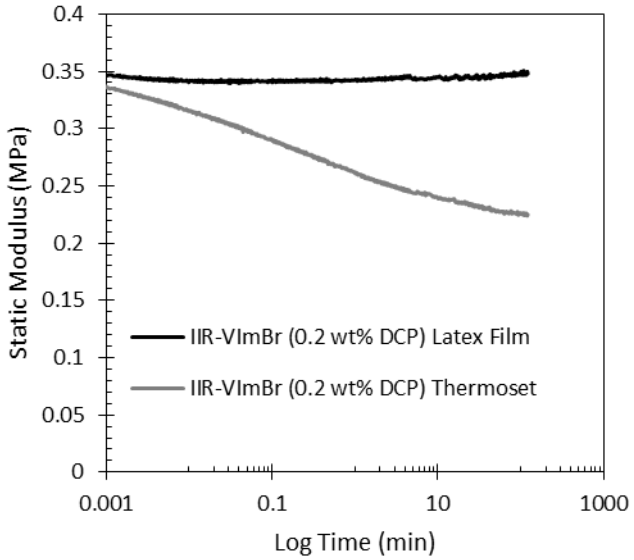

FIGURE 4.3 – Comparison of stress relaxation for the IIR-VImBr latex film and thermoset

The temperature sweep data shown in Figure 4.4 below reveals more of the characteristics of a hybrid ionic/covalent polymer network. The storage modulus declines with an increase in temperature for unvulcanized ionomers, owing to the reduction in ionic network strength,[11] whereas the modulus of non-ionic thermosets increases with temperature, due to the effect of temperature on entropy-driven elasticity.[12] These rheological test results indicate the latex film has superior bulk material properties compared to its thermoset counterpart and further indicates that its covalent network, despite the addition of the ionic surfmer, dominates its properties.

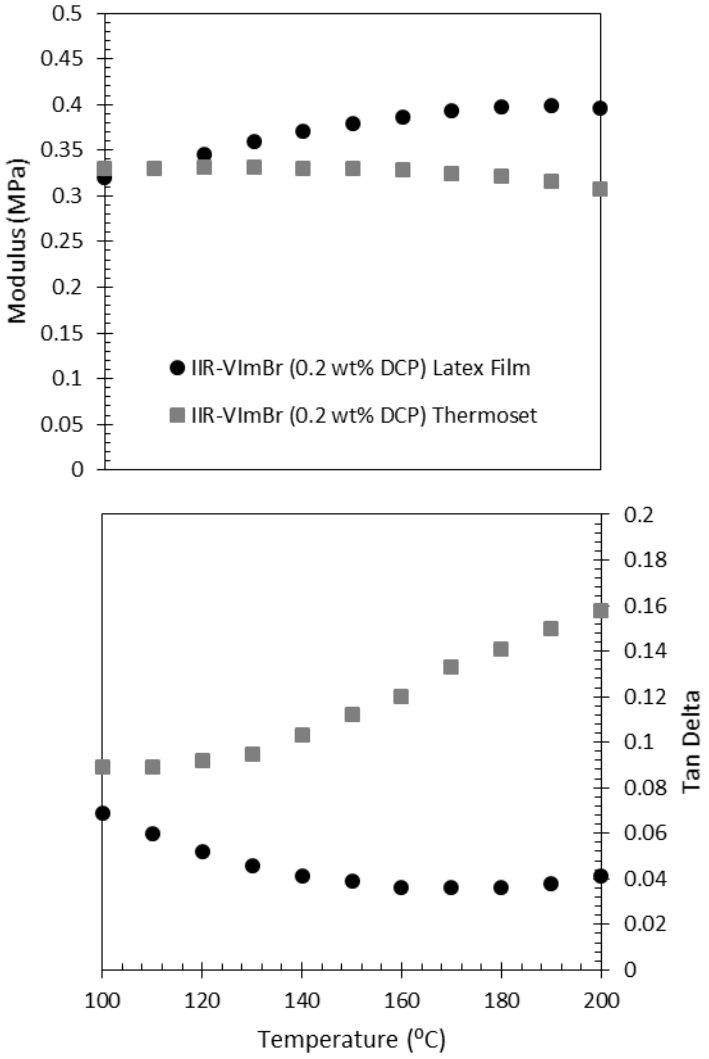

Figure 4.4 – IIR-VImBr latex film and thermoset temperature sweep comparison

4.4.4 Film Characterization

Tensile measurements were performed on dog-bones cut from a dried and crosslinked IIR-VImBr film (cast from an O/W emulsion) to determine its physical properties. These results were compared to a crosslinked IIR-VImBr bulk material thermoset, whose dog-bone dimensions were identical except for the thickness being approximately two millimetres greater. The low elongation and tensile stress at break (Table 4-2 below) for the two materials was attributed to their tight covalently crosslinked networks restricting the flow of the individual polymer chains through its entanglements.

The Young's modulus, calculated over a low elongation of 0-0.2 mm, and the ionic crosslinks are capable of reinforcing the material at these low strains but grow weaker with increased strain. The high value of the Young's modulus point to the combined strengths of the covalent network and ion pair aggregates.

TABLE 4.2 –Tensile Measurements for a Crosslinked IIR-VImBr Film and a Thermoset

Tensile Measurements	Crosslinked IIR-VImBr Latex Film	Crosslinked IIR-VImBr Thermoset
Tensile Extension at Break (mm)	325	300
Young's Modulus (MPa)	0.37	0.78
Tensile Strain at Break (mm/mm)	4.0	2.1

The crosslinked film and thermoset show comparable values for extension at break. However, the latex has a much smaller value for Young's Modulus as compared to the IIR-VImBr thermoset, which indicates a lower ionic content despite the addition of the ionic surfmer. Nevertheless, these results correlate well with the previous bulk material properties where the thermoset had shown results that correlate with a more labile network as a result of its ionic network. Whereas, the film's properties were dictated by its covalent nature and hence its lower value for Young's Modulus.

The crosslinked and un-crosslinked IIR-VImBr films did not attain weight after 30 days of submersion in water, indicating a lack of water absorption. The films shown in Figure 4.5 on page 83 also display no evidence of deformation resulting from exposure to water.

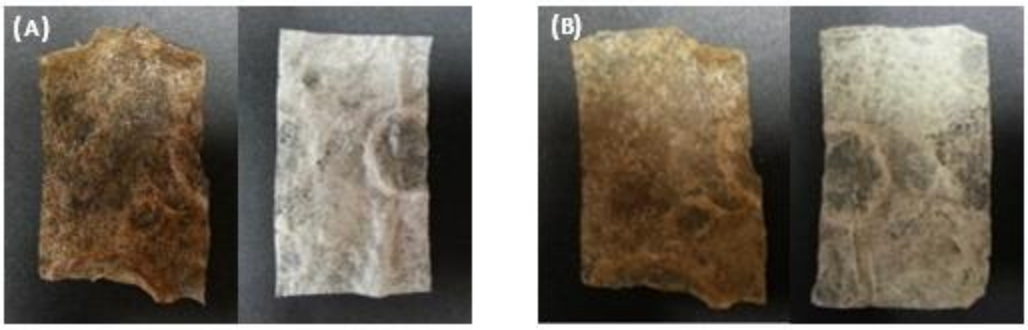

FIGURE 4.5 – IIR-VImBr films (A) before and (B) after submersion in water for 30 days. Left and right of each group are cured and uncured, respectively.

Gravimetric studies performed on the final IIR-VImBr-XL thermoset and latex was to determine the presence of leachables and extractables, specifically due to the surfmer. A sample refluxed in both toluene and chloroform suffered no loss in mass. Where one would assume a 15% weight loss with the use of a non-polymerizable surfactant. These results indicate neither the rubber nor surfmer will leach, thus resulting in an environmentally friendly end-product.

4.5 Conclusions

A vinylimidazolium grafted brominated poly(isobutylene-co-isoprene) elastomer was transformed into an oil-in-water emulsion via post-polymerization emulsification. This ionomer derivative of an isobutylene-rich elastomer has the ability of curing to a high crosslink density on exposure to low doses of free radical generating techniques. The polymerizable surfactant 3-dodecyl-1-vinylimidazolium bromide, when added to the emulsion formulation, successfully plasticized the ionomer, increased the extent of a free radical cure, provided additional ionic functionality to the material and stabilized the emulsion against coagulation. This class of surfactants, with its engagement of the polymer in co-curing eliminates the potential for leaching from the vulcanizate. The emulsion showed considerable stability towards centrifugation and freeze/thaw cycles. The films showed excellent rheological, tensile and water absorption properties.

REFERENCES

1. Becher, P., Emulsions: Theory and Practice, 3rd Ed.; Washington, D.C.:American Chemical Society; Oxford; New York: Oxford University Press, 2001.

2. Cosgrove, T., 2005. Colloid Science Principles, Methods and Applications. Blackwell Publishing, Bristol.

3. Bottino, F.A., Fabbri, E., Fragala, I.L., Malandrino, G., Orestano, A., Pilati, F., Pollicino, A. Polystyrene-Clay Nanocomposites Prepared with Polymerizable Imidazolium Surfactants, *Macromolecular Rapid Communications*, **24**, 1079–1084 (2003).

4. Ozvald, A.M. Reactive Ionomers: N-vinyliidazolium Bromide Derivatives of Poly(isobutylene-co-isoprene) and Poly(isobutylene-co-para-methylstyrene). Master of Applied Science Thesis, Queen's University (2012).

5. Bottino, F.A., Fabbri, E., Fragala, I.L., Malandrino, G., Orestano, A., Pilati, F., Pollicino, A. Polystyrene-Clay Nanocomposites Prepared with Polymerizable Imidazolium Surfactants, *Macromolecular Rapid Communications*, **24**, 1079–1084 (2003).

6. Lieberman, H.A., Rieger, M.M., Banker, G.S., 1988. Pharmaceutical Dosage Forms: Disperse Systems, vol. 1. Mercel Dekker, New York.

7. Cheng, S., Chen, Y., Chen, Z., Core-Shell Latex Containing Fluorinated Polymer Rich in Shell, *Journal of Applied Polymer Science*, **85(6)**, 1147-1153 (2002).

8. Puisieux, F., Seiller, M., 1983. Galenica—Agents de surface et émulsions. Lavoisier, Paris.

9. ASTM Standard D412 – 06a^{E2}, Standard Test Methods for Vulcanized Rubber and Thermoplastic Elastomers – Tension, *ASTM International*, West Conshohocken. PA. 2006, DOI: 10. 1520/D0412-06AE02, www.astm.org

10. ASTM Standard D4482 – 11, Standard Test Method for Rubber Property – Extension Cycling Fatigue, *ASTM International*, West Conshohocken, PA, 2007, DOI: 10. 1520/D4482-11, www.astm.org

11. Eisenberg, A., Kim, J.S. Introduction to Ionomers. 1st ed. New York: Wiley; 1998.

12. Gao, J., Weiner, J.H., Range of Validity of the Entropic Spring Concept in Polymer Melt Relaxation, *Macromolecules*, **25**, 3462 – 3467 (1992).

CHAPTER 5

COMPOSITES AND NANOCOMPOSITES OF A MIXED N-VINYLIMIDAZOLIUM AND N-BUTYLIMIDAZOLIUM DERIVATIVE OF BIMS

5.1 Introduction

Various systems that utilize fillers include organic, biological, biomimetic and polymeric materials. In polymeric materials, adding particulate fillers reduces cost and/or improves the mechanical and dynamic properties of compounds. Carbon black and silica are widely adopted fillers in the rubber industry.[1] Dispersion of these rigid fillers provides both abrasion resistance and reinforcement via an increase in modulus. Adsorption of polymer chain segments on filler surfaces generates a non-covalent network that resists relaxation to an applied load. Hence, a higher modulus, lower elongation at break and higher tensile strength at failure results if a finely divided filler with a high specific surface area disperses and distributes evenly throughout a rubber compound.[2]

Carbon black imparts strength and toughness to elastomers, improving rubber tear-resistance, abrasion, and flex fatigue, while increasing traction and durability. Carbon black, with over 30 grades manufactured for markets ranging from tires to industrial equipment, owes its reinforcing properties to the size of its aggregates, surface area of the particles and surface functionality (Table 5-1 on page 86).[2] Aggregate size influences the surface area to which elastomer chains can adsorb through van der Waals forces. The chemical composition of the filler surface, which includes small amounts of carbonyl and hydroxyl functional groups, determines the strength of the interactions between an elastomer and carbon black. Most grades of carbon black have relatively low surface energies compared to other particulate fillers and disperse easily in low-polarity elastomers, including BIIR and BIMS.[3,4]

TABLE 5.1 – Select Grades of Carbon Black[2]

ASTM Designation	Particle Size (nm)	Application
N220	20-25	Tires
N330	26-30	Tires
N475	31-39	Industrial Products
N762	61-100	Tire Carcasses

Silica has a weaker polymer-filler interaction and is extensively used where a high degree of reinforcement is not essential and where non-black colouring is required.[5] The high surface concentration of silanol (–Si–OH) functionality on these fillers imparts a high surface energy. Hence, silica has a strong tendency to aggregate making it difficult to disperse in non-polar elastomers. In these applications, silane-coupling agents are required to covalently-bond the filler to the elastomer during compound mixing. These coupling agents typically contain a trialkoxysilyl functionality that reacts with the silanol groups on the silica surface, and sulfur or amine functionality that can engage in rubber cure chemistry. Achieving good silica dispersion in isobutylene-based elastomers requires the use of a silane coupling agent strategy, as well as intense dispersive mixing of the rubber and filler.[4,6]

Polymer-layered silicate nanocomposites (PLSNs) are materials based on the intercalation of polymer chains into organically modified layered silicates. Compared to conventional filled polymer composites, they present improved physical, mechanical, barrier and flammability properties.[7] The most commonly used layered silicate in the preparation of PLSNs is montmorillonite (MMT), which has exchangeable cations such as Na^+, Ca^{2+}, K^+, Li^+ and Mg^{2+} in the interlayer region. Treating MMT with organic cations (o-MMT) renders the hydrophilic MMT more organophilic and increases interlayer spacing.

The different types of polymer-clay composite structures (Figure 5.1 on page 87) include a phase-separated microcomposite, exfoliated nanocomposite and intercalated nanocomposite. A phase-separated structure occurs when the polymer matrix chains are unable to penetrate between the layers of the silicate particles. In exfoliated composites, the clay particles are completely delaminated and the silicate layers do not show any periodicity in their arrangement. An intercalated structure forms when one or more of the polymer chains intercalate between the layers, resulting in increased interlayer spacing while retaining the clay particles in an ordered layer structure.

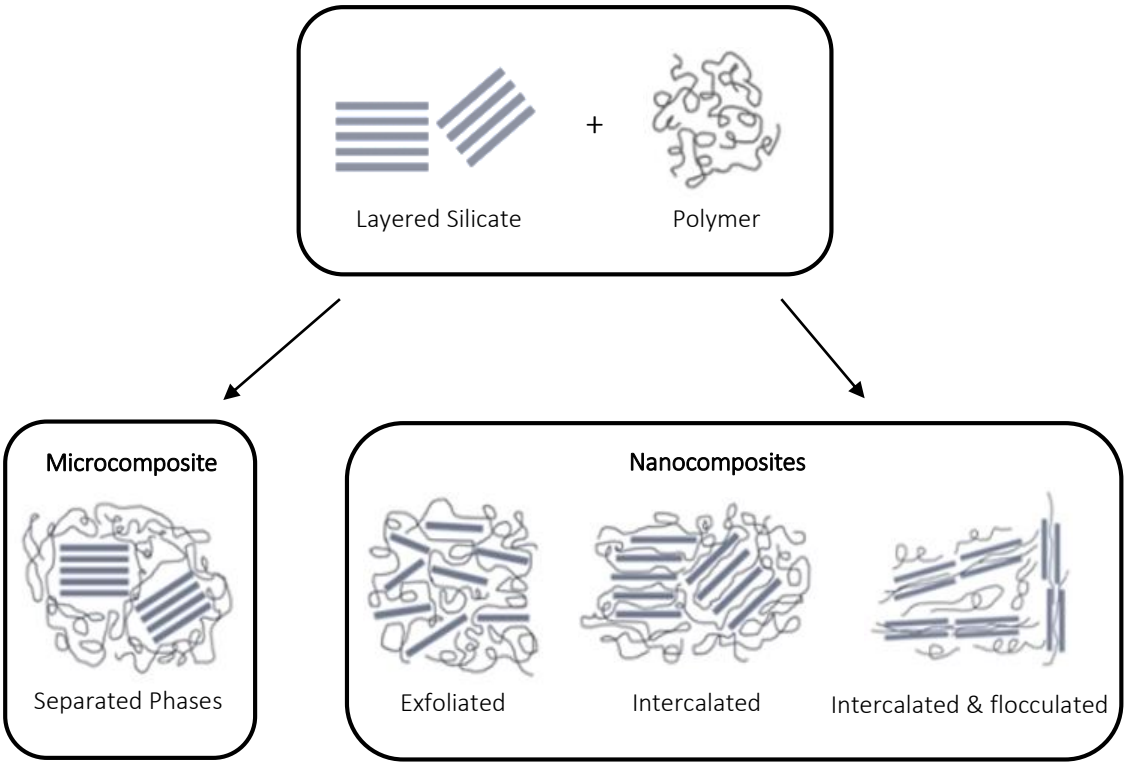

FIGURE 5.1 – Structures of polymer-clay composites[8]

Poor thermal stability is a drawback when using common cations, like long carbon-chain alkyl ammonium salts, in the preparation of polymer/o-MMT nanocomposites.[9] Especially via melt intercalation and during bulk processing, when elevated temperatures are usually required. Decomposition and alteration of the interface between filler and polymer occur if the processing temperature is greater than the thermal stability of the organic surfactant. The use of cations with greater thermal stability, such as phosphonium, pyridinium and imidazolium, to modify layered silicate may avoid this problem.[10]

To properly distribute and disperse fillers throughout a rubber matrix requires a mixing technique that generates high shear strains and shear stresses.[3] Distributive mixing involves spreading filler aggregates and agglomerates evenly throughout the elastomer matrix, achievable by division and re-orientation of the polymer flow path. Dispersive mixing breaks filler agglomerates into smaller structures by achieving high shear stresses resulting from the forced flow through spaces with narrow clearances.

Figure 5.2 below depicts a schematic of dispersive and distributive mixing with an ideally filled composite being both well distributed and well dispersed. This optimal situation requires the use of a heated two-roll mill, a batch mixer equipped with Banbury blades (for rubber composites) or an extruder.

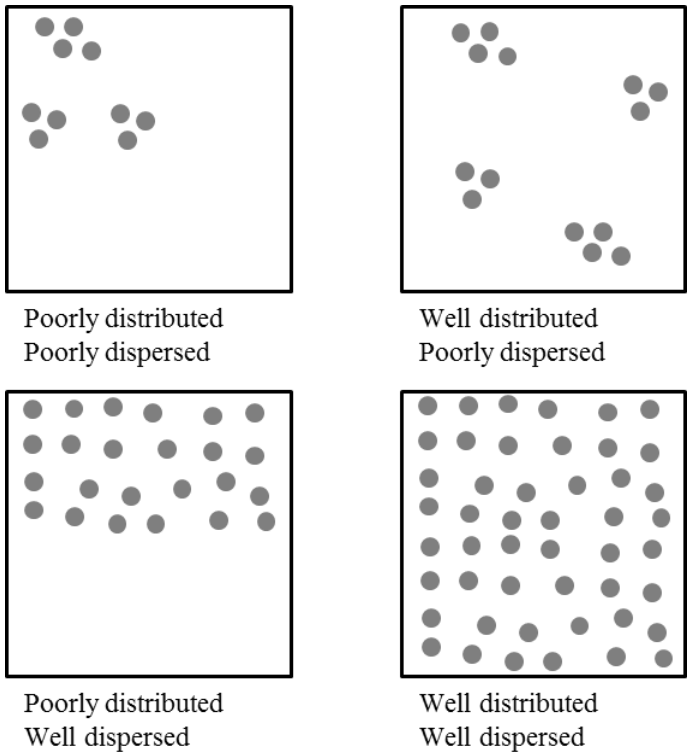

FIGURE 5.2 – Filler mixing in an elastomer[11]

Achieving adequate adhesion between the polymer and filler is challenging when generating good dispersive mixing in a rubber-compounding device. Strong interactions (van der Waals forces, hydrogen bonding, ion-dipole associations, etc.) between the polymer and filler are required if shear stresses are to be transferred through the elastomer to overcome inter-particle associations, thereby leading to filler aggregate breakdown into smaller particles. As previously discussed, silane coupling agents are the conventional means of achieving adhesion to siliceous fillers. However, previous work by Parent et al. has shown that incorporating phosphonium bromide functionality into BIIR will also provide requisite adhesion without the use of coupling agents. This incorporation facilitates the dispersion of silica and nano-clays throughout the butyl rubber compounds while using conventional polymer processing devices.[5,12] This ionomer

approach achieves polymer-filler adhesion through strong associations between the phosphonium bromide ion pairs and the surface silanol functionality of silica.

The elastomer studied in this work is the product of the mixed alkylation reaction of poly(isobutylene-co-methylstyrene) (BIMS) with both N-vinylimidazole and N-butylimidazole. Isobutylene-based elastomers are widely used in the automotive industry because these materials possess low permeability to gases. Additionally, one can control the mechanical properties by varying the level of isobutylene and para-methylstyrene, as well as filler content and crosslink density.[1]

This chapter extends previous work on filled ionomer compounds to the study of peroxide-cured, mixed alkylated BIMS thermosets via a solvent-free process. The clay nanocomposites incorporated an imidazolium salt, 3-dodecyl-1-vinylimidazolium bromide, to modify the montmorillonite clay, obtain improvement in thermal stability and facilitate the formation of partially exfoliated structures due to the presence of a polymerizable group in their structure. The filler composites and clay nanocomposites were characterized by cure reactivity, Payne analysis and tensile measurements. Further characterizations of the clay nanocomposites utilized X-Ray diffraction (XRD), transmission electron microscopy (TEM) and thermogravimetric analysis (TGA).

5.2 Experimental

5.2.1 Materials

BIMS (Exxpro 3745, 0.19 mmol benzylic bromide functionality/g BIMS) was used as supplied by Exxon Mobil Chemical (Baytown, Texas). N-vinylimidazole (VIm, 99+%), N-butylimidazole (BuIm, 98%), 1-bromododecane (97%), chloroform-d (99.8%D), methanol-d4 (99.8%D), toluene-d6 (99.6%D) and dicumyl peroxide (DCP, 98%) were used, as received, from Sigma Aldrich (Oakville, Ontario). 2,6-ditertbutyl-4- methylphenol (BHT, 99%) was used as received from Alfa Aesar. Carbon black (Cabot, N330) was used as received from the Green Centre (Kingston, ON). Amorphous precipitated silica (HiSil 233, PPG Industries, Pittsburg, Pennsylvania) was dried at 110 °C for 24 h prior to use. SCP Cloisite 30B and SCP Cloisite Na^+ was used as supplied by Southern Clay Products Inc. (Gonzales, Texas).

5.2.2 Synthesis of a Mixed Alkylation (MA) Product IMS-g-MImBr

A BIMS derivate containing 50% N-vinylimidazolium bromide and 50% N-butylimidazolium bromide functionality (M Product) was prepared. BIMS (40 g, 7.6 mmol benzylic bromide) was mixed with VIm (0.50 g, 0.50 mmol, 0.6 eq.) and BuIm (0.87 g, 0.87 mmol, 0.8 eq.) at 110 °C and 60 rpm using a Haake Polylab R600 internal batch mixer for 35 mins. Aliquots of the mixture (0.5 g) were removed from the mixer and characterized by ^{1}H NMR.

5.2.3 Synthesis of 3-Dodecyl-1-Vinylimidazolium Bromide

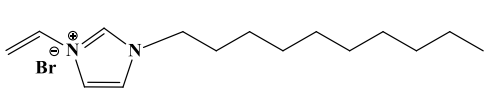

After combining 1-vinylimidazole (2.000 g), 1-bromododecane (6.582 g) and ethyl acetate (5.0 mL, spectrophotometric grade) the solution was stirred at room temperature for 12 hours. Subsequently, the solution was reacted at 55 ± 2°C for 24 hours. After a cool-down, the white precipitate was filtered-off and washed several times with ethyl acetate (spectrophotometric grade) and the solid product dried *in vacuo*. ^{1}H NMR (DMSO-d_6, δ, ppm): 9.53 (s, 1H, -N^+-C**H**-N-), 8.21 (d, 1H, CH_2=C**H**-N^+-), 7.94 (d, 1H, -N^+-C**H**=CH-N-), 7.30 (d, 1H, -N^+-CH=C**H**-N-), 5.96 (dd, 1H, C**H**$_2$=CH-N^+-), 5.42 (dd, 1H, C**H**$_2$=CH-N^+-), 4.19 (t, 2H, -N-C**H$_2$**-CH_2-), 1.80 (m, 2H, N-CH_2-C**H$_2$**-), 1.24 (m, 14H, -N-CH_2-CH_2-(C**H$_2$**)$_7$-CH_3), 0.85 (t, 3H, -CH_2-C**H$_3$**). Mass Spec: 263.2487(M^+), $C_{17}H_{31}N_2$, mp: 47°C.[13]

5.2.4 Preparation of o-MMT

An aqueous suspension of pre-washed MMT (2.088 g) in deionized water (200.0 mL) was added to a solution obtained by dissolving 3-dodecyl-1-vinylimidazolium bromide (2.506 mmol) in a 50:50 mixture of ethanol and deionized H_2O (10.00 mL). After the solution was stirred in an inert atmosphere overnight at room temperature the white powder was filtered off, washed several times with a mixture of ethanol and deionized water until no bromide ion could be detected by an $AgNO_3$ aqueous solution and then dried *in vacuo* overnight at room temperature.

5.2.5 Synthesis of IMS-g-AAcBr

Acrylic acid (0.29 mL, 4.0 mmol) was mixed with TBAOH (1.25 mL, 1.0 M in MeOH, 4.0 mmol), and stirred for 30 minutes at room temperature. Methanol was removed by Kugelrohr distillation (80 Pa, room temperature), yielding white crystals of tetra-N-butylammonium

acrylate. BIMS (20 g, 4.4 mmol benzylic bromide) was dissolved in toluene (200 mL, 10 wt%) and heated to 85°C. Tetra-N-butylammonium bromide (0.71 g, 2.2 mmol, 0.5 eq.) was added to the solution and the mixture isomerized for 1 hour. Next, tetra-N-butylammonium acrylate (1.50 g, 4.83 mmol, 1.1 eq.) and tetra-N-butylammonium acetate (2.65 g, 8.79 mmol, 2 eq.) was added to the solution and allowed to react for 2 hours, ensuring allylic bromide conversion. The esterification product was obtained by precipitation in excess acetone, purified by dissolution/precipitation using tetrahydrofuran/acetone and dried *in vacuo*.

5.2.6 Preparation of Filled Composites

The required amount of product was mixed with the required amount of filler or clay at 100 °C and 60 rpm for 10 min using a Haake Polylab R600 internal batch mixer. For example, a 30 wt% composite will contain 28 g of product and 12.0 g of organo-clay.

5.3 Instrumentation

^{1}H NMR characterization of the polymers was performed on a Bruker AM500 instrument with chemical shifts (δ) reported relative to tetramethylsilane in ppm.

To prepare a cured macro-sheet, 35.0 g of material with 0.5 wt% of DCP was sheeted with a two-roll mill and compression molded at 160 °C and 20 MPa for 25 min ($5t_{1/2}$ for DCP).[14] The sheeted product had a thickness of 2.00 ± 0.05 mm.

Rheological characterization was carried out in an oscillatory rheometer (Advanced Polymer Analyzer 2000, Alpha Technologies) operating in a parallel plate configuration. A 5.0 g sample of the uncured material was coated with 0.5 wt% of DCP in acetone and allowed to dry before being passed through a two roll mill ten times. The mixed compound was cured in the rheometer cavity at 160 °C for 60 min, at a 3° oscillation arc (30% applied strain) and 1 Hz frequency. Followed by a Payne analysis, which imposed an oscillating shear deformation at an increasing strain amplitude (0-30), constant frequency (0.1 Hz) and temperature (100 °C).

Tensile strength data was acquired using an INSTRON Series 3360 universal testing instrument operating at a crosshead speed of 500 mm/min at 23 ± 1 °C.[15] The Young's modulus was found by calculating the slope of the stress (MPa) vs. strain (mm/mm) curve from 0 mm to 0.2 mm of extension. Dogbones were cut using a specimen cutter described in ASTM D4482.[9] Five

replicate measurements were made for each sample to test the precision of the compounding and physical testing procedures.

The extent of clay exfoliation in the composites was determined by X-ray diffraction (XRD) using a Philips X'Pert Pro Diffractometer (Cu radiation λ = 1.54060Å, generator voltage = 45 kV, current = 40 μA). Pressed film samples were scanned in a 2θ range of 1 to 40° at a rate of 1°/min. Measurements were recorded every 0.03°. For comparative purposes, the XRD patterns were represented in terms of relative intensities.

The dispersion of the clay layers and their distribution in the polymer matrix were examined by transmission electron microscopy (TEM). Samples were analyzed at Mount Sinai Hospital, Toronto.

The stability, or change in mass, of the different clay fillers (Cloisite 30B, Cloisite Na^+ and o-MMT) were evaluated through thermogravimetric analysis (TGA) in a N_2 atmosphere for a temperature range of 30-700°C and rate of 10 °C/min. Negligible mass loss corresponds to little or no slope in the TGA trace.

5.4 Results and Discussion

It is both economical and environmentally responsible to conduct ionomer syntheses with a one-step solvent-free process. The N-alkylation of N-vinylimidazole (VIm) by BIIR under solvent-free conditions is extremely slow for commercial requirements. However, BIMS provides a more reactive electrophile which, based on reaction dynamics, is much closer to a commercially viable process. The solvent-free N-alkylation of one equivalent of VIm by BIMS, at 100 °C and 60 rpm, converted 70% of benzylic bromide to N-vinylimidazolium bromide functionality in 30 minutes providing an ion pair content of 0.13 mmol N-vinylimidazolium bromide functionality/g rubber.

N-alkylation of N-butylimidazole (BuIm) by BIMS is rapid in comparison to the reaction of N-vinylimidazole. The reaction is complete after 10 min converting 85% of the benzylic bromide functionality to N-butylimidazolium bromide functionality. This corresponds to an ion pair content of 0.16 mmol N-butylimidazolium bromide functionality/g rubber. The lower reactivity of VIm over BuIm may result from the delocalization of electron density from the imidazole ring to the vinyl group, thereby reducing nucleophilicity. Additionally, the modulus of the BIMS-based

ionomers becomes too high and hence does not mix well. However, the addition of a plasticizer to lower the modulus could allow the nucleophile to react faster. Alternatively, the addition of sodium iodide to form small amounts of the benzyl iodide species could allow quicker reactions with the nucleophiles. It may also be possible to prepare ionomeric, macromonomer derivatives of BIMS more efficiently if a methylene spacer group separated the imidazolium functionality from the vinyl functionality.

The mixed alkylation reaction of BIMS with both N-vinylimidazole and N-butylimidazole, Scheme 5-1 below, completed in approximately 35-40 min producing an ionomer containing 0.07 mmol of N-vinylimidazolium bromide functionality/g rubber and 0.08 mmol of N-butylimidazolium bromide functionality/g rubber, with the remainder composed of unreacted benzylic bromide functionality.

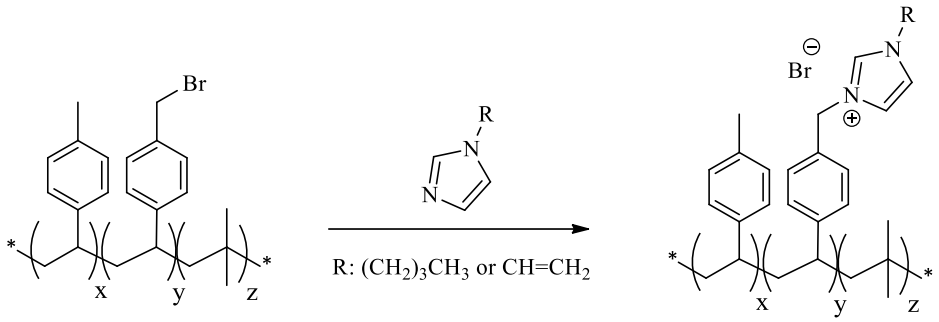

Scheme 5.1 – Mixed alkylation product of BIMS, IMS-MImBr

This study further evaluated the physical and rheological properties of an IMS-MImBr product against a non-ionic control compound. The control product, IMS-AAc, was achieved through the reaction of BIMS with 1.1 eq. of tetra-N-butylammonium acrylate and 2 eq. of tetra-N-butylammonium acetate in solution, Scheme 5-2 below. This mixed alkylation product, IMS-AAc, retains a similar crosslink density and cure reactivity as IMS-MImBr.

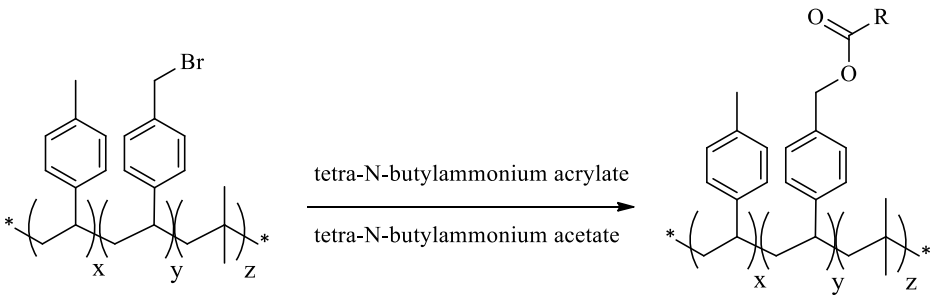

Scheme 5.2 – Mixed alkylation product of BIMS, IMS-AAc

5.5 Carbon Black Composites

Mixing IMS-MImBr with 18.5 µmol DCP/g rubber and varying amounts of N330 carbon black produced compounds with differing cure dynamics, as illustrated in Figure 5.3 below. The cure performance of IMS-MImBr is remarkable in its consistency, in that the change in storage modulus ($\Delta G' = G'_{max} - G'_{min}$) was relatively insensitive to filler loading. The small increase in $\Delta G'$ observed for the filled compounds is likely a result of synergistic effects between crosslinking and filler reinforcement. Generally, optimizing cure formulations is necessary for different filler loadings owing to the adsorption of curatives on the surface of carbon black. For example, diamine cures of halogenated polymers require changes be made to the curative levels when adding filler to the compounding mix.[2] The robustness of IMS-MImBr crosslinking in the presence of fillers is a clear advantage of reactive ionomer technology. The control sample, IMS-AAc, showed a greater increase in storage modulus with the addition of 15% carbon black, which exceeded the final storage modulus of the ionomer with 30% carbon black.

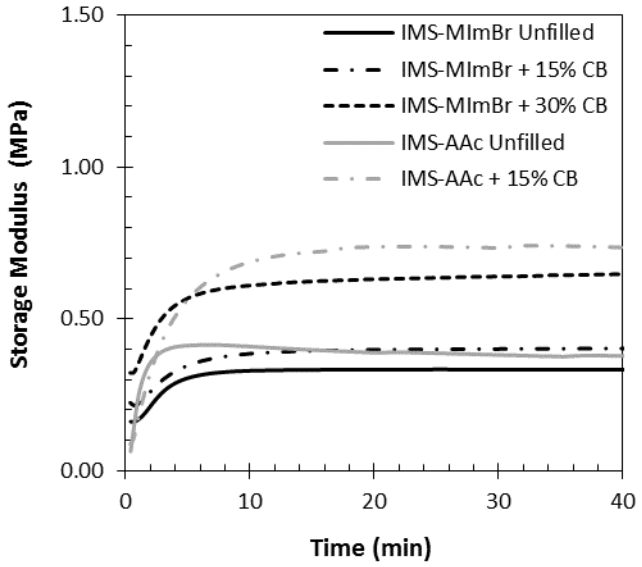

FIGURE 5.3 – Peroxide crosslinking dynamics for carbon black-filled IMS-MImBr and IMS-AAc (160°C, 1 Hz, 3°, 18.5 µmol DCP/g)

The aggregation of filler to yield a reticulate structure is not desirable as it leads to high stiffness at low elongations and survives poorly in the overall reinforcement of the composite. A continuous network of filler particles is relatively strong, yet disrupted at relatively low strains. A Payne analysis involves imposing an oscillating shear deformation at an ever-increasing strain amplitude at a constant frequency and temperature.[16] Although reticulate filler networks

generate a high modulus at low strain, the modulus decreases sharply as the strain increases. In contrast, a well-dispersed filler free of a reticulate network demonstrates a constant modulus over a wide range of strain amplitudes. Figure 5.4 below provides a Payne analysis of carbon black-filled elastomers, with both the unfilled and 15% carbon black-filled IMS-MImBr-XL demonstrating similar behaviour. When increasing the carbon black loading to 30 %, evidence of filler aggregation becomes apparent for both the ionic and non-ionic compounds. However, comparatively the ionomer has a lower modulus, an indication of less carbon black aggregation.

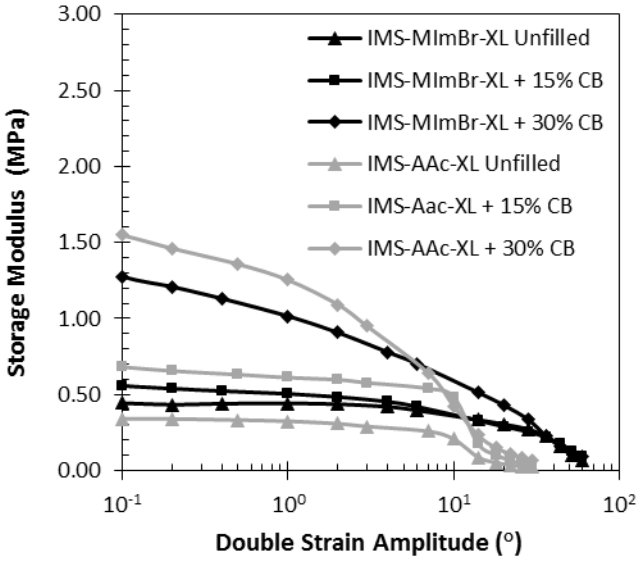

FIGURE 5.4 – Payne analysis for carbon black-filled IMS-MImBr-XL and IMS-AAc-XL (100 °C, 0.1 Hz)

Static tensile testing generated the representative stress-strain profiles plotted in Figure 5.5 on page 96 for IMS-MImBr-XL and its carbon black-filled analogues. The data is consistent with good filler reinforcement, with increasing Young's moduli and decreasing elongations at break observed at higher carbon black loadings. However, the ionomer containing 30% carbon black provided lower tensile strength than the 15% carbon black sample. Dilution of the cured elastomer, by carbon black filler, in the composite may account for the reduction in tensile strength. Additionally, this reduction may be symptomatic of relatively poor filler dispersion,

which was confirmed by Payne analysis. The low strain and elongation at break for the control samples are also confirmations of poor filler dispersion.

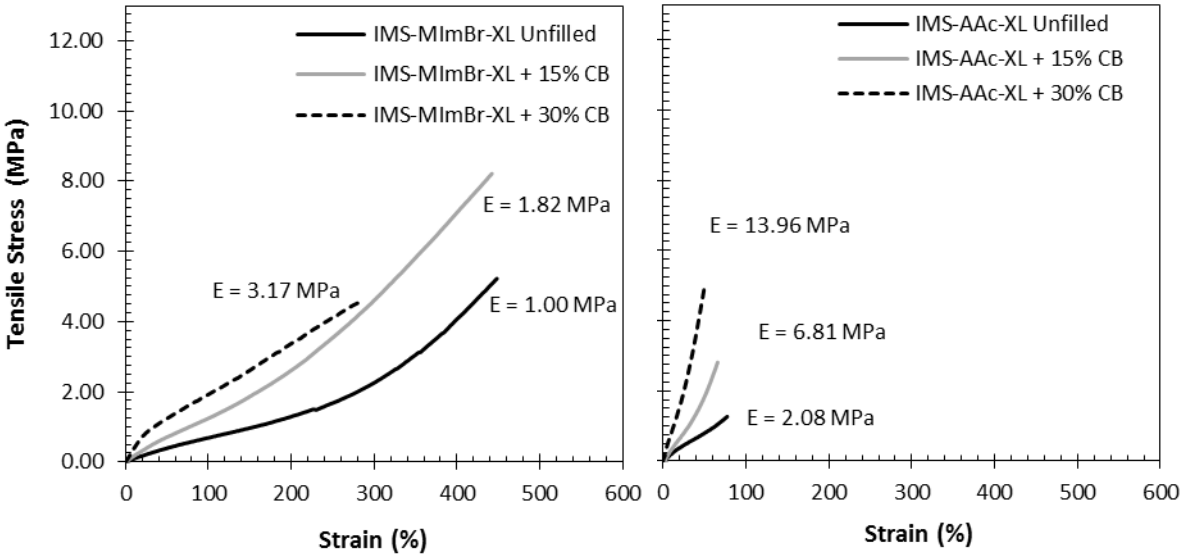

FIGURE 5.5 – Static tensile properties for carbon black-filled IMS-MImBr-XL and IMS-AAc-XL

5.6 Silica Composites

IMS-MImBr was mixed with 18.5 µmol DCP/g rubber and different silica loadings prior to curing the compound at 160°C (Figure 5-6 on page 97). As observed for the carbon black-filled ionomer, the dynamics and rates of peroxide curing were insensitive to filler loading. It is interesting to note, that the extent of reinforcement by silica was greater than that observed for carbon black. However a high G', in the cure rheology data, can be indicative of poor silica dispersion.

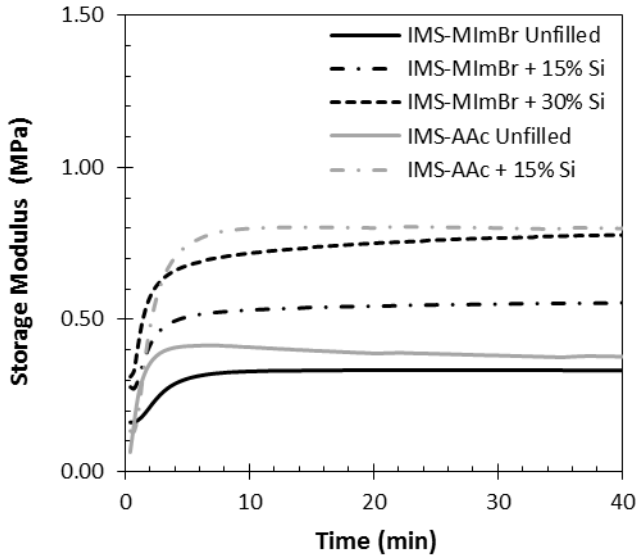

FIGURE 5.6 –Peroxide crosslinking dynamics for silica-filled IMS-MImBr and IMS-AAc (160°C, 1 Hz, 3°, 18.5 µmol DCP/g)

Payne analysis of these composites (Figure 5.7 on page 98) reveals very good silica dispersion at the 15% filler loading, while the behaviour of the 30% composite was better than that observed for carbon black. Both the unfilled and 15% silica-filled composites have a stable modulus plateau at low strain and decreases at high modulus, indicative of good filler dispersion. Upon increasing the silica loading to 30% there appears to be some reticulate network formation as the storage modulus begins to decrease at lower strain values. For the control sample at a 30% silica loading, the instrument achieved its maximum torque limit at 10° and hence the measurement stopped at this point. However, results clearly indicate the non-ionic polymer shows strong reticulate network formation at higher filler loadings, a result of poor dispersion, clearly demonstrating the advantage of using an ionomer. Nevertheless, as with the carbon black-filled composites, these silica-filled composites would benefit from further work focused on the improvement of dispersive mixing.

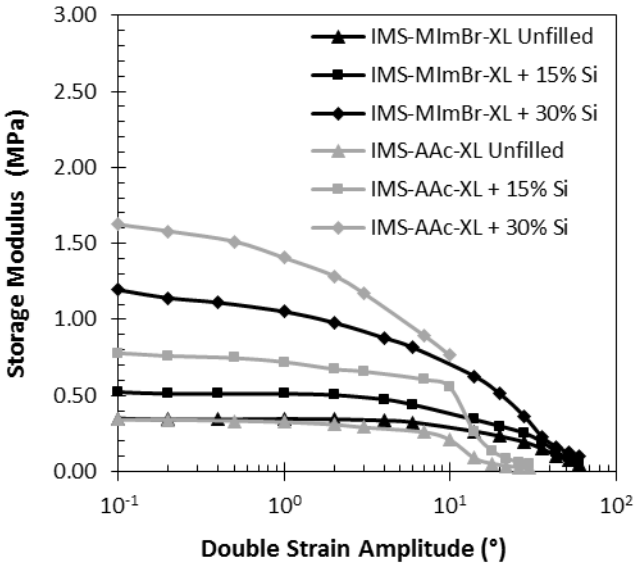

FIGURE 5.7 – Payne analysis for silica-filled IMS-MImBr-XL and IMS-AAc-XL (100 °C, 0.1 Hz)

The behaviour of the silica-filled composites observed in the Payne analysis is similar to the carbon black-filled articles. However, the silica-filled composites display better reinforcement towards static tensile properties (Figure 5.8 on page 99). Outstanding reinforcement was observed at all elongations, indicating extensive silica dispersion. A Young's modulus of 6.9 MPa observed at the 30% silica loading indicated no sign of low strain yielding arising from a reticulate filler network. This is likely due to the surface functionality of these fillers, as the high concentration of silanol functionality on the surface of precipitated silica offers more opportunity for hydrogen bonding with the ionomer.[17] Carbon black has a much lower concentration of acidic surface functionality that could participate in hydrogen bonding with the ionomer.[18] In the carbon black-filled composites, van der Waals interactions between the isobutylene backbone and the carbon black surface become more important than hydrogen bonding with the ionomer functionality. Observations indicate that carbon black dispersion could be difficult in other isobutylene-based elastomers at high filler loadings.[16] These differing surface functionalities likely contribute to the improved tensile properties of IMS-MImBr at high silica loadings and the poor tensile properties at high carbon black loadings.

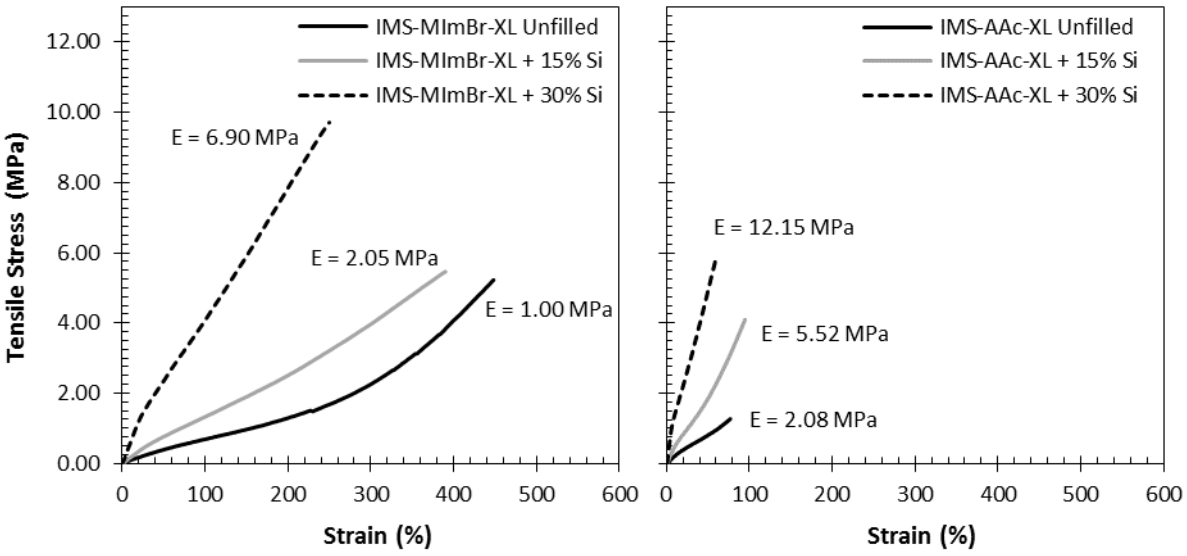

FIGURE 5.8 – Static tensile properties for silica-filled IMS-MImBr-XL and IMS-AAc-XL

For the silica control samples, similar results were observed as for the carbon black samples where very low elongations at break and low strains indicate poor filler dispersion. It should also be noted that all of these compounds contained no dispersing aids or compatibilization agents commonly used in commercial rubber compounds. Hence, the performance of IMS-MImBr stands to be greatly improved from these preliminary evaluations.

5.7 Clay Nanocomposites

Montmorillonite (MMT, $M_x(Al_{4-x}Mg_x)Si_8O_{20}(OH)_4$) is a nanoparticle with an anisotropic, plate-like, high aspect-ratio morphology providing a variety of benefits at very low-loadings. Its morphology leads to improved modulus, tensile and barrier properties, and increased dimensional stability at a low reinforcement loading. MMT will develop a similar increase in modulus and tensile strength at 3-5% loading compared to 20-60% loading of conventional reinforcing agents like kaolin, talc, silica and carbon black.[19] The work herein involves the organic modification of MMT using a cationic polymerizable surfactant, 3-dodecyl-1-vinylimidazolium bromide, capable of increasing the space between the clay platelets and improving interactions with the polymer matrix. Cloisite® additives consist of organically modified nanometer scale, layered magnesium aluminum silicate platelets. The silicate platelets are 1 nanometer thick and 70-150 nanometers across. The two additives used herein include an ion-exchanged Cloisite® 30B

with a reactive alkyl quaternary ammonium salt bentonite, and a pure non-reactive natural bentonite Cloisite® Na^+. Cloisite® 30B and Cloisite® Na^+ have a modifier concentration of 90 and 92.6 meq/100g of clay, respectively.

The TGA trends for o-MMT, Cloisite® 30B and Cloisite® Na^+ (Figure 5.9 below) indicate superior stability for Cloisite® Na^+. Cloisite® Na^+ experienced the least amount of weight loss, approximately 15%, when brought to a temperature of 700°C as compared to o-MMT, which lost almost 50% of its mass at only 450°C.

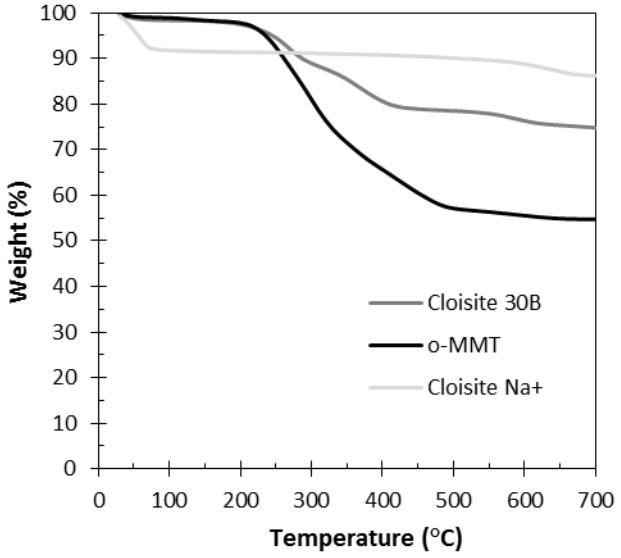

FIGURE 5.9 – TGA results for Cloisite® 30B, o-MMT and Cloisite® Na^+ clay

The preparation of nanocomposites requires extensive delamination of the layered clay structure and complete dispersal of the resulting platelets throughout the polymer matrix. Nanocomposite synthesis by conventional polymer processing operations requires strong interfacial interactions between the polymer matrix and the clay in order to generate shear forces of sufficient strength. This is achieved readily with high surface energy polymers such as polyamides, where polarity and hydrogen-bonding capacity generates considerable adhesion between the polymer and clay phases.[20] However, low energy materials such as polyethylene and polypropylene interact only weakly with mineral surfaces, making the synthesis of polyolefin nanocomposites by melt compounding considerably more difficult.

Difficulties persist in the dispersion of nanolayers due to the high face-to-face stacking of layers in agglomerated tactoids and their intrinsic hydrophilicity.[21] The incompatibility of

hydrophilic clay layers with hydrophobic polymer chains prevents the dispersion of clay nanolayers within a polymer matrix, thus causing weak interfacial interactions. Modification of clay layers with hydrophobic agents renders them more compatible with the polymer chains by reducing their surface energy and matching their surface polarity with the polymer polarity, permitting them to intercalate within the interlayer spacing. For example, grafting pendant anhydride groups on polyolefin resins overcomes problems associated with poor phase adhesion in polyolefin/clay systems.

The cure data in Figure 5.10 below for the ionomer and control compounds indicate very similar ΔG' for all filler loadings of Cloisite® 30B.

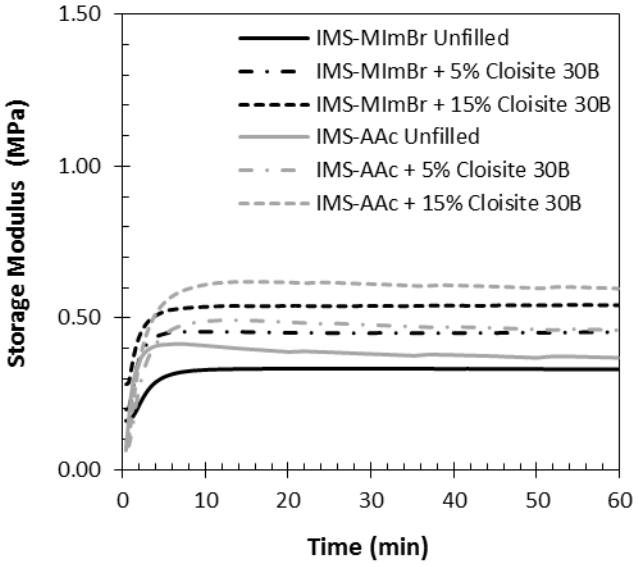

FIGURE 5.10 – Peroxide crosslinking dynamics for Cloisite® 30B clay-filled IMS-MImBr and IMS-AAc (160°C, 1 Hz, 3°, 18.5 µmol DCP/g)

The representative static tensile properties for the Cloisite® 30B samples in Figure 5.11 on page 102 reveal excellent reinforcement for IMS-MImBr-XL at all elongations, an indication of extensive clay dispersion. A Young's modulus of 3.1 was observed at the 15% clay loading with no sign of low strain yielding that typically arise from a reticulate filler network. The control samples presented similar Young's moduli but with significantly lower strains.

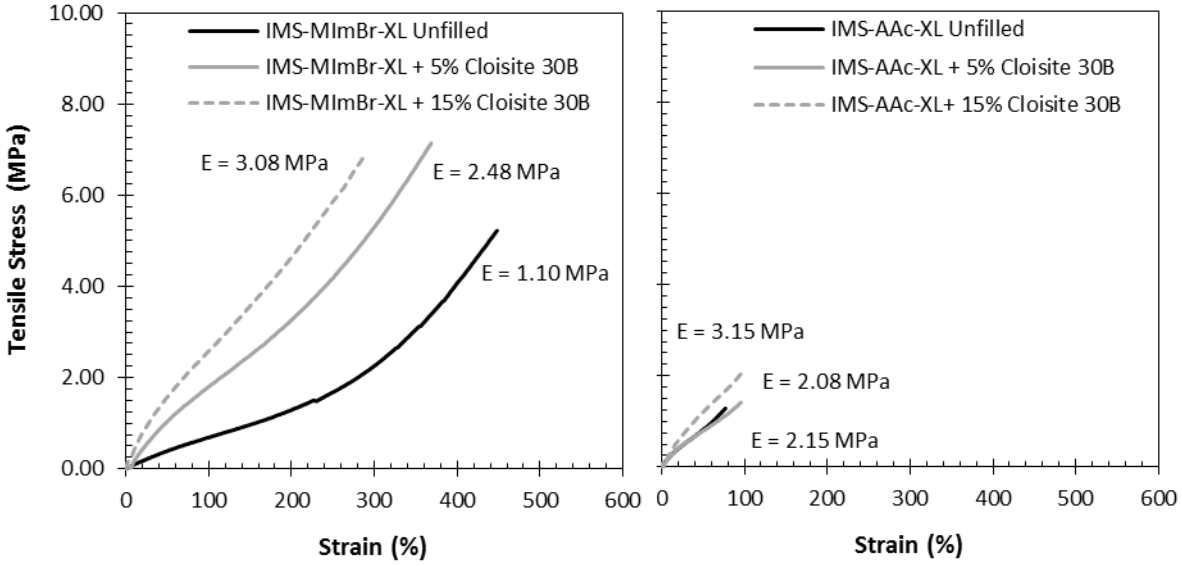

FIGURE 5.11 – Static tensile properties for Cloisite® 30B clay-filled IMS-MImBr-XL and IMS-AAc-XL

The reduction in the intensity of the diffraction peak (Figure 5.12 below), which represents the structural collapse of the clay due to the removal of the ion, for the 15 wt% Cloisite 30B clay-filled IMS-MImBr indicates that partial exfoliation took place. In comparison, more intense and clear XRD signals remained for the non-ionic species, indicating almost no exfoliation.

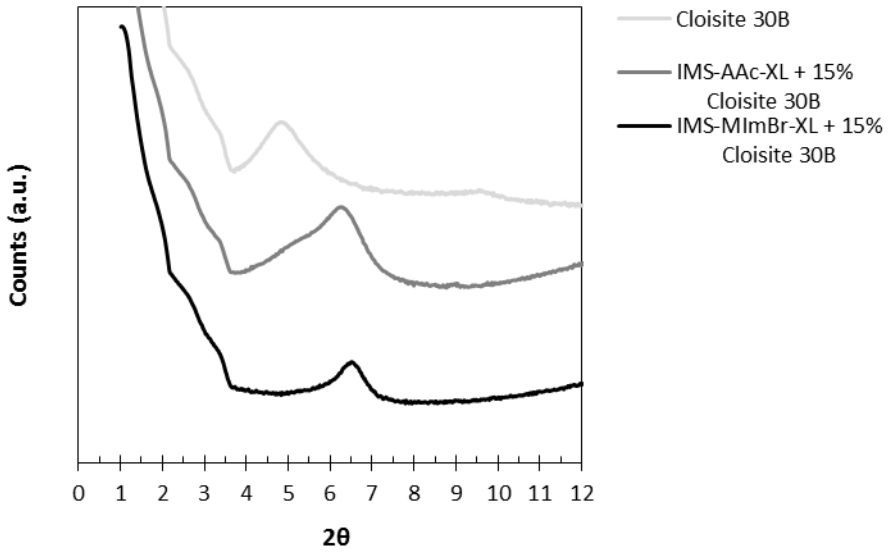

FIGURE 5.12 – XRD for Cloisite® 30B clay-filled IMS-MImBr-XL and IMS-AAc-XL, and the Cloisite 30B clay

The organo-modification of MMT is an important step in the preparation of polymer layered silicate nanocomposites (PLSNs). In fact, the layer separation and therefore the achievement of exfoliated morphologies depends on the establishment of favourable interactions

between the polymer and the clay surface. The interfacial adhesion between the organic and inorganic phases of the nanocomposite plays a role of primary importance. Therefore, the initial aim of this work was to modify the clay surface using a cationic polymerizable surfactant able to increase the space among the layers and improve the interaction with the polymer matrix. Moreover, this chosen organic cation will enhance the thermal stability of the o-MMT. For this reason, knowing that the delocalized imidazolium cation has better thermal stability than the alkylammonium and pyridinium cations, the synthesis of a thermally stable imidazolium salt, containing a vinyl group expecting to bind to the polymer and facilitate the formation of exfoliated nanomorphologies, was performed.

The ionomer showed a significant improvement in cure, with increasing filler loading (Figure 5.13 below). However, no cure boost was provided for the control sample, indicating very poor filler dispersion and hence the benefit of using an ionomeric system.

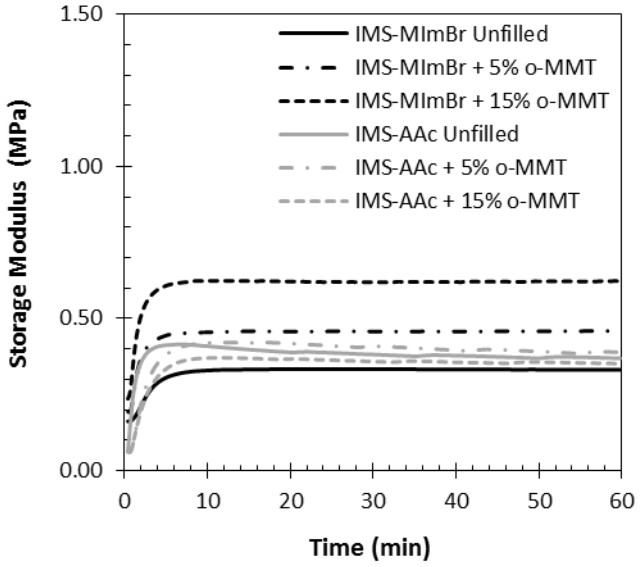

FIGURE 5.13 – Peroxide crosslinking dynamics of o-MMT clay-filled IMS-MImBr and IMS-AAc (160°C, 1 Hz, 3°, 18.5 µmol DCP/g)

The representative static tensile properties for the o-MMT filled ionomer product shows exceptional tensile stress at break as compared to the other filled materials (Figure 5.14 below), where the control samples again indicate low elongations at break and low strains. The addition of the o-MMT clay significantly deteriorated the tensile stress of the control materials.

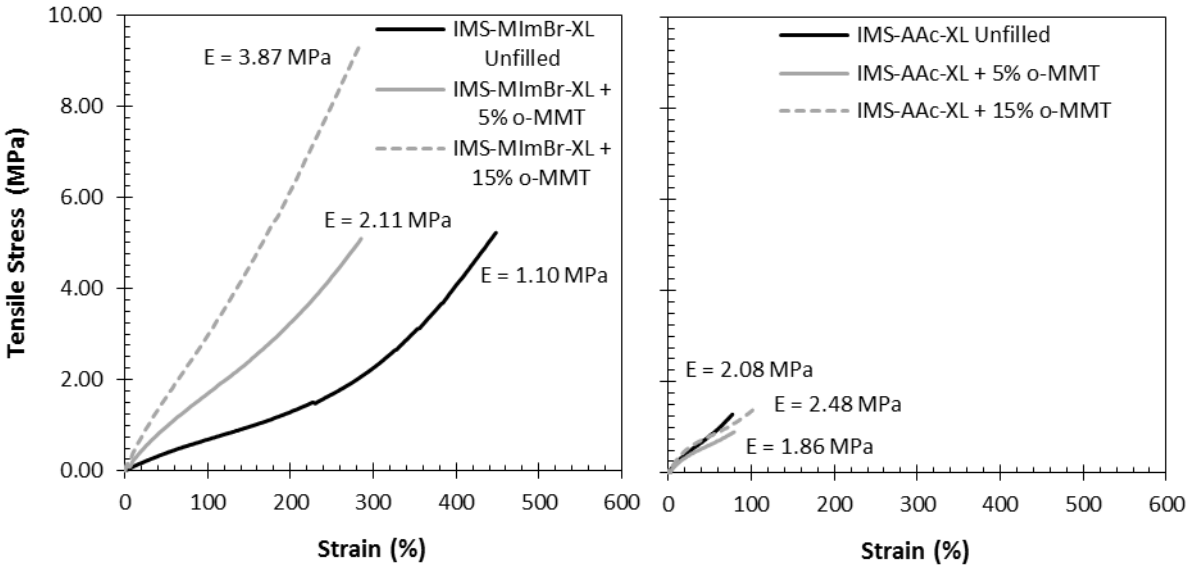

FIGURE 5.14 – Static tensile properties for o-MMT-filled IMS-MImBr-XL and IMS-AAc-XL

The substantial reduction in the intensity of the diffraction peaks for the 15 wt% o-MMT clay-filled IMS-MImBr-XL (Figure 5.15 on page 105) indicates that clay exfoliation took place. In comparison, intense and clear XRD signals remained for the non-ionic species.

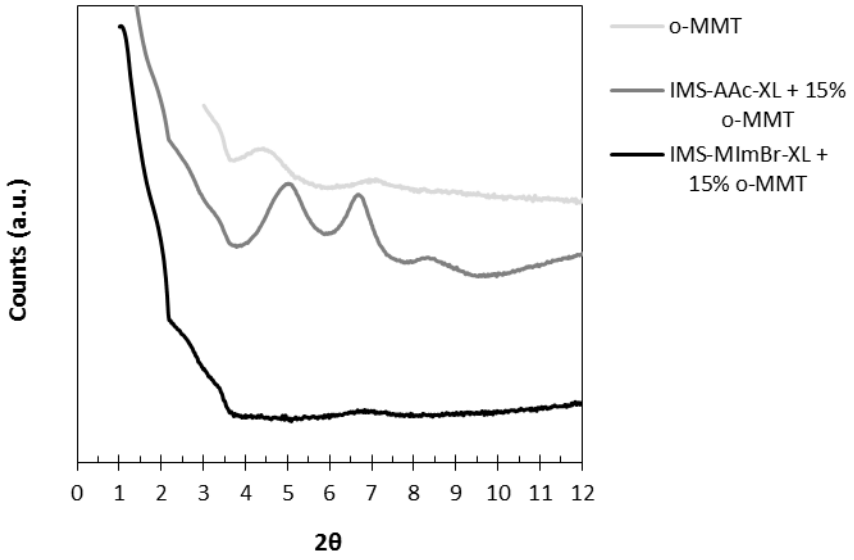

FIGURE 5.15 – XRD for o-MMT clay-filled IMS-MImBr-XL and IMS-AAc-XL, and the o-MMT clay

TEM images (Figure 5.16 on page 106) were performed to demonstrate the differences in exfoliation between the o-MMT clay-filled ionic (A) and non-ionic (B) nanocomposites. Clay platelets were clearly identified for the IMS-MImBr-XL product, which is not seen for the control sample. Partial exfoliation was demonstrated for the ionic species, which correlates well with its XRD spectra, indicating improvement in dispersive mixing is required.

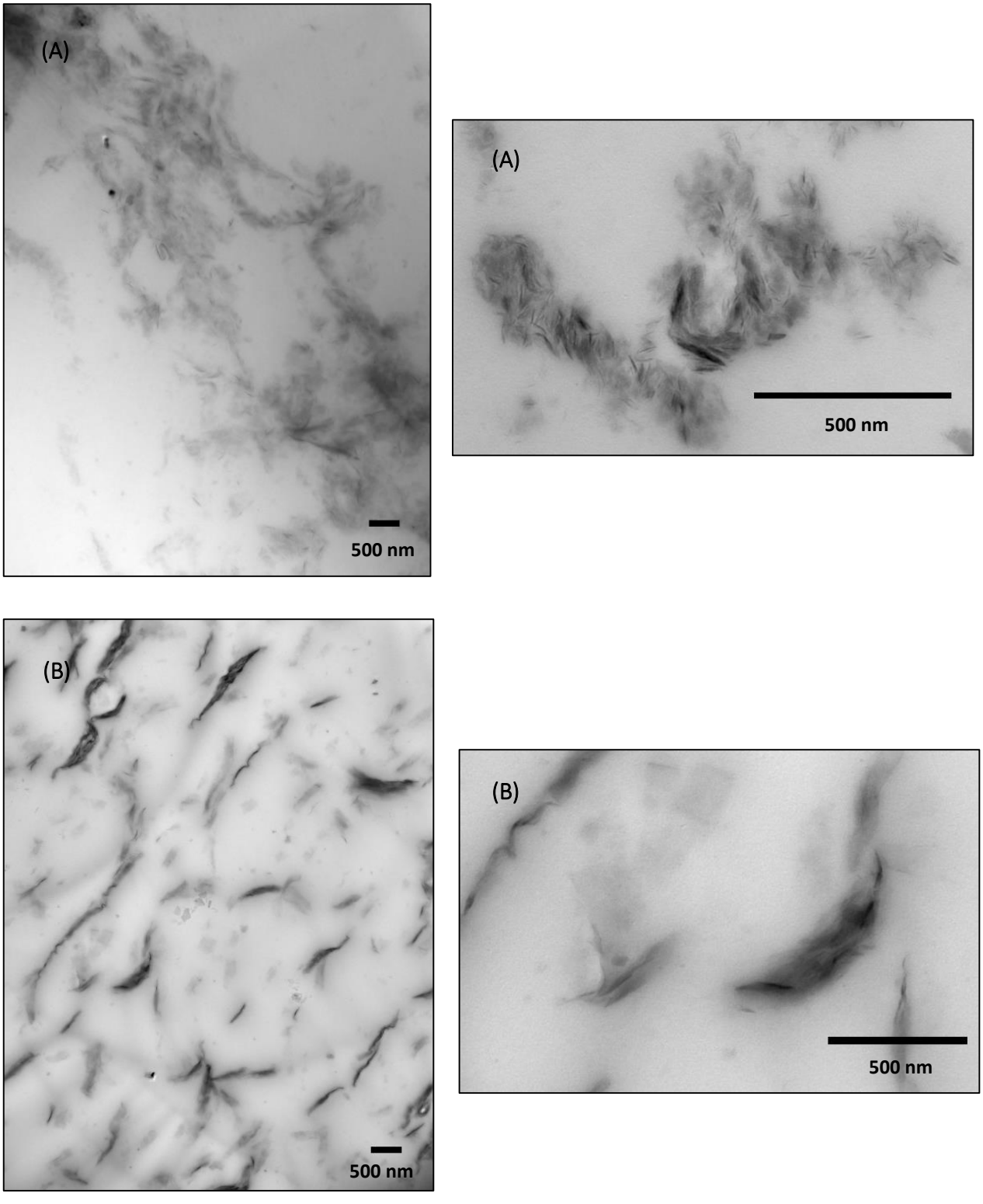

FIGURE 5.16 – TEM images of (a) IMS-MImBr-XL with 15 wt% o-MMT and (b) IMS-AAc-XL with 15 wt% o-MMT

The promising results given by the Cloisite® Na^+ filled ionomer along with the ease of acquiring a sodium-derived clay clearly identifies the superiority of the following compounds. The cure data, Figure 5.17 below, for the ionomer and control compounds shows very similar ΔG' for all filler loadings of Cloisite® Na+.

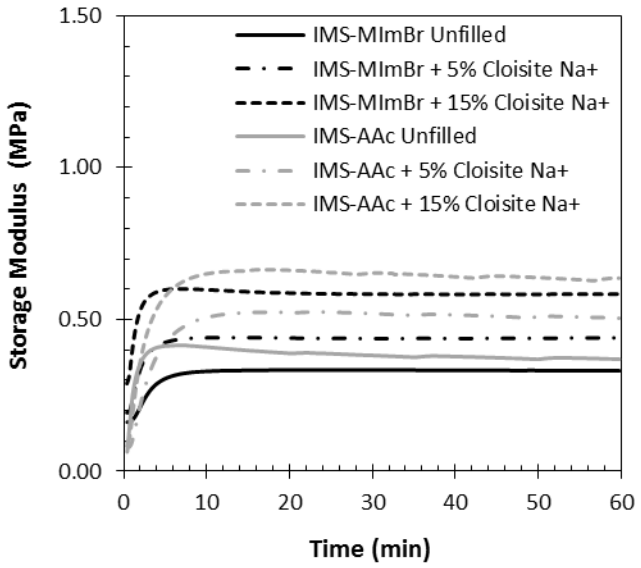

FIGURE 5.17 – Peroxide crosslinking dynamics of Cloisite® Na^+ clay-filled IMS-MImBr and IMS-AAc (160°C, 1 Hz, 3°, 18.5 µmol DCP/g)

The representative static tensile properties for the Cloisite® Na^+ samples in Figure 5.18 on page 108 reveal excellent reinforcement for the ionomer at all elongations, indicating extensive clay dispersion. A Young's modulus of 2.5 MPa is observed at the 15% clay loading with no sign of low strain yielding typically arising from a reticulate filler network. The control samples show both lower Young's moduli and significantly lower strains.

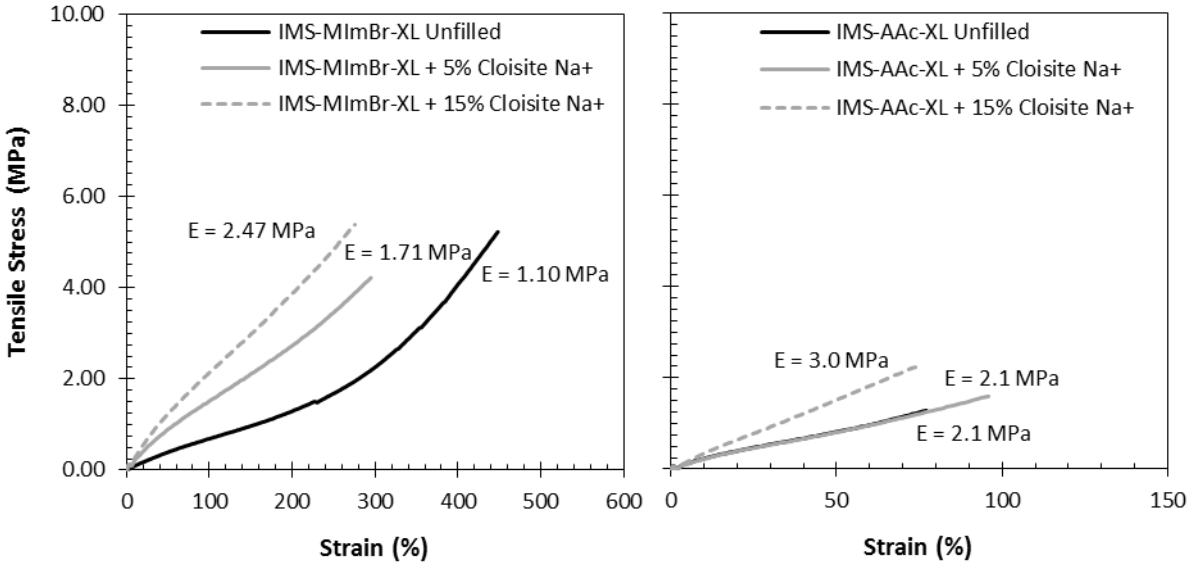

FIGURE 5.18 – Static tensile properties for Cloisite® Na^+ clay-filled IMS-MImBr-XL and IMS-AAc-XL

The substantial reduction in the intensity of the diffraction peaks for the 15 wt% Cloisite Na^+ clay-filled IMS-MImBr-XL (Figure 5.19 below) indicates that clay exfoliation took place. In comparison, intense XRD signals remained for the non-ionic species.

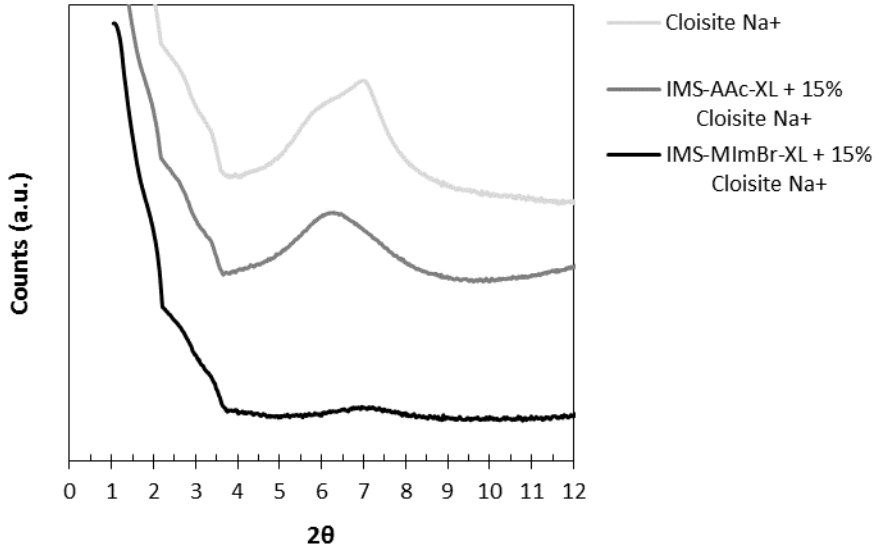

FIGURE 5.19 – XRD for Cloisite® Na^+ clay-filled IMS-MImBr-XL and IMS-AAc-XL, and the Cloisite® Na^+ clay

TEM images (Figure 5.20 on page 109) were performed to demonstrate differences in exfoliation between the Cloisite Na^+ clay-filled ionic (A) and non-ionic (B) nanocomposites. Clay platelets are clearly identified for the IMS-MImBr-XL product, which is not seen for the control sample. Superior exfoliation is demonstrated for the ionic species, which correlates well with its

XRD spectra, as compared to the 15 wt% o-MMT clay filled IMS-MImBr-XL. These results are encouraging in terms of industrial applications, since sodium clay is easily attainable and not financially costly.

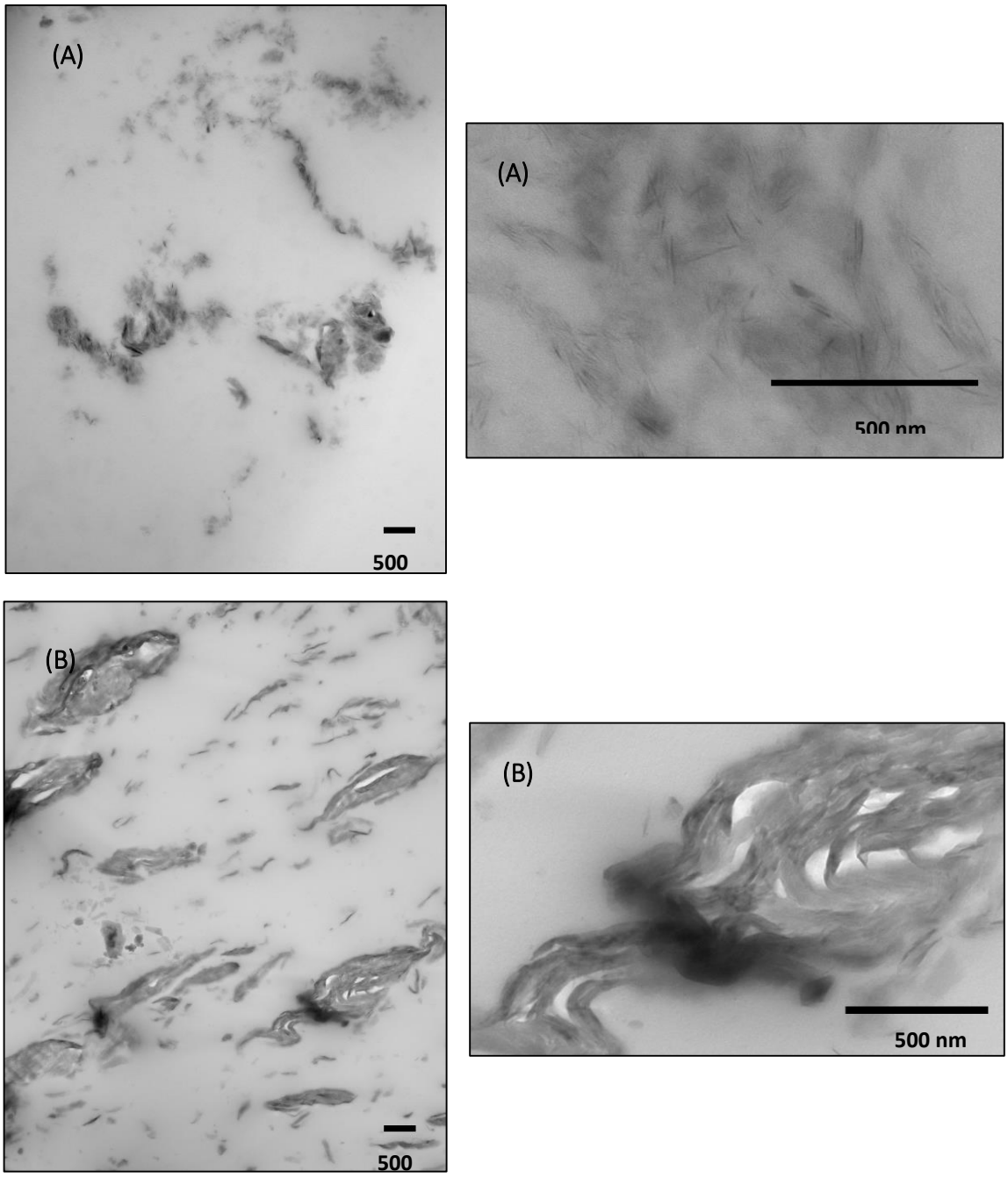

FIGURE 5.20 – TEM images of (a) IMS-MImBr-XL with 15 wt% Cloisite® Na^+ clay and (b) IMS-AAc-XL with 15 wt% Cloisite® Na^+ clay

5.8 Conclusions

A reactive ionomer derivative of BIMS was prepared under solvent-free conditions by the N-alkylation of N-vinylimidazole and N-butylimidazole. Peroxide crosslinking of the mixed alkylation product occurred efficiently yielding a thermoset containing an ionic network and a covalent crosslink network. These radical cures were robust, in that the cure formulations did not require optimization for different carbon black, silica or clay loadings. Physical properties of the mixed alkylation thermosets showed excellent reinforcement and little evidence of filler agglomeration. The static stress-strain curves showed the Young's modulus increased with an increase in filler loading, consistent with elastomer reinforcement. A dynamic Payne analysis indicated the ionomers do disperse conventional rubber fillers and clays, although some reticulate filler networks may form at higher filler loadings. Overall, the ionomer reveals superior qualities over the non-ionic species through its physical properties, XRD and TEM.

REFERENCES

1. Zhang, Y., Ge, S., Tang, B., Koga, T., Rafailovich, M.H., Sokolov, J.C., Peiffer, D.G., Li, Z., Dias, A.J., McElrath, K.O, Lin, M.Y., Satija, S.K., Urquhart, S.G., Ade, H., Nguyen, D. Effect of Carbon Black and Silica Fillers in Elastomer Blends, *Macromolecules*, **34,** 7056-7065 (2001).

2. Donnet, J.–B., Custodero, E., Reinforcement of Elastomers by Particulate Fillers, from *Science and Technology of Rubber*, 3rd Edition, 367 – 400, Mark, J.E., Erman, B., Eirich, F.R., Elsevier Academic Press, Boston (2005).

3. Tse, M.F., Wang, H. –C., Rogers, J.E., Rheological Behaviour of a New Isobutylene-based Elastomer Blended with a Filler, *Rubber World*, **216**, 39 – 45 (1997).

4. Tsou, A.H, Measmer, M.B., Dispersion of Layered Organosilicates in Isobutylene-Based Elastomers, *Rubber Chemistry and Technology*, **79**, 281 – 306 (2006).

5. Micouin, J.M., Chevallier, Y., U.S. Patent 6,191,205, 2001.

6. Hopkins, W., von Hellens, W., Koski, A., Rausa, J., Bromobutyl in Tire Treads, *Rubber World*, **226**, 38 – 43 (2002).

7. E. Giannelis, Adv. Mater. 1996, 8, 29.

8. Galimberti, M., 2012. Advanced Elastomers – Technology, Properties and Applications, Chapter 4 : Rubber Clay Nanocomposites. ISBN 978-953-51-0739-2.

9. W. Xie, Z. Gao, W.P.Pan, D. Hunter, A. Singh, R. Vaia, Chem. Mater. 2001, 13, 2979.

10. Z.M. Liang, J. Yin, J.J. Xu, Polymer 2003, 44, 1391.

11. Ozvald, A.M. Reactive Ionomers: N-vinyliidazolium Bromide Derivatives of Poly(isobutylene-co-isoprene) and Poly(isobutylene-co-para-methylstyrene). Master of Applied Science Thesis, Queen's University (2012).

12. Parent, J.S., Liskova, A., Resendes, R., Isobutylene-Based Ionomer Composites: Silicious Filler Reinforcement, Polymer, 45, 8091 – 8096 (2004).

13. Bottino, F.A., Fabbri, E., Fragala, I.L., Malandrino, G., Orestano, A., Pilati, F., Pollicino, A. Polystyrene-Clay Nanocomposites Prepared with Polymerizable Imidazolium Surfactants, *Macromolecular Rapid Communications*, **24**, 1079–1084 (2003).

14. ASTM Standard D3182 – 07, Standard Practice for Rubber – Materials, Equipment and Procedures for Mixing Standard Compounds and Preparing Standard Vulcanized

Sheets, ASTM International, West Conshohocken, PA, 2007, DOI: 10. 1520/D03182 - 07, www.astm.org.

15. ASTM Standard D412 – 06aE2, Standard Test Methods for Vulcanized Rubber and Thermoplastic Elastomers – Tension, ASTM International, West Conshohocken. PA. 2006, DOI: 10. 1520/D0412-06AE02, www.astm.org

16. Payne, A.R., Whittaker, R.E., Low Strain Dynamic Properties of Filled Rubbers, *Rubber Chemistry and Technology*, 44, 440 – 478 (1971).

17. Zaborski, M., Vidal, A., Ligner, G., Balard, H., Papirer, E., Burneau, A., Comparative Study of the Surface Hydroxyl Groups of Fumed and Precipitated Silicas. 1. Grafting and Chemical Characterization, *Langmuir*, 5, 447 – 451 (1989).

18. Bertrand, P., Weng, L.T., Carbon Black Surface Characterization by TOF-SIMS and XPS, *Rubber Chemistry and Technology*, 72, 384 – 398 (1999).

19. Cloisite Additives: Nano-scale additives for reinforced plastics. Rockwood Clay Additives GMBH. Accessed: August 6 2013. http://www.nanoclay.com/benefits2.asp

20. Gopakumar, T.G., Lee, J.A., Kontopoulou, M., Parent, J.S. Influence of clay exfoliation on the physical properties of montmorillonite/polyethylene composites, *Polymer*, **43** 5483–5491 (2002).

21. Ali Olad (2011). Polymer/Clay Nanocomposites, Advances in Diverse Industrial Applications of Nanocomposites, Dr. Boreddy Reddy (Ed.), ISBN: 978-953-307-202-9, InTech, Available from: http://www.intechopen.com/books/advances-in-diverse-industrial-applications-of-nanocomposites/polymerclay-nanocomposites.

CHAPTER 6

CONCLUSIONS AND RECOMMENDATIONS

6.1 Conclusions

The N-alkylation of different functional groups, including imidazole derivatives, produces ionomeric, peroxide-curable derivatives of BIIR and BIMS. The benzylic bromide functionality in BIMS shows greater reactivity towards N-alkylation of different imidazole derivatives and supports a solvent-free preparation. These reactive ionomers readily crosslink with peroxide at elevated temperatures producing thermosets made of a hybrid ionic/covalent network. The presence of ionic and covalent crosslink networks provide these materials with unique physical properties. At high temperatures and high stresses, where the ionic crosslink network is labile, the covalent crosslink network provides support to the material. At low temperature and low elongation, stiffness generated by the ionic network is more comparable to that given by the covalent network. Additionally, anti-microbial studies of different BIIR derivatives determined the inclusion of imidazolium functionality in the elastomer film prevents the viability of bacterial cell growth, whereas non-imidazolium derivatives do not discourage cell proliferation.

The effects of ion pair aggregation on macromonomer crosslinking dynamics and yields were studied by comparing macromonomers bearing simple ester functionality to analogues bearing imidazolium bromide functionality. Additionally, the structure/reactivity of BIIR and BIMS study provided an enriching insight into the effects of polymer backbone reactivity on peroxide-cure outcomes. The subtle difference in chemical functionality and composition distribution of BIIR and BIMS provided unique cure characteristics, particularly for macromonomers bearing relatively unreactive oligomerizable functionality.

Rendering an IIR-VImBr ionomer into a stable O/W emulsion is possible using a polymerizable imidazolium surfactant. The use of a polymerizable surfactant allows for its engagement of the polymer in co-curing, thereby eliminating the potential for leaching from the vulcanizate. With these, the ionomers potentially plasticize, increase the extent of free radical cures, provide the material additional ionic functionality, deliver a reactive anion to the formulation and stabilize the emulsion against coagulation. The final emulsion targets adhesive

surface-coating applications requiring an interfacial bond, or cure, and anti-microbial properties for various conditions and environments.

A mixed alkylation of VIm and BuIm was performed on BIMS via a solvent-free compounding technique. This reactive ionomer demonstrated compatibility with conventional rubber fillers including carbon black and precipitated silica. A BIMS-clay nanocomposite was prepared using Cloisite 30B, Cloisite Na+ and an organically modified montmorillonite with use of an imidazolium salt. The latter obtains an improvement in thermal stability compared to montmorillonite modified with a standard alkylammonium cation. The synthesized cations facilitated the formation of partially exfoliated structures resulting from the presence of a polymerizable group in their structure. There were no adverse effects observed on the peroxide crosslinking of the elastomers and a constant peroxide loading is usable regardless of the filler loading. Carbon black, precipitated silica and the three different clays provide reinforcement to the final elastomer products, as observed in the tensile stress-strain profiles. Payne analysis show good filler dispersion at low filler loading, however some evidence indicate reticulate filler network formation at high filler loadings. Overall, the sodium-based clay showed the most promising results, which is very encouraging in terms of industrial applications.

6.2 Recommendations

a. Use lower strains in future measurements. The rheological measurements conducted in this research monitored crosslink yields at high strains (3° arc), which could be disruptive to crosslinked networks.

b. Explore different functionalities in addition to the functional macromonomer derivatives of IIR and IMS as reported in this investigation. For example, IIR or IMS containing amino silane functional groups have the potential to enhance silica dispersion within a polymer.

c. Explore the multiplet morphology of IIR-VImBr and the role of a peroxide crosslink. The mechanism of peroxide crosslinking in IIR-VImBr is unclear as N-vinylimidazolium salts do not homopolymerize well, yet IIR-VImBr has similar cure dynamics to IIR-Acrylate, a more reactive macromonomer.

d. Explore anion metathesis and possibly introduce alternative anions, which may alter physical properties or aid in crosslinking reactions.

e. Conduct more tests in determining the fatigue-to-failure and hysteretic properties of materials.

f. Conduct more tests to determine the influence of functional group reactivity, polymer backbone structures and ion pair aggregation on cure reactivity.

g. Determine which additives best increase the solids content of an ionomeric emulsion without rubber precipitation during solvent removal, and analyze the adhesivity of the resulting latex film.

APPENDIX A

A.1 ^{1}H NMR Spectra for IIR-BuImBr and IIR-VImBr

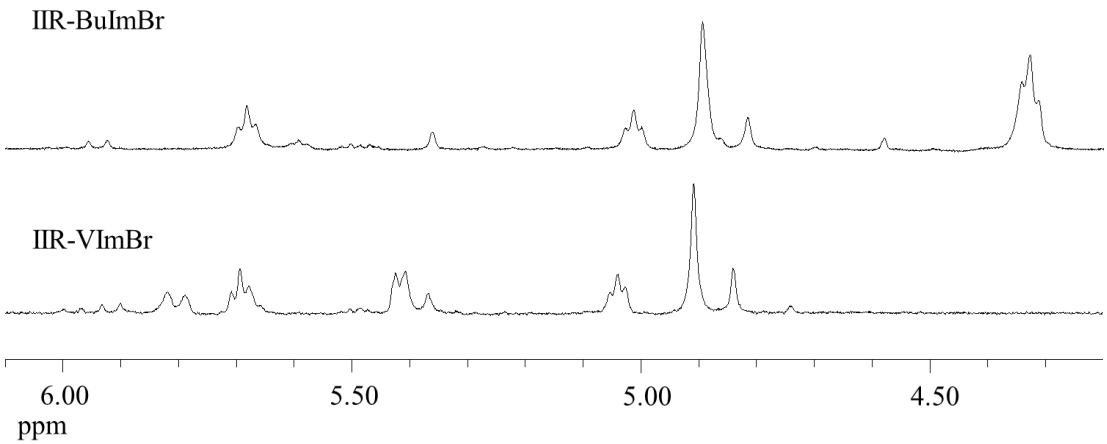

FIGURE A.1 - ^{1}H NMR Spectra of IIR-BuImBr and IIR-VImBr